HYDRODYNAMICS OF NEUTRON STAR INTERIORS AND LABORATORY SUPERFLUIDS

Thesis by

Tassilo Andreas Reisenegger

In Partial Fulfillment of the Requirements

for the Degree of

Doctor of Philosophy

California Institute of Technology

Pasadena, California

1993

(Defended April 30, 1993)

Thesis Advisor:

Professor Peter Goldreich

To my parents and to Ana María
with gratitude and love,
To Renate and her generation
with joy and hope.

Lee and Kevin Rauch, should also be specially thanked for putting up with me, with my questions about how to do this and that on the computer, and with many phone calls.

I am grateful to Kip Thorne for his excellent teaching in Ph 136 (Applications of Classical Physics) and Sterl Phinney and Peter Goldreich for their very original course Ph 103 (Order of Magnitude Physics). From these courses, I learned a significant fraction of all the physics I know, and mainly the most important things: to be able to connect physics to the real world (which it is, of course, supposed to explain) and to identify the main physical ingredients relevant for a particular problem.

Many thanks go also to our friends and neighbors Nina and Olivier Espinosa, Marcela and Fernando Echeverría, and Yarona and Ilan Grave, for making Ana María's and my life in Pasadena much easier than it would otherwise have been.

Those individuals who contributed to particular parts of this thesis, as well as the institutions that provided the financial support, are thanked at the end of each chapter.

Abstract

This thesis contains the following papers:

1) *A new class of g-modes in neutron stars* (*Astrophys. J.*, **395**, 240 (1992)): In the fluid core of a neutron star, the ratio of the number densities of charged particles (protons and electrons) to neutrons is an increasing function of the mass density. This composition gradient stably stratifies the matter, giving rise to *g*-modes with periods ranging upward from a few milliseconds. Some of these modes are computed and their damping mechanisms are discussed.

2) *Magnetic field decay in isolated neutron stars* (*Astrophys. J.*, **395**, 250 (1992)): We investigate mechanisms that promote the loss of magnetic flux from an isolated neutron star. *Ambipolar diffusion* involves a drift of the magnetic field and charged particles relative to the neutrons, opposed by frictional drag. Variants of it include both the buoyant rise and the dragging by superfluid neutron vortices of magnetic flux tubes. The charged particle flux decomposes into a solenoidal and an irrotational component. The irrotational component perturbs the chemical equilibrium, generating pressure gradients that effectively choke it. The solenoidal component can transport magnetic flux from the outer core to the crust on a short timescale. Flux that threads the inner core is permanently trapped unless particle interactions can rapidly smooth departures from chemical equilibrium. We speculate that *Hall drift* may lead to a turbulent cascade of the magnetic field in the solid crust, terminated by ohmic dissipation at small scales.

3) *The spin-up problem in helium II* (To appear, *J. Low Temp. Phys.*, **92** (1/2) (July 1993)): The laminar spin-up of helium II is studied by solving the linearized two-fluid equations in a simple case. No direct interactions between vortex lines and container walls are included. Two mechanisms are identified for the transfer of angular momentum from the container to the interior fluid. Both involve a poloidal secondary flow. An analytic expression for the spin-up time is found.

Contents

Chapter 1

INTRODUCTION

This thesis includes three research papers directly or indirectly related to the dynamics of neutron star interiors. Thus, in this introduction, I will give a brief background on neutron stars, focusing mainly on some open theoretical questions that motivated this work, and a summary of the three papers, placed in this context.

Neutron stars are the densest objects in the Universe that can be observed directly. They are believed to be the remnants of fairly massive stars that have undergone supernova explosions. Since no nuclear burning occurs in neutron stars, and in their early life they cool quite efficiently by emitting neutrinos, they are supported against gravity only by the degeneracy pressure (and strong interactions) of the neutrons and other fermions contained in their interiors. Their mean density is even higher than that of atomic nuclei, providing a unique environment in which to study the physics of extremely dense matter. Among the exotic physics to be encountered in this medium, it is believed that the neutrons and protons in the fluid core of the star, and also the neutrons permeating the inner part of the solid crust, form Cooper pairs that allow them to condense into a BCS-type superfluid (or, in the case of the protons, superconducting) state. A good review of the superfluid properties of neutron stars is given by Sauls (1989). Even more exotic physics, such as a kaon condensate (Brown et al. 1992) or quark droplets (Heiselberg, Pethick, & Staubo 1993) may be encountered in the deeper regions of the core. For more details on the physics of neutron stars, the reader is referred to Shapiro and Teukolsky (1983).

Neutron stars are observed both as radio pulsars and as x-ray binaries. Radio pulsars are believed to be rapidly rotating, strongly magnetized neutron stars, in which charged particles streaming along the open magnetic field lines coming out of the magnetic poles of the star emit a fairly narrow beam of radiation. Since the rotational and magnetic axes of the star are in general not aligned with each other, this beam sweeps through space as the star rotates. If the Earth happens to lie in the path of this beam, a pulse of radiation is observed in every rotation period.

These pulses can be timed very accurately, yielding interesting information about the stars. For example, from the pulse period, P, and its time derivative, $\dot{P}$, one obtains an estimate for the age of the pulsar (the "spin-down age," $t_s = P/2\dot{P}$) that roughly agrees with independent estimates such as those from historical records of supernovae, kinematics of preserved supernova remnants, and the "kinetic ages" inferred from the space velocity of pulsars and their distance to the galactic plane, where they are believed to be born.

The surface magnetic field strength of a pulsar can also be inferred from P and $\dot{P}$ (and theoretical estimates for its radius and moment of inertia) if it is assumed that the pulsar is an oblique magnetic dipole rotating in vacuum that loses rotational energy due to emission of electromagnetic radiation. This is of course a gross oversimplification, but a more refined model (Goldreich & Julian 1969) that considers a pulsar with a magnetosphere, but with its rotational and magnetic axes aligned with each other, gives very similar results. For the vast majority of the observed pulsars, one infers $10^{11.5}\,\mathrm{G} < B_s < 10^{13}\,\mathrm{G}$.

In addition to a secular spin-down trend, several young radio pulsars exhibit "glitches," i. e., sudden changes in the rotation period, followed by a much slower relaxation back to a slow spin-down behavior (Lyne & Graham-Smith 1990). These phenomena are generally thought to be associated with differential rotation of the crustal neutron superfluid with respect to the other components of the star, and detailed models have been proposed (Pines & Alpar 1985, Baym, Epstein, & Link 1992). However, recent observations (Flanagan 1990, Lyne, Graham Smith, & Pritchard 1992) show that the post-glitch relaxation process is more complicated than previously expected, with at least three different time scales involved in it, and current models fall short of explaining all the details of these observations (Blandford 1992).

There is a special class of radio pulsars formed by the so-called "millisecond pulsars" ($P \lesssim 10\,\mathrm{ms}$), binary radio pulsars (i. e., systems in which the pulsar has a binary companion), and globular cluster pulsars. Most of these are inferred

to be very old, on grounds of their spin-down ages, the age of their companions (Kulkarni 1986), or their position in a globular cluster, where no star formation has taken place in recent times. One interesting fact about these pulsars is that their (inferred) B_s values are n the range $10^8 \, G < B_s < 10^{11} \, G$ (Bhattacharya & van den Heuvel 1991, Chanmugam 1992), much lower than those of the "classical" radio pulsars.

X-ray binaries are believed to be systems in which a neutron star is accreting matter from a non-degenerate companion. As this matter falls onto the surface of the neutron star, x-rays are emitted. These systems fall into two classes: 1) x-ray pulsars, in which the strong magnetic field of the neutron star channels the accreted matter onto its poles, creating a similar effect to that seen in radio pulsars (although generally the pulses are broader, and the periods are longer), and 2) low-mass x-ray binaries, in most of which the magnetic field is not strong enough to significantly influence the flow of the infalling matter, and therefore no pulses are seen. From the lifetimes of the companion stars, it can be inferred that the x-ray pulsars are young systems, whereas the low-mass x-ray binaries are much older. The spectra of some x-ray pulsars show features that have been identified as being due to resonant electron cyclotron scattering. These allow one to make estimates of the surface magnetic field strengths of these neutron stars, $B_s \sim (0.5 - 4) \times 10^{12} \, G$ (Nagase 1989, Chanmugam 1992), in the same range as those of young radio pulsars.[1] The absence of pulses in the low-mass x-ray binaries constrains the surface field strength to much lower values.

As is also discussed in Chapter 3, the different surface field strengths of young and old neutron stars suggest that the magnetic field may decay with time, either spontaneously or due to accretion. Whether the observational data from classical, single (and therefore not accreting) radio pulsars show evidence for field decay remains controversial. (See Wakatsuki et al. 1992, and specially Harrison, Lyne,

---

[1]This may partly be due to selection effects, since fields far outside this range could not have been detected. However, the fact that several x-ray pulsars do have fields in this range is probably already significant.

and Anderson 1993, in addition to the references given in Chapter 3.) It was realized early on that, due to the high conductivity of the degenerate neutron star matter (even in the absence of superconductivity), the ohmic decay of the magnetic field proceeds extremely slowly, so that it cannot account for the observed differences in the field strengths between young and old neutron stars. It also means that B_s is not necessarily representative of the magnetic field in the interior of the neutron star, which may be much weaker (Blandford, Applegate, & Hernquist 1983) or much stronger than the surface field.

The long time scale for ohmic decay implies that a significant evolution of the magnetic field can only occur if it is transported by a bulk flow of charged particles, into which it is effectively frozen. Similar flows of matter may be expected also to be associated with the rotational evolution of the neutron star, both in the secular spin-down (Easson 1979b) and in the glitches and post-glitch relaxation (Easson 1979a), as it occurs in the spin-up and spin-down of ordinary laboratory fluids.

In Chapter 2, it is shown that the radial gradient in the composition of the matter in the neutron star core (the number of charged particles per neutron decreases monotonically with increasing radius) has the effect of stably stratifying the fluid. Thus, perturbations to the equilibrium configuration of the star can give rise to buoyant restoring forces. The neutron star supports a set of oscillation modes (g-modes) whose periods, wave functions, and damping times are calculated (or estimated) and discussed. The fact that the periods are quite short (only an order of magnitude longer than the dynamical time scale of the star) gives an indication of the strength of the restoring forces.

In the future, one might hope to do astroseismology with neutron stars, as is already done, e. g., with the Sun and white dwarf stars, in order to obtain direct information about the physical conditions of the stellar interiors. However, there are no convincing detections so far of any neutron star oscillations. Thus, at this point in time, probably the most important consequence of the stable stratification of the neutron star core is that it impedes the bulk flows mentioned above,

and therefore affects the magnetic (and possibly also the rotational) evolution of neutron stars.

The possible mechanisms for the decay of the magnetic field in a neutron star that is not accreting matter from a companion are studied in Chapter 3. The two-fluid equations of motion for protons and electrons moving through (and experiencing a drag force from) a static background of neutrons (effectively immobilized due to the stable stratification) are manipulated in order to derive an equation for the evolution of the magnetic field. This equation shows the effects of 1) ohmic diffusion, which is confirmed to occur only on extremely long time scales, 2) ambipolar diffusion, i.e., the coupled motion of protons and electrons, driven by magnetic stresses, that convects the magnetic field, and 3) Hall drift, in which the magnetic field is carried only by the electric currents supporting it. The latter two mechanisms, including their time scales and their possible significance for real neutron stars, are discussed in some detail. The equations derived are strictly valid only for non-superfluid particles, and therefore probably do not apply directly to a real neutron star during most of its lifetime. It is possible, to some extent, to make extrapolations to a state that includes superfluid neutrons and/or superconducting protons, but the validity of these is somewhat uncertain.

Interesting ideas about a coupled rotational and magnetic evolution of neutron stars, based on the dynamics and interactions of the quantized, magnetized vortices of the neutron and proton superfluids, have recently been proposed (Sauls 1989, Srinivasan et al. 1990, Ruderman 1991abc, Chau, Cheng, & Ding 1992), but complete, convincing models are still lacking. It should be interesting to investigate these ideas more deeply by a more complete description of the superfluid dynamics that incorporates the physical intuition gained in the study of the dynamics of normal fluids in this context, as described in Chapters 2 and 3.

In the last chapter, I follow the "philosophy" that, before attempting to understand the dynamics of a system as complex and remote as a neutron star, one should try to understand the analogous processes in a simpler and more accessible

system, as is available in this case with laboratory superfluids such as the two isotopes of helium, ^{4}He and ^{3}He. It turns out that no complete model for the superfluid spin-up process (i.e., the response of the superfluid to a change in the rotation rate of its container) has been given in the literature. Since this seems to be an important step towards the understanding of the relaxation of the neutron star superfluids after a glitch, and it might also give clues to more general aspects of superfluid dynamics, it is the subject of Chapter 4.

In order to understand the general principles involved in the spin-up process, imagine a classical fluid (say, water) is placed in a uniformly rotating, axisymmetric container and allowed to reach its equilibrium state of solid-body rotation at the same angular velocity as the container. Then, the rotation rate of the container is suddenly changed. The first response of the fluid will be to create a viscous boundary layer at the upper and lower boundaries of the container (those which are roughly perpendicular to the axis of rotation). In the interior of the fluid (i.e., away from the boundary layers) the fluid is still rotating at its original speed, and the centrifugal force is balanced by a radial pressure gradient. The same pressure gradient exists in the boundary layer, but the fluid there is rotating at a somewhat different speed (essentially that of the container), and therefore these two forces do not balance, with the effect of creating a radial flow. This flow returns (also radially) through the interior of the fluid, carrying angular momentum with it, which is used to change the angular velocity of the interior fluid. Angular momentum is only created (or destroyed) in the relatively thin boundary layer, and the secondary flow takes care of distributing it in the way needed for the fluid to achieve solid-body rotation at the container's speed. This process is significantly faster than would be expected from pure viscous diffusion.

A laboratory superfluid is more complex than a classical fluid. Its hydrodynamics, more details about which can be found, e.g., in Tilley and Tilley (1990) or Donnelly (1991), can be described by two separate components: 1) a truly superfluid component of density ρ_s and velocity $\mathbf{v}_s$, which is irrotational ($\nabla \times \mathbf{v}_s = 0$)

and has zero viscosity, and 2) a "normal fluid" (composed of the thermal excitations of the superfluid) with density ρ_n, velocity $\mathbf{v}_n$, and a finite viscosity. The superfluid component can only rotate by forming discrete, quantized vortex lines in whose cores $\rho_s \to 0$, allowing the superfluid to circulate around them. The superfluid and normal fluid components are coupled by a "mutual friction" force that arises from the scattering of thermal excitations by the normal cores of the vortex lines.

It is shown in Chapter 4 that, despite its greater complexity, the spin-up process in a laboratory superfluid should be similar to that occurring in a classical fluid. The normal component will form viscous boundary layers that in two ways cause a secondary flow to appear. In the first place, the same force imbalance mentioned in the classical case drives a secondary flow in the normal fluid. Secondly, the mutual friction force between the boundary layer fluid and the superfluid vortex lines will bend these and induce a secondary flow in the superfluid component. Due to the tight coupling between the two components, these mechanisms combine in a nontrivial way, and allow both components to spin up at essentially the same rate, regardless of which of the two mechanisms is dominant.

For several reasons, this model cannot be directly applied to the spin-up (or spin-down) of the fluid core of a neutron star. In the first place, the stable stratification of the core matter will strongly resist any secondary flows. Also, the magnetic stress, which is enhanced in the superconducting core due to the concentration of the magnetic flux in thin tubes (Easson & Pethick 1977), is likely to have an important effect on the spin-up process (Easson 1979, Srinivasan et al. 1990, Chau et al. 1992). The interaction between these flux tubes and the (also magnetized) neutron vortices may well introduce dissipation throughout the bulk of the fluid, giving the spin-up process a completely different character. However, it is likely that the processes described in this thesis will give some guidance in an attempt to understand the evolution of a neutron star's magnetic field and its rotation rate.

REFERENCES

Baym, G., Epstein, R. I., & Link, B. 1992, *Physica B* **178**, 1.

Baym, G., Pethick, C., & Pines, D. 1969, *Nature* **224**, 674.

Bhattacharya, D. & van den Heuvel, E. P. J. 1991, *Phys. Reports* **203**, 1.

Blandford, R. D. 1992, *Nature* **359**, 675.

Blandford, R. D., Applegate, J. H., & Hernquist, L. 1983, *MNRAS* **204**, 1025.

Brown, G. E., Kubodera, K., Rho, M., & Thorsson, V. 1992, *Phys. Lett. B* **291**, 355.

Chanmugam, G. 1992, *Ann. Rev. Astron. Astrophys.* **30**, 143.

Chau, H. F., Cheng, K. S., & Ding, K. Y. 1992, *Astrophys. J.* **399**, 213.

Donnelly, R. J. 1991, *Quantized Vortices in Helium II* (Cambridge Univ. Press, Cambridge).

Easson, I. 1979a, *Astrophys. J.* **228**, 257.

Easson, I. 1979b, *Astrophys. J.* **233**, 711.

Easson, I. & Pethick, C. 1977, *Phys. Rev. D* **16**, 275.

Flanagan, C. S. 1990, *Nature* **345**, 416.

Goldreich, P. & Julian, W. H. 1969, *Astrophys. J.* **157**, 869.

Greenspan, H. P. 1968, *The Theory of Rotating Fluids* (Cambridge Univ. Press, Cambridge).

Harrison, P. A., Lyne, A. G., & Anderson, B. 1993, *MNRAS* **261**, 113.

Heiselberg, H., Pethick, C. J., & Staubo, E. F. 1993, *Phys. Rev. Lett.* **70**, 1355.

Kulkarni, S. R. 1986, *Astrophys. J.* **306**, L95.

Lyne, A. G. & Graham-Smith, F. 1990, *Pulsar Astronomy* (Cambridge Univ. Press, Cambridge).

Lyne, A. G., Graham Smith, F., & Pritchard, R. S. 1992, *Nature* **359**, 706.

Nagase, F. 1989, *Publ. Astron. Soc. Japan* **41**, 1.

Pines, D. & Alpar, M. A. 1985, *Nature* **316**, 27.

Ruderman, M. 1991a, *Astrophys. J.* **366**, 261.

Ruderman, M. 1991b, *Astrophys. J.* **382**, 576.

Ruderman, M. 1991c, *Astrophys. J.* **382**, 587.

Sauls, J. A. 1989, in *Timing Neutron Stars*, H. Ögelman & E. P. J. van den Heuvel, eds., p. 457 (Kluwer Academic Publishers, Dordrecht & Boston).

Shapiro, S. L., & Teukolsky, S. A. 1983, *Black Holes, White Dwarfs, and Neutron Stars* (John Wiley & Sons, New York).

Srinivasan, G., Bhattacharya, D., Muslimov, A. G., & Tsygan, A. I. 1990, *Current Sci.* **59**, 31.

Tilley, D. R. & Tilley, J. 1990, *Superfluidity and Superconductivity*, third edition (Adam Hilger, Bristol & New York).

Wakatsuki, S., Hikita, A., Sato, N., & Itoh, N. 1992, *Astrophys. J.* **392**, 628.

Chapter 2

A NEW CLASS OF G-MODES IN NEUTRON STARS

ABSTRACT

Because a neutron star is born hot, its internal composition is close to chemical equilibrium. In the fluid core, this implies that the ratio of the number densities of charged particles (protons and electrons) to neutrons, $x \equiv n_c/n_n$, is an increasing function of the mass density. This composition gradient stably stratifies the matter giving rise to a Brunt-Väisälä frequency $N \sim (xg/2H)^{1/2} \sim 500\text{s}^{-1}$, where g is the gravitational acceleration, and H is the density scale height. Consequently, a neutron star core provides a cavity that supports gravity modes (g-modes). These g-modes are distinct from those previously identified with the thermal stratification of the surface layers and the chemical stratification of the crust. We compute the lowest-order, quadrupolar, g-modes for cold, Newtonian, neutron star models with $M/M_\odot = 0.581$ and $M/M_\odot = 1.405$ and show that the crustal and core g-modes have similar periods. We also discuss damping mechanisms and estimate damping rates for the core g-modes. Particular attention is paid to damping due to the emission of gravitational radiation.

1. INTRODUCTION

The nonradial oscillations of neutron stars have been analyzed extensively in a series of papers by Thorne and collaborators (Thorne and Campolattaro 1967, Price and Thorne 1969, Thorne 1969a, b, Campolattaro and Thorne 1970, Ipser and Thorne 1973). These authors assumed that chemical equilibrium rendered cold neutron stars neutrally stable, and therefore concluded that their g-modes were degenerate at zero frequency (e.g., Thorne 1969a, Van Horn 1980, and McDermott, Van Horn, and Scholl 1983). McDermott et al. (1983) calculated g-modes associated with *thermal stratification* and found the quadrupole modes of completely fluid models with temperatures $T \sim 10^8 \mathrm{K}$ to be concentrated within 10 m of the stellar surface and to have periods $P > 50$ ms. [1]

Later, Finn (1987) pointed out that the *nonuniform chemical composition of the neutron star crust* would perturb the g-modes away from zero frequency. He studied modes associated with discrete changes in composition that occur at densities in the range $8 \times 10^6 < \rho < 4 \times 10^{11} \mathrm{g\ cm}^{-3}$. These are located in the outer kilometer of the star. Finn's calculations show that the lowest order, crustal g-modes have periods of a few milliseconds, shorter than those of thermal g-modes of the same multipole order.

In addition to discrete changes of chemical composition in the crust, there is also a *smooth change of chemical composition in the core* of a neutron star. More specifically, the equilibrium concentration of charged particles (protons and electrons) depends on density, and increases toward the center of the star. This concentration gradient stably stratifies the core, thus giving rise to an additional series of g-modes. The purpose of our paper is to provide a rough description of these core g-modes.

In §2, we derive equations that govern the linear oscillations of a fluid star.

---

[1] McDermott, Hansen, Van Horn, and Buland (1985) and McDermott, Van Horn, and Hansen (1988) studied neutron star models with a solid crust and found an additional set of thermal g-modes in the fluid material just below the crust, with even longer periods.

Then we obtain the WKB dispersion relation which approximates the g-mode frequencies in terms of the Brunt-Väisälä frequency, N.

The stable stratification of the material in the core of a neutron star is investigated in §3. We evaluate the Brunt-Väisälä frequency, thereby obtaining a numerical estimate for the periods of the core g-modes. These turn out to be of the same order of magnitude as those of the discontinuity modes computed by Finn (1987). We also provide crude estimates for the damping timescales of these modes.

Section 4 outlines the numerical computation of the g-mode eigenfunctions, periods, and damping times due to emission of gravitational waves. We explain the differential equations, boundary conditions, and stellar equilibrium models used, emphasizing the models for the Brunt-Väisälä frequency due to the composition gradients in the core and crust.

In §5, we present and discuss the results of the numerical calculations of quadrupole f- and g-modes for two model neutron stars, comparing them to earlier work.

Finally, in §6, we give a short summary of the conclusions of the present work and its implications for other aspects of neutron star physics.

2. NONRADIAL OSCILLATIONS OF A NEWTONIAN, FLUID STAR

In this section we derive differential equations that govern the linear oscillations of a nonrotating, unmagnetized, inviscid, fluid star. We apply *Newtonian* mechanics and make the *Cowling approximation* (Cowling 1941), that is, we neglect the Eulerian perturbations of the local gravitational potential. Similar derivations can be found elsewhere (e.g. Cox 1980, Unno, Osaki, Ando, and Shibahashi 1970); we offer ours for completeness and to clarify the notation and approach of the present paper.

Under our assumptions, the equilibrium configuration of the star is spherically

symmetric, and the equilibrium density and pressure, ρ_0 and p_0, depend only on the radial coordinate, r. Oscillations are characterized by a displacement vector field, $\boldsymbol{\xi}(\mathbf{r}, t)$, together with the *Eulerian* (or "local") *perturbations* of the density and pressure, $\delta\rho$ and δp. In addition, it is convenient to use the *Lagrangian* (or "convective") *perturbations*, $\Delta\rho$ and Δp. Eulerian and Lagrangian perturbations are formally related by

$$\Delta = \delta + \boldsymbol{\xi} \cdot \boldsymbol{\nabla}. \tag{1}$$

Written in terms of these variables, the continuity equation reads

$$\Delta\rho = -\rho_0 \boldsymbol{\nabla} \cdot \boldsymbol{\xi}, \tag{2}$$

and the equation of motion takes the form

$$\frac{\partial^2 \boldsymbol{\xi}}{\partial t^2} = -\frac{1}{\rho_0 + \delta\rho} \boldsymbol{\nabla}(p_0 + \delta p) + \mathbf{g}, \tag{3}$$

where the local gravitational acceleration, $\mathbf{g}$, is taken to be constant at a fixed location in space (Cowling approximation). The equation of motion decomposes into an equilibrium equation,

$$\frac{1}{\rho_0} \boldsymbol{\nabla} p_0 = \mathbf{g}, \tag{4}$$

in which both sides are time-independent radial vectors, and a linearized equation for the perturbations,

$$-\omega^2 \boldsymbol{\xi} = -\frac{1}{\rho_0} \boldsymbol{\nabla}(\delta p) + \frac{\delta\rho}{\rho_0} \mathbf{g}, \tag{5}$$

where all perturbation variables depend on time through the factor $e^{-i\omega t}$.

Since the last term in equation (5) is purely radial, the component of the displacement vector perpendicular to the radial direction satisfies

$$\xi_\perp = \frac{1}{\rho_0 \omega^2} \nabla_\perp (\delta p), \tag{6}$$

where $\nabla_\perp$ is the analogous component of the gradient operator. Substituting this expression into the continuity equation (2), and taking the Eulerian pressure perturbation in a given mode to be the product of a spherical harmonic $Y_l^m(\theta, \phi)$ and an arbitrary function of radius, we obtain

$$\frac{1}{r^2} \frac{\partial}{\partial r} (r^2 \xi_r) - \frac{l(l+1)}{r^2 \omega^2} \frac{\delta p}{\rho_0} + \frac{\Delta \rho}{\rho_0} = 0. \tag{7}$$

To relate the density perturbations to the pressure perturbations, it is useful to introduce the variables

$$c_s^2 \equiv \left(\frac{\partial p}{\partial \rho} \right)_{\text{adiabatic}} = \frac{\Delta p}{\Delta \rho}, \tag{8}$$

where c_s is the adiabatic sound speed, and

$$c_{eq}^2 \equiv \left(\frac{\partial p}{\partial \rho} \right)_{\text{equilibrium}} = \frac{dp_0/dr}{d\rho_0/dr}. \tag{9}$$

Using these definitions, it is straightforward to rewrite equation (7) in terms of the radial displacement and the Eulerian pressure perturbation as

$$\frac{1}{r^2} \frac{\partial}{\partial r} (r^2 \xi_r) - \frac{g}{c_s^2} \xi_r + \left(\frac{1}{c_s^2} - \frac{l(l+1)}{r^2 \omega^2} \right) \frac{\delta p}{\rho_0} = 0, \tag{10}$$

where $g \equiv |\mathbf{g}|$. Similarly, the radial component of the equation of motion (equation [5]) takes the form

$$\frac{1}{\rho_0} \frac{\partial \delta p}{\partial r} + \frac{g}{c_s^2} \frac{\delta p}{\rho_0} + (N^2 - \omega^2) \xi_r = 0, \tag{11}$$

where the *Brunt-Väisälä frequency*

$$N \equiv g \left(\frac{1}{c_{eq}^2} - \frac{1}{c_s^2} \right)^{\frac{1}{2}}. \tag{12}$$

From equations (10) and (11), it is clear that ξ_r is a function of radius times the spherical harmonic $Y_l^m(\theta, \phi)$, and that the same is true for Δp, $\delta \rho$, and $\Delta \rho$.

To obtain the WKB dispersion relation, we assume that the radial wavelength is much smaller than both r and the density scale height $H \equiv (d \ln \rho_0 / dr)^{-1} = c_{eq}^2 / g \sim c_s^2 / g$. Under these conditions, the perturbations are proportional to $\exp[i \int^r dr' \, k(r')]$, where $|d \ln k / dr| \ll k$. In this short wavelength limit, equations (10) and (11) reduce to

$$ik\xi_r \approx - \left(\frac{1}{c_s^2} - \frac{l(l+1)}{r^2 \omega^2} \right) \frac{\delta p}{\rho_0}, \tag{13}$$

and

$$ik\frac{\delta p}{\rho_0} \approx -(N^2 - \omega^2)\xi_r. \tag{14}$$

When combined, equations (13) and (14) yield the WKB dispersion relation,

$$\left(N^2 - \omega^2 \right) \left(\frac{l(l+1)}{r^2 \omega^2} - \frac{1}{c_s^2} \right) \approx k^2. \tag{15}$$

In the fluid core of a neutron star, $0 < c_s - c_{eq} \ll c_{eq} \sim c_s$, so $N \ll g/c_s \ll c_s k$. This inequality implies that the dispersion relation has two well-separated branches. On the higher frequency (pressure) p-mode branch

$$\omega^2 \approx \left[(kr)^2 + l(l+1) \right] \left(\frac{c_s}{r} \right)^2, \tag{16}$$

whereas on the lower frequency (gravity) g-mode branch

$$\omega^2 \approx \frac{l(l+1)}{(kr)^2 + l(l+1)} N^2. \tag{17}$$

Stable g-modes exist whenever $N^2 > 0$ (i.e. $(\partial p/\partial \rho)_{adiabatic} > (\partial p/\partial \rho)_{equilibrium}$) in some region of the star.

3. G-MODES IN NEUTRON STAR CORES

3.1. Derivation of the Brunt-Väisälä Frequency

Neutron star cores are believed to contain a fluid mixture of several species of particles. At nuclear density ($\rho_{nuc} = 2.8 \times 10^{14} \text{g cm}^{-3}$), the only particles present are neutrons, protons, and electrons. For simplicity, we will assume that no other particles exist in the core, although additional particle species appear at only slightly higher densities (Pandharipande 1971; see Lattimer et al. 1991 for more recent references).

Because of the high density, small fractional differences between the number densities of protons and electrons create huge electric fields that quickly restore equilibrium. Thus, we can safely use a single variable, n_c, to denote the number densities of both charged particle species. In this sub-section, we follow Shapiro and Teukolsky (1983) in deriving a simplified expression for the ratio $x \equiv n_c/n_n$, where n_n is the number density of neutrons, by neglecting all interactions among particles. Then, we show that its density dependence gives rise to a non-zero Brunt-Väisälä frequency and hence to stable stratification.

The equilibrium value of x is determined by the condition of chemical potential equilibrium for neutron beta decay, $n \longrightarrow p + e^- + \bar{\nu}_e$, and its inverse reaction, $p + e^- \longrightarrow n + \nu_e$.[2] Since neutrinos and antineutrinos escape from the star their chemical potential vanishes, and the equilibrium condition takes the form

$$\mu_n = \mu_p + \mu_e, \tag{18}$$

where μ_n, μ_p, and μ_e are the internal chemical potentials of the three species

---

[2] Neutron star matter is expected to be close to chemical equilibrium since the stars are born hot.

of massive particles. Under typical conditions, neutrons contribute most of the density, and each species of massive particle is highly degenerate.

The neutrons and protons are (approximately) nonrelativistic, so their Fermi energies (not including the rest-mass energy $m_N c^2$) are given by

$$E_{Fi} \approx \frac{\hbar^2}{2m_N}(3\pi^2 n_i)^{\frac{2}{3}}, \tag{19}$$

where m_N is the nucleon mass (approximately equal for protons and neutrons) and $i = n, p$ labels the particle species. Taking $n_n \approx \rho/m_N$, we find $E_{Fn} \approx 10^{-4}(\rho/\rho_{nuc})^{2/3}$erg $\approx 60(\rho/\rho_{nuc})^{2/3}$MeV. The electrons are extremely relativistic, so their Fermi energy is

$$E_{Fe} = \hbar c(3\pi^2 n_c)^{\frac{1}{3}}. \tag{20}$$

If interactions among particles and finite-temperature effects are neglected, the chemical potentials can be written as

$$
\begin{aligned}
\mu_n &\approx m_N c^2 + E_{Fn}, \\
\mu_p &\approx m_N c^2 + E_{Fp}, \\
\mu_e &\approx E_{Fe}.
\end{aligned}
\tag{21}
$$

Since $n_c \ll n_n$, and therefore $E_{Fp} \ll E_{Fn}$, the equilibrium condition (equation [18]) reduces to

$$E_{Fe} \approx E_{Fn}. \tag{22}$$

Thus, the equilibrium density ratio

$$x = \frac{n_c}{n_n} \approx \left(\frac{\hbar}{2m_N c}\right)^3 3\pi^2 n_n \approx 6 \times 10^{-3}\frac{\rho}{\rho_{nuc}}. \tag{23}$$

In an adiabatic perturbation the composition remains unchanged, so

$$\left(\frac{\partial n_c}{\partial n_n}\right)_{\text{adiabatic}} = \frac{n_c}{n_n}, \tag{24}$$

whereas, since $n_c \propto n_n^2$ in chemical equilibrium,

$$\left(\frac{\partial n_c}{\partial n_n}\right)_{\text{equilibrium}} = 2\frac{n_c}{n_n}. \tag{25}$$

The pressure and mass density of the fluid, neglecting the small contributions of the protons in the first case, and of the electrons in the second, are

$$p = \frac{2}{5}n_n E_{Fn} + \frac{1}{4}n_c E_{Fe}, \tag{26}$$

and

$$\rho \approx m_N(n_n + n_c). \tag{27}$$

To linear order in the density ratio x,

$$c_s^2 = \left(\frac{\partial p}{\partial \rho}\right)_{\text{adiabatic}} \approx \frac{2}{3}\frac{E_{Fn}}{m_N}\left(1 - \frac{1}{2}x\right) \approx \frac{5}{3}\frac{p}{\rho}\left(1 - \frac{1}{8}x\right), \tag{28}$$

and

$$c_{eq}^2 = \left(\frac{\partial p}{\partial \rho}\right)_{\text{equilibrium}} \approx \frac{2}{3}\frac{E_{Fn}}{m_N}(1 - x) \approx \frac{5}{3}\frac{p}{\rho}\left(1 - \frac{5}{8}x\right). \tag{29}$$

Equations (28) and (29) show that the equilibrium composition gradient stably stratifies the fluid core of a cold neutron star. A piece of matter raised above (lowered below) its equilibrium position, slowly enough so that its pressure can adjust to that of its surroundings, but quickly enough to freeze its chemical composition, is denser (less dense) than the surrounding matter. Thus, the buoyancy force opposes the displacement.

The Brunt-Väisälä frequency (equation [12]) becomes

$$N \approx \left(\frac{x}{2}\right)^{\frac{1}{2}} \frac{g}{c_{eq}} = \left(\frac{x}{2}\frac{g}{H}\right)^{\frac{1}{2}} \sim 500\mathrm{s}^{-1} \tag{30}$$

for typical neutron star parameters ($g \sim 10^{14}\mathrm{cms}^{-2}$, $H \sim 10\mathrm{km}$, and $\rho \sim \rho_{nuc}$). The oscillation periods of the core g-modes range upward from $P_{min} \sim 2\pi/N \sim$ 10ms. They are of the same order of magnitude as the periods of the crustal discontinuity modes found by Finn (1987), and significantly shorter than the periods of the thermal g-modes computed by McDermott et al. (1983).

We have implicitly assumed that neutrons and charged particles will move together on all timescales comparable to the oscillation periods. This is clearly true if the neutrons are "normal" (not superfluid). In this case, binary collisions between neutrons and protons (or between neutrons and electrons if the protons are superconducting) effectively bind the neutrons and charged particles together on extremely short timescales (see, e. g., Yakovlev and Shalybkov 1990 for the numbers). If the neutrons are superfluid, relative motions between neutrons and charged particles may occur (Epstein 1988, Mendell 1991a). Nevertheless, the motions of superfluid neutrons and superconducting protons are not independent of each other, so the core g-modes would still exist, and would have periods similar to those computed here.

3.2. Damping Mechanisms

Three damping mechanisms for g-modes come to mind. They are: the *relaxation toward chemical equilibrium* of the oscillating fluid, *viscous* damping, and damping due to the emission of *gravitational waves*. These three mechanisms are evaluated, in order, below. Afterwards, we briefly discuss the mechanism of *mutual friction* between two superfluid species (neutrons and protons), recently suggested by Mendell (1991b).

As the core fluid oscillates at fixed chemical composition, the instantaneous

equilibrium composition also oscillates. Thus, the oscillating fluid is out of chemical equilibrium. Under nonequilibrium conditions, the net rate of direct plus inverse beta decays tends to relax the composition back toward equilibrium. The relaxation weakens the restoring force acting on displaced fluid elements, thus damping the oscillation[3]. It is not difficult to show that the damping timescale is comparable to the characteristic relaxation timescale.

The equilibration timescale, expressed in terms of the net beta reaction rate per unit volume, $\delta\Gamma \equiv \Gamma(p + e^- \to n + \nu_e) - \Gamma(n \to p + e^- + \bar{\nu}_e)$, reads

$$\tau_{chem} \sim -\frac{\delta n_n}{\delta\Gamma} \sim \frac{\delta n_c}{\delta\Gamma}, \tag{31}$$

where δn_n and δn_c are the amounts by which the number densities of neutrons and charged particles differ from their equilibrium values. For reactions at constant density, $\delta n_c = -\delta n_n$. Otherwise (say, at constant pressure), δn_c and $-\delta n_n$ differ by a factor of order unity.

The deviation from chemical equilibrium is conveniently characterized by the chemical potential difference, $\delta\mu \equiv \mu_p + \mu_e - \mu_n$, which can be estimated as

$$\delta\mu = \delta E_{Fp} + \delta E_{Fe} - \delta E_{Fn} \approx \delta E_{Fe} \approx \frac{1}{3} E_{Fn} \frac{\delta n_c}{n_c}, \tag{32}$$

since $|\delta E_{Fp}| \ll |\delta E_{Fn}| \ll |\delta E_{Fe}|$, and $E_{Fe} \approx E_{Fn}$.

If both neutrons and protons are normal (not superfluid), and $|\delta\mu| \ll kT$, the differential reaction rate is

$$\delta\Gamma = \lambda\delta\mu, \tag{33}$$

where λ is a temperature-dependent proportionality constant that characterizes the reaction speed.

---

[3]The energy lost by the oscillation mode is emitted in the form of neutrinos.

If, as it has been believed until recently, only the modified URCA reactions can operate (Chiu and Salpeter 1964), this parameter takes the value

$$\lambda \approx 5 \times 10^{33} T_9^6 \left(\frac{\rho}{\rho_{nuc}} \right)^{\frac{2}{3}} \text{erg}^{-1} \text{cm}^{-3} \text{s}^{-1} \tag{34}$$

(Sawyer 1989)[4], where T_9 is the temperature in units of 10^9K.

Substitution of equations (32)-(34) into equation (31) yields the *relaxation time toward chemical equilibrium*

$$\tau_{chem} \sim \frac{3n_c}{\lambda E_{Fn}} \sim \frac{0.2}{T_9^6} \left(\frac{\rho_{nuc}}{\rho} \right)^{\frac{2}{3}} \text{yr}, \tag{35}$$

which is the approximate timescale for g-mode damping due to neutrino emission.[5]

Incidentally, equation (35) justifies our use of an adiabatic equation of state in the derivation of the wave equation since for stars with core temperatures $T \ll 3 \times 10^{10}$K the damping timescale is much longer than the periods of the lowest-order g-modes ($\tau_{chem}/P \sim 10^9 T_9^{-6}$).

If the regular URCA reactions can operate, as has been suggested by Lattimer, Pethick, Prakash, and Haensel (1991), λ is increased by a factor $\sim 5 \times 10^5 T_9^{-2}$, τ_{chem} is *decreased* by the same factor, and the temperature below which the g-modes are weakly damped is reduced to $\sim 3 \times 10^9$K.

In all likelihood, superfluidity of one or more particle species would *reduce* the reaction rates, thus increasing the damping time.

The *viscous damping timescale* is set by the rate at which momentum diffuses across a wavelength. We write

$$\tau_{visc} \sim \frac{L^2}{\nu}, \tag{36}$$

---

[4]For convenience, our sign convention for λ is opposite to Sawyer's.

[5]This damping time is related to the cooling time due to thermal neutrino emission by a factor of order n_c/n_n.

where L is a characteristic wavelength of the oscillation mode and ν is the kinematic viscosity. Using the formulae of Cutler and Lindblom (1987) for the viscosity, and defining $L_6 = L/(10^6\,\text{cm})$, we obtain

$$\tau_{visc} \sim 80 L_6^2 T_9^2 \left(\frac{\rho_{nuc}}{\rho}\right)^{\frac{5}{4}} \text{yr} \tag{37}$$

if the material in the star is "normal," and

$$\tau_{visc} \sim 20 L_6^2 T_9^2 \left(\frac{\rho_{nuc}}{\rho}\right) \text{yr} \tag{38}$$

if both neutrons and protons are superfluid. In the former case, ν is primarily due to the neutrons, and in the latter, it is almost completely due to the electrons.

The evaluation of the *damping timescale due to emission of gravitational radiation* is more subtle. Below, we give an approximate lower bound, which is later checked by numerical evaluation of the damping time for specific modes of our model stars.

The *e*-folding time for the oscillation amplitude can be written as

$$t_g = \frac{2E}{P_g}, \tag{39}$$

where E is the total energy stored in the oscillations, and P_g is the power released by emission of gravitational waves.

In order to estimate this timescale, it is convenient to introduce the variables η_r, $\eta_\perp$, and ρ_1 defined by the relations

$$\begin{aligned}
\xi_r(r,\theta,\phi,t) &= \eta_r(r)Y_l^m(\theta,\phi)e^{-i\omega t}, \\
\frac{\delta p(r,\theta,\phi,t)}{\omega^2\rho_0 r} &= \eta_\perp(r)Y_l^m(\theta,\phi)e^{-i\omega t}, \\
\delta\rho(r,\theta,\phi,t) &= \rho_1 Y_l^m(\theta,\phi)e^{-i\omega t}.
\end{aligned} \tag{40}$$

Note that η_r and $\eta_\perp$ are related to the radial and horizontal components of the displacement, ξ_r and $\xi_\perp$, respectively. For the simple case of azimuthal symmetry ($m = 0$), $\xi_r = \eta_r(r)P_l(\cos\theta)$ and $\xi_\theta = \eta_\perp(r)dP_l(\cos\theta)/d\theta$, where $P_l(x)$ denotes the l-th Legendre polynomial.

In terms of these variables, the mode energy can be written as

$$E = \frac{\omega^2}{2} \int_0^R \rho_0 r^2 [\eta_r^2 + l(l+1)\eta_\perp^2]dr, \tag{41}$$

and the radiated power (in the weak-gravity approximation) is

$$P_g = \frac{G}{8\pi c^{2l+1}} \frac{(l+1)(l+2)}{(l-1)l} \left[\frac{4\pi\omega^{l+1}}{(2l+1)!!} \int_0^R \rho_1 r^{l+2} dr \right]^2 \tag{42}$$

(Thorne 1969b), where $(2l+1)!! \equiv (2l+1) \times (2l-1) \times (2l-3) \times \cdots \times 3 \times 1$.

Using the relations in §2, it is possible to express the Eulerian density perturbation in terms of the two components of the displacement vector

$$\frac{\rho_1}{\rho_0} = \frac{N^2}{g}\eta_r + \frac{\omega^2 r}{c_s^2}\eta_\perp = \frac{x}{2H}(\eta_r + \beta\eta_\perp), \tag{43}$$

where $\beta \equiv (rg/c_s^2)(\omega/N)^2$. Thus,

$$P_g = \frac{G}{8\pi c^{2l+1}} \frac{(l+1)(l+2)}{(l-1)l} \left[\frac{4\pi\omega^{l+1}}{(2l+1)!!} \int_0^R \rho_0 \frac{x}{2H}(\eta_r + \beta\eta_\perp) r^{l+2} dr \right]^2. \tag{44}$$

For g-modes, β is of order unity or less everywhere in the core of the neutron star. Hence, an order-of-magnitude estimate of their damping time due to emission of gravitational waves (39) is

$$\tau_g^g \sim 8[(2l+1)!!]^2 \frac{(l-1)l}{(l+1)(l+2)} \frac{c^{2l+1}}{GMR^{2l-2}x^2\omega^{2l}}$$

$$\sim 10^2 \left(\frac{M}{M_\odot}\right)^{-1} \left(\frac{R}{10\text{km}}\right)^{-2} \left(\frac{x}{0.01}\right)^2 \left(\frac{P}{10\text{ms}}\right)^4 \text{yr}, \tag{45}$$

where $l = 2$ in the numerical evaluation. For comparison, for quadrupole f- and p-modes (for which $\beta \sim x^{-1}$ rather than unity, so that $\rho_1/\rho_0 \sim \eta_\perp/H$), a similar estimate yields

$$\tau_g^f \sim 0.2 \left(\frac{M}{M_\odot}\right)^{-1} \left(\frac{R}{10\text{km}}\right)^{-2} \left(\frac{P}{0.4\text{ms}}\right)^4 \text{s}. \tag{46}$$

Equation (46) provides an adequate estimate of the damping times of f-modes. However, equation (45) should be regarded as a lower bound, because cancellation in the integral in equation (44) due to nodes in the eigenfunctions is not accounted for in its derivation. In both cases, the damping times of higher-order (p- and g-)modes are underestimated by progressively larger factors. These expectations are confirmed by the results of numerical computations of the damping times reported in §5.

A comparison of equations (35) and (38) indicates that viscous damping dominates over neutrino emission in stars whose core temperatures are lower than $\sim 6 \times 10^8 L_6^{-1/4}$ K if only modified URCA reactions occur, and $\sim 5 \times 10^7 L_6^{-1/3}$ K if regular URCA reactions can operate. Damping due to emission of gravitational radiation is not likely ever to be important for g-modes, in sharp contrast to f- and p-modes (see also McDermott et al. 1988 and Cutler, Lindblom, and Splinter 1990).

Mendell (1991b) has pointed out that *mutual friction* might damp the oscillations of rotating neutron stars if at least two particle species (e. g., neutrons and protons) are superfluid. Using Mendell's results, we find that the damping time due to mutual friction is always shorter than $10^5(\rho_{nuc}/\rho)(P_{rot}/0.1\text{s})$s (where P_{rot} is the stellar rotation period), making it the most important damping mechanism for g-modes in the interesting temperature range $10^7 L_6^{-1}(P_{rot}/0.1\text{s})^{1/2} < T/\text{K} < 2 \times 10^9(P_{rot}/0.1\text{s})^{-1/6}$.

4. NUMERICAL CALCULATIONS AND RESULTS

In order to advance our understanding of neutron star g-modes, we compute eigenvalues and eigenfunctions for the lowest few quadrupole g-modes of two model neutron stars.

4.1. Differential Equations and Boundary Conditions

With the change of variables given in equations (40), equations (10) and (11) are rewritten as

$$\frac{d\eta_r}{dr} = -\left(2 - \frac{gr}{c_s^2}\right)\frac{\eta_r}{r} + \left(l(l+1) - \frac{\omega^2 r^2}{c_s^2}\right)\frac{\eta_\perp}{r} \tag{47}$$

and

$$\frac{d\eta_\perp}{dr} = \left(1 - \frac{N^2}{\omega^2}\right)\frac{\eta_r}{r} - \left(1 - \frac{N^2 r}{g}\right)\frac{\eta_\perp}{r}. \tag{48}$$

The origin is a singular point of these equations; as $r \to 0$ each of the four coefficients multiplying η_r and $\eta_\perp$ on the right-hand sides of these equations diverges as r^{-1}. The physically meaningful solutions are regular at $r = 0$ and have the form

$$\eta_r \approx l\eta_\perp \sim r^{l-1} \tag{49}$$

as $r \to 0$.

The pressure (but not necessarily the density) must vanish at the surface ($r = R$) of an unperturbed neutron star. Perturbations must satisfy the boundary condition that the Lagrangian pressure perturbation vanish, $\Delta p = 0$. Written in terms of the variables η_r and $\eta_\perp$, this boundary condition becomes

$$(\omega^2 r\eta_\perp - g\eta_r)\rho_0 = 0 \qquad \text{at} \quad r = R. \tag{50}$$

In our numerical calculations, equations (47) and (48) are integrated, for two closely spaced trial values of ω, from a point near to $r = 0$, where $\eta_r = l\eta_\perp$ is imposed, out to $r = R$, where the left-hand side of equation (50) is evaluated. Then, a new trial value for ω is chosen by interpolation to reduce this value, and the procedure is iterated until an accurate eigenvalue is obtained.

4.2. Stellar equilibrium models

We compute g-modes for two neutron star models, both based on the Pandharipande (1971) equation of state that includes hyperonic matter (model B in the classification of Arnett and Bowers 1974), the same as used by Finn (1987). Since only a table containing the values of the density ρ and pressure p at a relatively small number of discrete points[6] is available to us, we obtain the intermediate values necessary for the construction of the stellar model by approximating the equation of state in each interval between tabulated points by a polytrope, $p = k\rho^{1+1/n}$, with the constants k and n determined by the values of ρ and p at the endpoints. This interpolation procedure allows us to calculate the important derivative

$$c_{eq}^2 \equiv \left(\frac{\partial p}{\partial \rho}\right)_{eq} = \left(1 + \frac{1}{n}\right)\frac{p}{\rho} \tag{51}$$

without a numerical differentiation.

The models are constructed by integrating the *Newtonian* equations of stellar structure outward from the center of the star, in this way determining ρ, p, c_{eq}^2, and the local gravitational acceleration g as functions of the radial coordinate r. We use Newtonian equations for consistency with the equations for the modes, which are much more easily written and understood in their Newtonian form. At any rate, larger uncertainties are introduced in our calculation by the lack of knowledge about the correct equation of state and the composition of the star than by this simplification.

---

[6]The ratio between the densities at consecutive points in the important range $5 \times 10^{14} < \rho < 2 \times 10^{15}$g cm^{-3} fluctuates between 1.2 and 1.4.

Model I, with central density $\rho_c = 0.8 \times 10^{15} \text{g cm}^{-3}$, radius $R = 10.98$ km, and total mass $M = 0.581 M_\odot$, is similar to Finn's "fiducial" model. *Model II* represents a more standard neutron star, and has central density $\rho_c = 1.6 \times 10^{15} \text{g cm}^{-3}$, radius $R = 10.94$ km, and total mass $M = 1.405 M_\odot$.

4.3. Models for the Brunt-Väisälä Frequency

Unfortunately, currently available neutron star models do not provide enough information for us to extract the speed of sound, c_s, and the Brunt-Väisälä frequency, N, directly from them. Our procedure is to estimate N taking into account the *composition discontinuities in the crust* (Finn 1987) and the *continuous composition gradient in the core* and then to evaluate c_s from equation (12).

In the upper crust (ρ less than neutron drip density), where the density discontinuities occur, relativistically degenerate electrons dominate the pressure, and

$$p = \frac{1}{4} n_e E_{Fe} = \frac{1}{4} (\hbar c)^{\frac{1}{3}} \left(\frac{\rho}{\alpha m_N} \right)^{\frac{4}{3}}, \tag{52}$$

where m_N is the mass of a nucleon, and α is the number of nucleons per electron. In an adiabatic perturbation, α is constant, so

$$\frac{1}{c_s^2} \equiv \left(\frac{\partial \rho}{\partial p} \right)_{\text{adiabatic}} = \frac{3\rho}{4p}, \tag{53}$$

but, since the equilibrium value of α varies with pressure,

$$\frac{1}{c_{eq}^2} \equiv \left(\frac{\partial \rho}{\partial p} \right)_{\text{equilibrium}} = \frac{3\rho}{4p} \left(1 + \frac{4}{3} \frac{d \ln \alpha}{d \ln p} \right). \tag{54}$$

Thus, from equation (12), we obtain

$$N_{crust}^2 = \left(\frac{4}{3} \frac{d \ln \alpha}{d \ln p} \right) \frac{g^2}{c_s^2} \approx \left(\frac{4}{3} \frac{d \ln \alpha}{d \ln p} \right) \frac{g^2}{c_{eq}^2}. \tag{55}$$

In Finn's model, $\alpha(p)$ changes in $D(= 11)$ discrete steps:

$$\frac{d\ln\alpha}{d\ln p} = \sum_{i=1}^{D} \Lambda_i \delta\left(\ln\frac{p}{p_i}\right).\tag{56}$$

Here, $\delta(x)$ is the Dirac delta function, p_i is the pressure at which the i-th discontinuity occurs, and Λ_i is the difference between the values of $\ln\alpha$ on opposite sides of the discontinuity, or equivalently, the fractional jump in the density as shown in Finn's Table 2. Since our numerical integrator cannot handle delta functions, we make a continuous approximation to equation (56)[7]:

$$\frac{d\ln\alpha}{d\ln p} \approx \sum_{i=1}^{D} \frac{\Lambda_i}{(2\pi\sigma^2)^{\frac{1}{2}}} \exp\left[-\frac{1}{2\sigma^2}\left(\ln\frac{p}{p_i}\right)^2\right].\tag{57}$$

Our choice of $\sigma = 0.2$ compromises the convenience of a smooth function against the need to accurately model the discontinuities. Also, we do not include Finn's outermost discontinuity; it is too close to the surface to be properly taken into account by our computer code, and it appears not to affect Finn's lowest order modes.

The contribution to N^2 from the continuous chemical gradient in the core follows from equations (30) and (23):

$$N^2_{core} \approx 3 \times 10^{-3} \left(\frac{\rho}{\rho_{nuc}}\right) \frac{g^2}{c^2_{eq}}.\tag{58}$$

To account for the stratification in both regions, we write the Brunt-Väisälä frequency as

$$N^2 = N^2_{crust} + N^2_{core}.\tag{59}$$

---

[7]This computation can be done more elegantly by imposing "jump" conditions at the discontinuities (Finn 1987, McDermott 1990), but this is not convenient for us.

4.4. Damping Time due to Emission of Gravitational Radiation

We evaluate the mode damping times due to gravitational radiation reaction numerically from[8]

$$\tau_g = \frac{c^{2l+1}}{2\pi G\omega^{2l}} \frac{(l-1)[(2l+1)!!]^2}{l(l+1)(l+2)} \frac{\int_0^R \rho_0 r^2 [\eta_r^2 + l(l+1)\eta_\perp^2]dr}{\left(\int_0^R \rho_0 r^{l+1} [\eta_r + (l+1)\eta_\perp]dr\right)^2} \quad (60)$$

(see, e. g., Balbinski and Schutz 1982). Substantial cancellation occurs in the denominator of this expression (cf. equation [45]). The integral

$$\int_0^R \rho_0 r^{l+1} [\eta_r + (l+1)\eta_\perp]dr$$

is smaller by a factor $\sim x$ than both $|\int_0^R \rho_0 r^{l+1} \eta_r dr|$ and $(l+1)|\int_0^R \rho_0 r^{l+1} \eta_\perp dr|$. Thus, a naive order-of-magnitude estimate based on equation (60) underestimates the true damping time by at least a factor $\sim x^2 \sim 10^{-4}$. Furthermore, numerical evaluation of the damping time from equation (60) requires that the functions $\eta_r(r)$ and $\eta_\perp(r)$ be known accurately enough to allow such a subtle cancellation.

5. RESULTS

5.1. The "fiducial" models

For Model I with $N = N_{crust}$ (see §4.3), the input physics and model parameters are similar to those used by Finn (1987)[9]. As can be seen by comparing Fig. 1 with Finn's Fig. 5, our g-modes are qualitatively very similar to his, giving us confidence that the smoothing of the discontinuities (see equation [57]) in our calculation of the Brunt-Väisälä frequency does not introduce substantial errors. The periods do not agree exactly, since our use of Newtonian rather than relativistic physics introduces errors of order $GM/Rc^2 \sim 8\%$. Taking this into account, the

---

[8]This expression can be obtained by using the continuity equation, $\delta\rho = -\nabla \cdot (\rho_0\xi)$, to integrate equation (42) by parts, and replacing the result and equation (41) in (39).

[9]Finn's model star has the parameters $M = 0.522M_\odot$, $\rho_c = 10^{15}\text{gcm}^{-3}$, and $R = 9.83\text{km}$.

agreement is satisfactory (see Table 1). Our damping times are smaller than Finn's by factors ~ 10. The Newtonian approximation and the strong dependence of τ_g on stellar radius and mode period (see the analytical estimates by Finn 1987) may account for part of this discrepancy. Similar discrepancies between relativistic and quasi-Newtonian estimates of the damping time of quadrupole f-modes due to gravitational radiation reaction forces have been reported by Balbinski and Schutz (1982).

An additional simplification which changes our results compared to Finn's is our use of the *Cowling approximation*. The extent to which this approximation affects f-mode periods can be appreciated by considering a *Newtonian, incompressible, uniform density, fluid star*. For this simple model, analytical calculations give the ratio

$$\frac{P(\text{Cowling approximation})}{P(\text{exact})} = \left(1 - \frac{3}{2l+1}\right)^{\frac{1}{2}} \approx 0.63 \qquad \text{for} \quad l = 2. \qquad (61)$$

Since neutron stars are centrally condensed, this ratio is closer to unity for them. The Cowling approximation is more accurate for the g-modes than it is for the f-mode, because radial nodes weaken the perturbations of the gravitational field.

McDermott et al. (1988) used Newtonian equations of motion and the Cowling approximation to calculate periods of oscillation modes of a relativistic neutron star model very similar to Finn's ($M = 0.503 M_\odot$, $\rho_c = 9.44 \times 10^{14} \text{gcm}^{-3}$, $R = 10.1 \text{km}$) and obtained $P = 0.398 \text{ms}$ for the quadrupole f-mode, very close to our value.

The periods of the crustal discontinuity modes change very little (by a few percent upward) as the stellar mass is increased by a factor ~ 2.4 (see Table 1).

The periods of the core g-modes (see Table 2) agree well with the estimate given in §3.1, and are similar to those of the crustal discontinuity modes. Comparing the results for Models I and II, one sees that these periods decrease strongly with increasing stellar mass.

The damping times of the core modes due to the emission of gravitational radiation exceed the estimate of equation (45) by a large factor ($\sim 10^2$ for g_1^c and more than 10^3 for the higher-order modes in both models), showing that this is an extremely inefficient damping mechanism for g-modes.

A comparison of Figs. 2 and 3 reveals that the oscillation energy of the core g-modes is distributed throughout the inner 90% in radius of the star, whereas discontinuity modes are concentrated in the outer crust, i. e. the outermost 10% in radius.

When both contributions to the stratification are taken into account, the crust and core modes retain their separate identities, as Figs. 4 and 5 show. The core and crust act as a pair of weakly coupled resonant cavities, with modes in one cavity being little affected by the existence of the other cavity. Fractional period changes due to the presence of the second cavity are smaller than 10^{-3} for all modes listed. The gravitational radiation damping times of the core modes are also changed very little ($\sim$ few percent) by the existence of stratification in the crust, but the damping times of some crustal modes are decreased significantly (up to factors $\sim 10^2$) by the core stratification. This latter result follows because small motions in the core (whose density is several orders of magnitude higher than that of the outer crust) substantially increase the oscillations of the stellar quadrupole moment.

5.2. Modifications and Further Discussion

Possibly the most important source of errors in the present determination of the core g-modes is our neglect of the *strong interactions among nucleons*, which leads us to significantly underestimate the composition ratio, x. A fit to the results obtained by R. Smith (see Table I of Sauls et al., 1982), who took the strong interactions into account, gives

$$x \approx 0.05(\rho/\rho_{nuc})^{0.4}, \tag{62}$$

instead of $x \approx 0.006\rho/\rho_{nuc}$ from our equation (23). Substitution of equation (62) into equation (30) for the Brunt-Väisälä frequency yields periods for the four lowest-order, quadrupolar, core g-modes of Model I that are shorter than our previous results by a factor ~ 2.5. These periods are listed in the column labeled *"Model I-int"* in Table 2. This procedure is not completely consistent, since the strong interactions are neglected in the derivation of equation (30), but it gives an idea of the importance of the approximations made[10].

Throughout this paper, we have taken the neutron stars to be completely fluid. This assumption was also made by Finn (1987), but was criticized by McDermott (1990), who pointed out that the *shear modulus of the crystalline stellar crust* will significantly affect the discontinuity modes. Neutron star models that take into account the finite shear modulus of the crust (but not the stable stratification associated with composition gradients) were studied by McDermott, Hansen, Van Horn, and Buland (1985) and McDermott, Van Horn, and Hansen (1988). These authors find a sequence of shear (s-) modes in the crust and two sequences of interfacial (i-) modes, one trapped at the interface between the upper crust and the fluid ocean above, and the other at the boundary between the lower crust and the fluid core below.

The solid crust with its finite shear modulus modifies both the crustal discontinuity modes and the core g-modes. However, its effect on the core modes should be small. To verify this, we calculate the periods of the f-mode and the first four core g-modes of Model I (with $N = N_{core}$) with the *modified boundary condition* $\eta_r(r_{ccb}) = 0$, where $r_{ccb} = 7.81\,\text{km}$ is the location of the crust-core boundary, taken to be where $\rho = 2.4 \times 10^{14}\text{g cm}^{-3}$. This is equivalent to setting both the shear modulus and the mass of the crust equal to infinity. However, the g-mode periods (listed in the column labeled *"Model I-rc"* in Table 1) are longer by only 7 to

---

[10]The difference between the real value and our results for non-interacting particles is probably somewhat less striking than this comparison would suggest, because the dependence of x on ρ is less strong in equation (62) than in equation (23).

15% than those of the "fiducial" Model I.[11] The f-mode period is more strongly changed (and in the opposite direction). However, in a more realistic calculation with a crust of finite shear modulus, McDermott et al. (1988) find that the f-mode period is almost identical to its value for a completely fluid model.

We have been assuming that the entire neutron star (except the outer crust) is composed of neutrons, protons and electrons. However, *additional species of particles* (muons, kaons, hyperons, and others) undoubtedly appear at densities only slightly above nuclear density (see, e.g., Lattimer et al. 1991 for references), and these would contribute to the stable stratification of the neutron star core, decreasing the periods of the g-modes. Furthermore, the lower crust is stably stratified by the *density dependent concentration of neutrons*, which contribute an important share of the mass density without adding much to the pressure.

6. CONCLUSIONS

The present work shows that the core of a neutron star is stably stratified, and that it supports a set of core g-modes. These modes have periods ranging upward from a few milliseconds, similar to those of the discontinuity modes identified and investigated by Finn (1987), and considerably shorter than the thermal g-modes studied by McDermott et al. (1983).

It is unfortunate that, to date, no convincing detections of neutron star oscillations have been reported (see McDermott et al. 1988 for references and for a discussion of the possibilities). However, the stable stratification identified here may have other important consequences. For example, it restricts secular motions of matter inside neutron stars, because neutrons and charged particles cannot move together over large radial distances on timescales shorter than those over which weak interactions can maintain chemical equilibrium. How this might impact the

---

[11]The counterintuitive effect of *increasing* the period by *decreasing* the size of the resonant cavity can be understood by a glance at the WKB dispersion relation for g-modes (equation [17]), which shows that the frequency *decreases* with increasing radial wavenumber.

evolution of neutron star magnetic fields will be discussed in a separate paper (Goldreich and Reisenegger, 1992).

ACKNOWLEDGEMENTS

REFERENCES

Arnett, W. D., & Bowers, R. L. 1974, Neutron Star Structure: A Survey (Austin: University of Texas)

Balbinski, E., & Schutz, B. F. 1982, MNRAS 200, 43p

Campolattaro, A., & Thorne, K. S. 1970, ApJ, 159, 847

Chiu, H., & Salpeter, E. E. 1964, Phys. Rev. Lett., 12, 413

Cowling, T. G. 1941, MNRAS, 101, 367

Cox, J. P. 1980, Theory of Stellar Pulsation (Princeton: Princeton University Press)

Cutler, C., & Lindblom, L. 1987, ApJ, 314, 234

Cutler, C., Lindblom, L., & Splinter, R. J. 1990, ApJ, 363, 603

Epstein, R. I. 1988, ApJ, 333, 880

Finn, L. S. 1987, MNRAS, 227, 265

Goldreich, P., & Reisenegger, A. 1992, ApJ, submitted

Ipser, J. R., & Thorne, K. S. 1973, ApJ, 181, 181

Lattimer, J. M., Pethick, C. J., Prakash, M., & Haensel, P. 1991, Phys. Rev. Lett., 66, 2701

McDermott, P. N. 1990, MNRAS, 245, 508

McDermott, P. N., Hansen, C. J., Van Horn, H. M., & Buland, R. 1985, ApJ, 297, L37

McDermott, P. N., Van Horn, H. M., & Hansen, C. J. 1988, ApJ, 325, 725

McDermott, P. N., Van Horn, H. M., & Scholl, J. F. 1983, ApJ, 268, 837

Mendell, G. 1991a, ApJ, 380, 515

Mendell, G. 1991b, ApJ, 380, 530

Pandharipande, V. 1971, Nucl. Phys. A, 178, 123

Price, R., & Thorne, K. S. 1969, ApJ, **155**, 163

Sauls, J. A., Stein, D. L., & Serene, J. W. 1982, Phys. Rev. D, **25**, 967

Sawyer, R. F. 1989, Phys. Rev. D **39**, 3804

Shapiro, S. L., & Teukolsky, S. A. 1983, Black Holes, White Dwarfs, and Neutron
    Stars (New York: Wiley)

Thorne, K. S. 1969a, ApJ, **158**, 1

Thorne, K. S. 1969b, ApJ, **158**, 997

Thorne, K. S., & Campolattaro, A. 1967, ApJ, **149**, 591

Unno, W., Osaki, T., Ando, H., & Shibahashi, H. 1970, Nonradial Oscillations of
    Stars (Tokyo: Tokyo University Press)

Van Horn, H. M. 1980, ApJ, **236**, 899

Yakovlev, D. G. & Shalybkov, D. A. 1990, Sov. Astr. Lett., **16**, 86

Table 1

Crustal Discontinuity Modes

Mode	P [ms] (Finn 1987)	τ_g [s] (Finn 1987)	P [ms] (Model I)	τ_g [s] (Model I)	P [ms] (Model II)	τ_g [s] (Model II)
f	.528	6.49 –01	.397	1.03 –01	.298	1.10 –02
g_1^d	5.13	1.09 +12	5.22	1.60 +11	5.54	2.24 +12
g_2^d	10.5	9.56 +15	10.8	7.84 +14	11.3	2.61 +15
g_3^d	14.2	1.93 +16	14.9	2.72 +15	15.6	4.52 +15
g_4^d	15.3	2.46 +17	16.5	1.84 +16	17.1	1.14 +16

Periods (in ms) and damping times due to emission of gravitational radiation (in s) for the quadrupole ($l = 2$) f-mode and first four g-modes of model neutron stars whose crusts are stably stratified due to composition discontinuities. Shown are the results of Finn (1987) for a relativistic $0.522 M_\odot$ neutron star model, and our results for the Newtonian Models I ($M = 0.581 M_\odot$) and II ($M = 1.405 M_\odot$), in which we took the Brunt-Väisälä frequency to be $N = N_{crust}$ (see equation [55]).

Table 2

Core g-Modes

Mode	P [ms] (Model I)	τ_g [s] (Model I)	P [ms] (Model II)	τ_g [s] (Model II)	P [ms] (Model I-int)	P [ms] (Model I-rc)
f	.397	1.03 −01	.298	1.10 −02	.397	.247
g_1^c	10.8	3.34 +11	4.66	7.30 +08	4.21	12.4
g_2^c	15.0	3.47 +13	7.25	7.15 +10	6.39	16.0
g_3^c	18.8	2.22 +14	10.1	1.47 +12	7.66	21.0
g_4^c	24.3	2.04 +15	12.4	5.33 +12	9.22	26.8

Periods (in ms) and damping times due to emission of gravitational radiation (in s) for the quadrupole ($l = 2$) f-mode and first four g-modes of neutron star models that are stably stratified due to a smooth composition gradient in the stellar core. The first four columns of numbers show results for our Newtonian Models I ($M = 0.581 M_\odot$) and II ($M = 1.405 M_\odot$) with Brunt-Väisälä frequency $N = N_{core}$ (see equation [58]), which are analyzed in §5.1. The last two columns contain results for modified versions of Model I, as discussed in §5.2. In the first case (labeled "Model I-int"), the density ratio x is taken to be as given by equation (62), in order to get an estimate of the effect of the strong interactions among nucleons, and in the second (labeled "Model I-rc"), the crust is taken to be perfectly rigid, i.e. the boundary condition $\xi_r = 0$ is imposed at the crust-core boundary ($r = r_{ccb} = 7.81$km, where $\rho(r_{ccb}) = 2.4 \times 10^{14}$gcm^{-3}).

Fig. 1: The first four (quadrupole) g-modes of our neutron star Model I ($M = 0.581M_\odot$), when only the stable stratification due to the discontinuities in the stellar crust is taken into account ($N = N_{crust}$). The radial displacement is plotted as a function of $\log(1-r/R)$, where R is the radius of the star, for easy comparison with Fig. 5 of Finn (1987). The modes are normalized by the condition $\eta_r(R)/R = 1$.
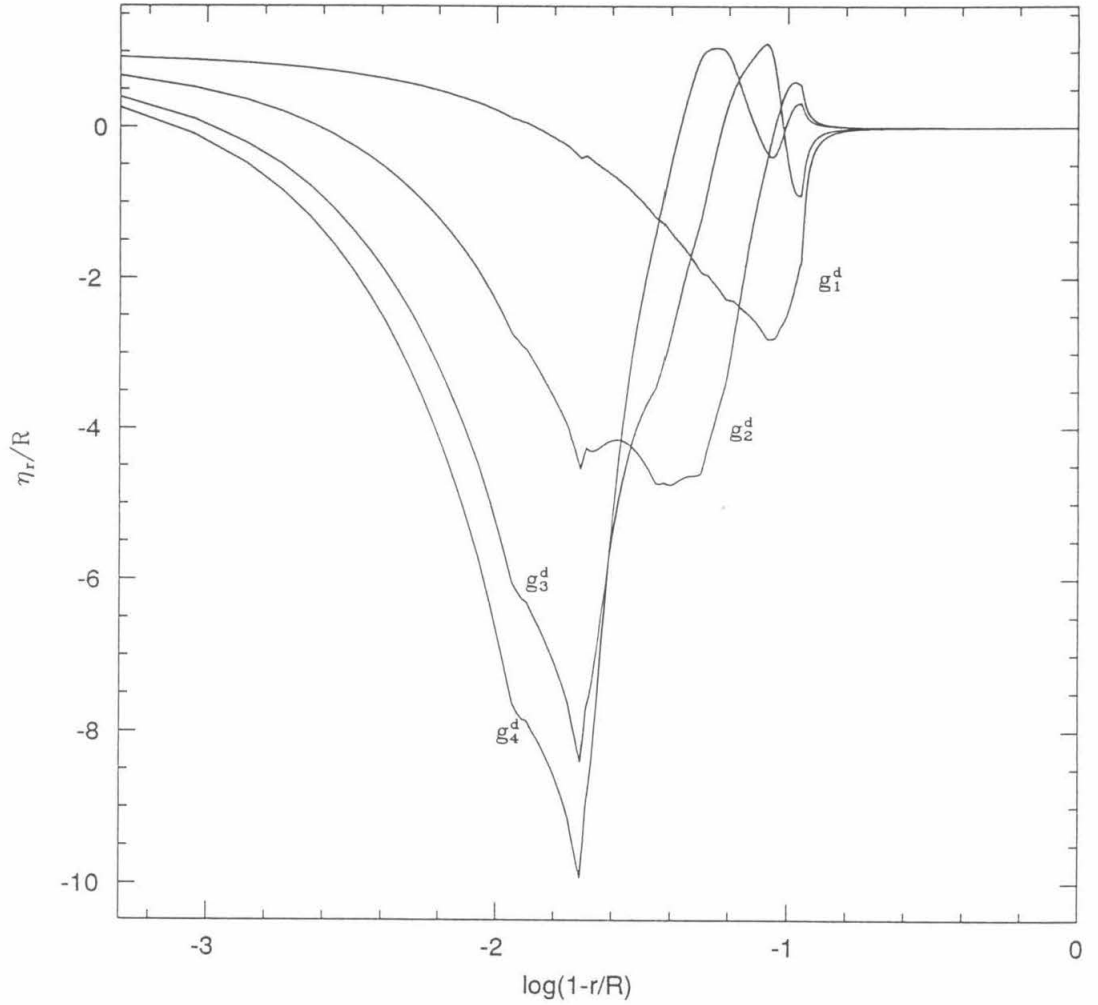
Fig. 2: Oscillation energy per unit radial distance, $\epsilon = (1/2)\omega^2 \rho_0 r^2(\eta_r^2 + l(l+1)\eta_\perp^2)$, as a function of radius for the first two g-modes of our Model I with $N^2 = N_{crust}^2$. The modes are normalized by the condition $\eta_r(R)/R = 1$.
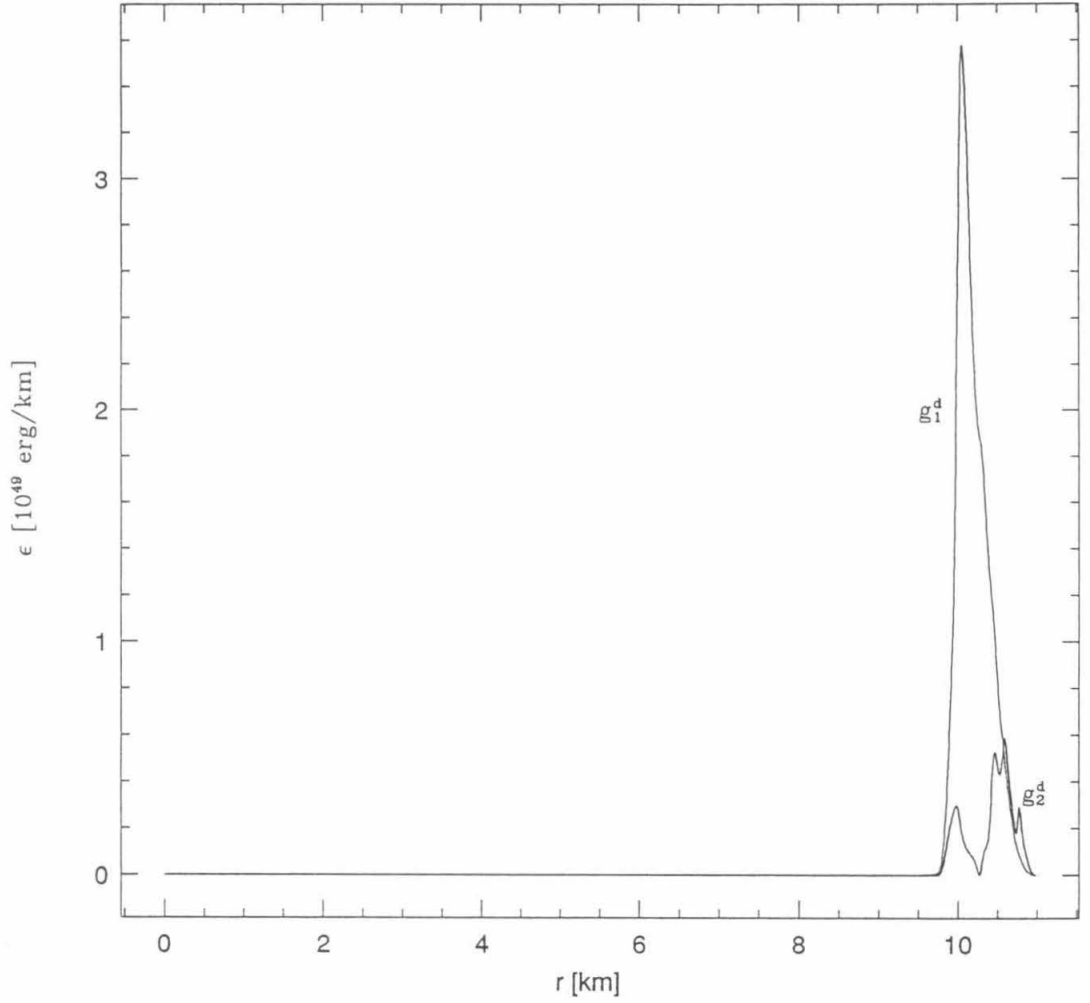
Fig. 3: Oscillation energy per unit radial distance as a function of radius for the first two g-modes of our Model I with $N^2 = N^2_{core}$. The normalization condition is $\eta_r(R)/R = 1$.
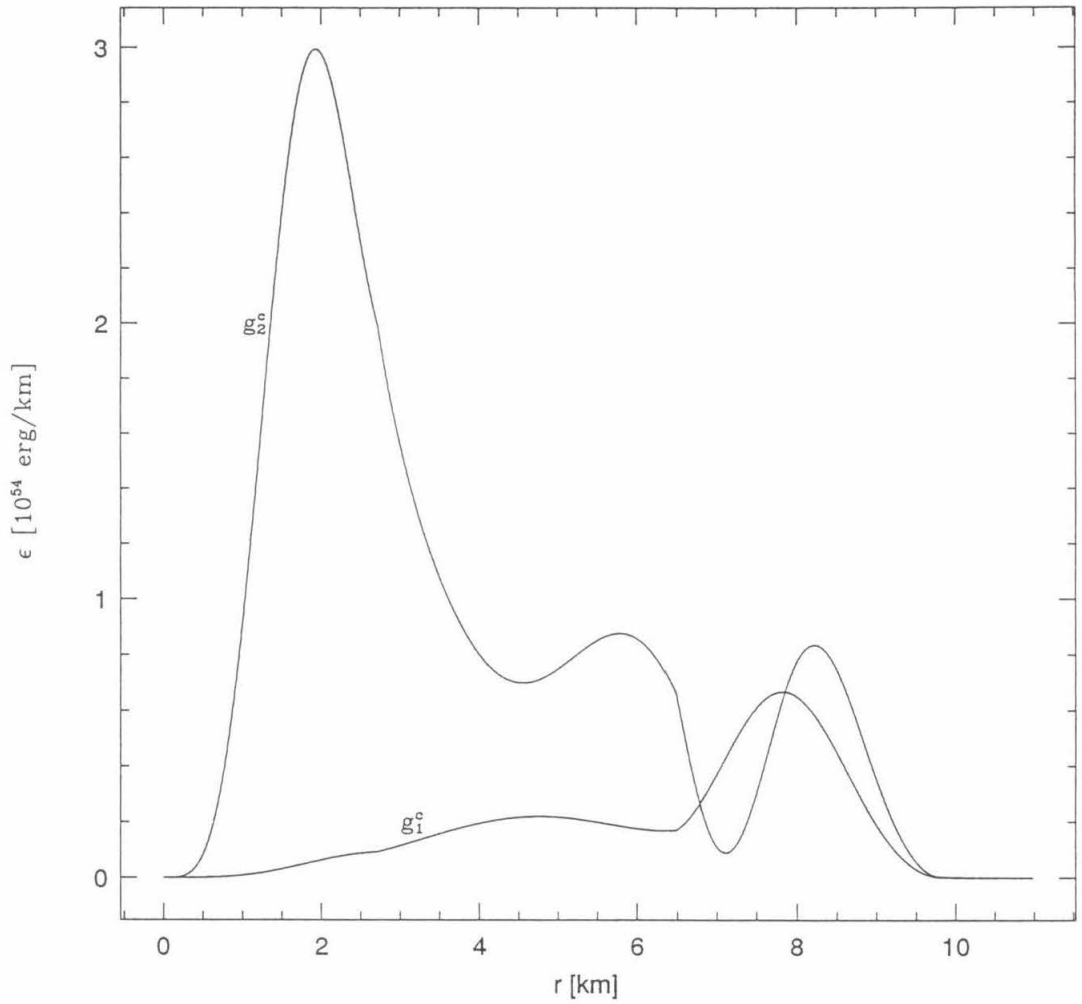
Fig. 4: Oscillation energy per unit radial distance as a function of radius for the first two crustal g-modes of our Model I with $N^2 = N^2_{crust} + N^2_{core}$. Again, the modes are normalized by the condition $\eta_r(R)/R = 1$.
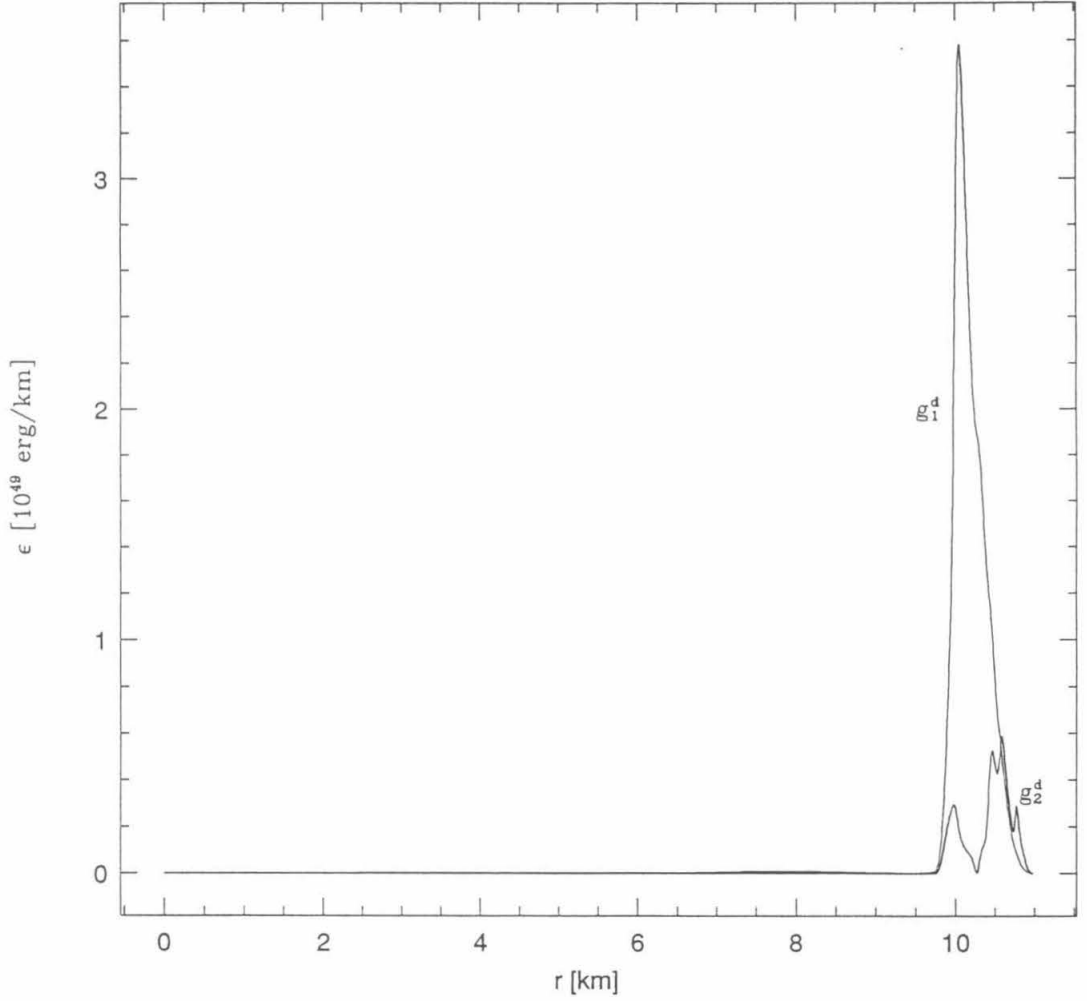
Fig. 5: Oscillation energy per unit radial distance as a function of radius for the first two core g-modes of our Model I with $N^2 = N^2_{crust} + N^2_{core}$. Again, the normalization condition is $\eta_r(R)/R = 1$.
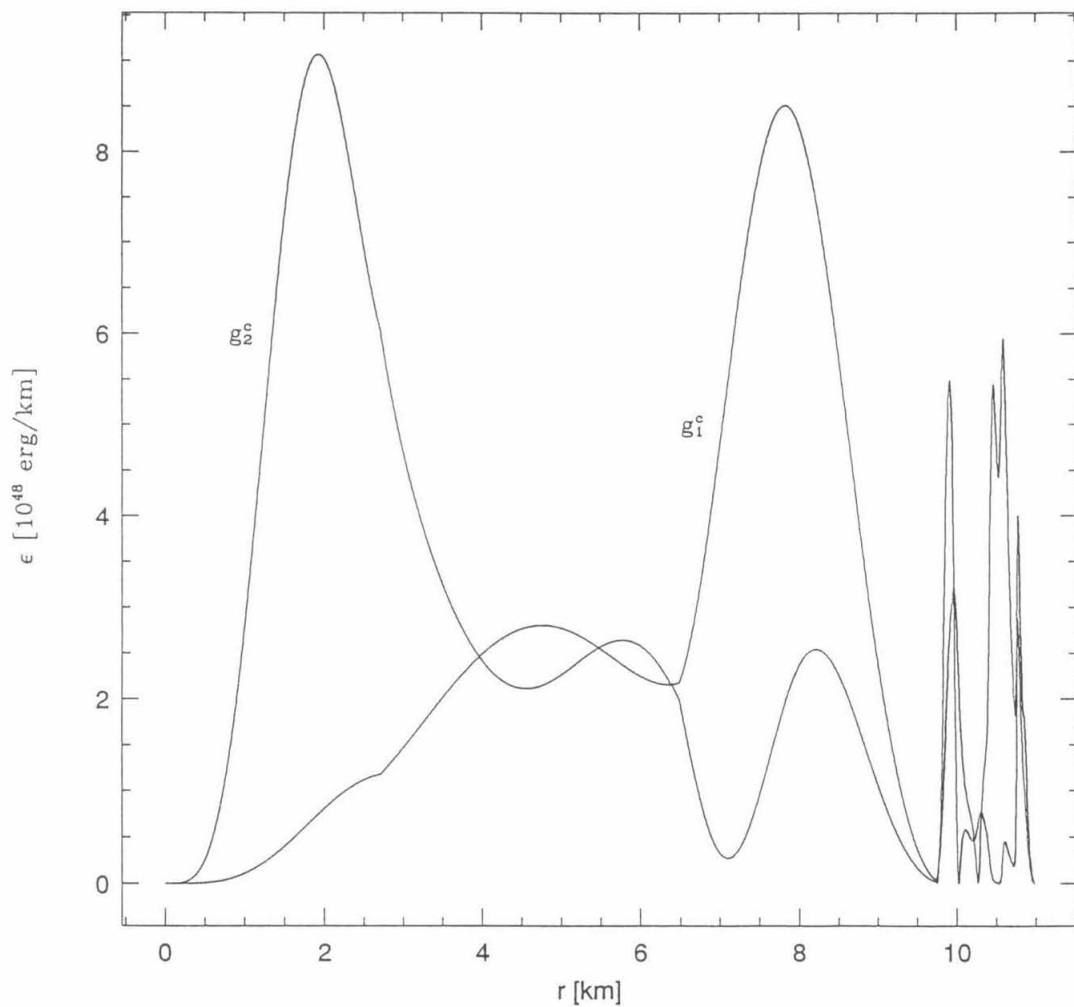
Chapter 3

MAGNETIC FIELD DECAY IN ISOLATED NEUTRON STARS

ABSTRACT

We investigate three mechanisms that promote the loss of magnetic flux from an isolated neutron star.

Ohmic decay produces a diffusion of the magnetic field with respect to the charged particles. It proceeds at a rate that is inversely proportional to the electric conductivity and independent of the magnetic field strength. Ohmic decay occurs in both the fluid core and solid crust of a neutron star, but it is too slow to directly affect magnetic fields of stellar scale.

Ambipolar diffusion involves a drift of the magnetic field and charged particles relative to the neutrons. The drift speed is proportional to the second power of the magnetic field strength if the protons form a normal fluid. Variants of ambipolar diffusion include both the buoyant rise and the dragging by superfluid neutron vortices of magnetic flux tubes. Ambipolar diffusion operates in the outer part of the fluid core where the charged particle composition is homogeneous, protons and electrons being the only species. The charged particle flux associated with ambipolar diffusion decomposes into a solenoidal and an irrotational component. Both components are opposed by frictional drag. The irrotational component perturbs the chemical equilibrium between neutrons, protons, and electrons, thus generating pressure gradients that effectively choke it. The solenoidal component is capable of transporting magnetic flux from the outer core to the crust on a short timescale. Magnetic flux that threads the inner core, where the charged particle composition is inhomogeneous, would be permanently trapped unless particle interactions could rapidly smooth departures from chemical equilibrium.

Magnetic fields undergo a *Hall drift* related to the Hall component of the electric field. The drift speed is proportional to the magnetic field strength. Hall drift occurs throughout a neutron star. Unlike ohmic decay and ambipolar diffusion which are dissipative, Hall drift conserves magnetic energy. Thus, it cannot by itself be responsible for magnetic field decay. However, it can enhance the rate

of ohmic dissipation. In the solid crust, only the electrons are mobile and the tangent of the Hall angle is large. There, the evolution of the magnetic field resembles that of vorticity in an incompressible fluid at large Reynolds number. This leads us to speculate that the magnetic field undergoes a turbulent cascade terminated by ohmic dissipation at small scales. The small scale components of the magnetic field are also transported by Hall drift waves from the inner crust where ohmic dissipation is slow to the outer crust where it is rapid. The diffusion of magnetic flux through the crust takes about $5 \times 10^8 / B_{12}$ years, where B_{12} is the crustal magnetic field strength measured in units of 10^{12}G.

1. INTRODUCTION

Young neutron stars are seen as ordinary radio pulsars and X-ray pulsars. Their surface magnetic field strengths are deduced to be of order $10^{12} - 10^{13}$G. Older neutron stars are observed as recycled pulsars and low mass X-ray binaries. Their surface fields are weaker, $\lesssim 10^{10}$G. The association of weaker fields with older objects suggests that the magnetic fields of neutron stars are subject to decay. Since the neutron stars found in recycled pulsars and low mass X-ray binaries have accreted substantial amounts of matter, it is difficult to resolve whether the decay results from age or accretion (Bisnovatyi-Kogan and Komberg 1975). Evidence favoring age comes from some statistical studies of ordinary, single, radio pulsars which conclude that the magnetic fields of these objects decay on timescales of order 10^7 years (Lyne, Manchester, and Taylor 1985, Narayan and Ostriker 1990). However, other studies reach the opposite conclusion (Bhattacharya, Wijers, Hartman, and Verbunt 1991). The detection in γ-ray burst spectra of what appear to be cyclotron lines formed in $10^{12} - 10^{13}$G fields (Murakami et al. 1988) would provide evidence in favor of accretion should the bursts emanate from old neutron stars (Shibazaki, Murakami, Shaham, and Nomoto 1989).

The purpose of this paper is to identify decay mechanisms for the magnetic field of an isolated neutron star and to estimate their timescales. We do not address questions related to the origin of the field. We merely assume that the initial field threads the interior of the star and inquire as to how it would evolve. To do so, we solve the equations of motion for charged particles in the presence of a magnetic field and a fixed background of neutrons while allowing for the creation and destruction of particles by weak interactions. Strictly speaking, these equations apply to normal neutrons and protons. However, we extend our interpretations of their solutions to cover cases of neutron superfluidity and proton superconductivity.

The organization of the paper is set out below. We present continuity equations and equations of motion for the protons and electrons in §2. These equations

are manipulated to prove that, in the presence of a magnetic force, the charged particles can not be simultaneously in magnetostatic equilibrium and in chemical equilibrium with the neutrons. In §3, the equations are solved and two mechanisms for the decay of the magnetic energy are identified, *ohmic dissipation* and *ambipolar diffusion*. Speculations concerning turbulent field evolution by *Hall drift* are offered in §4. Finally, §5 contains a discussion of the application of our results to real neutron stars.

Each of the three mechanisms we investigate, ohmic decay, ambipolar diffusion and Hall drift, has already received attention in relation to neutron star magnetic fields. Baym, Pethick, and Pines (1969b) were the first to properly calculate the ohmic decay time in the fluid core under the assumption that the neutrons and protons were normal (not superfluid and superconducting). Ewart, Guyer, and Greenstein (1975) and Sang and Chanmugam (1987) estimated the ohmic decay of fields supported by currents in the solid crust. The ambipolar diffusion timescale for normal neutrons and protons was evaluated by Haensel, Urpin, and Yakovlev (1990), although these authors mistakenly attributed it to enhanced ohmic decay (Pethick 1991). Harrison (1991) properly appreciated the connection between ambipolar diffusion and the buoyant rise of flux tubes. Hall drift was part of the picture of the thermoelectric generation of magnetic fields detailed by Blandford, Applegate, and Hernquist (1983). Jones (1988) proposed that Hall drift could transport magnetic flux across neutron star crusts. Relations between our results and those obtained in earlier papers are mentioned in §5.

2. EQUATIONS OF MOTION FOR THE CHARGED PARTICLES

We model the interior of a neutron star as a lightly ionized plasma consisting of neutrons, protons and electrons labeled by the indices n, p, and e. The equation of state for each particle species is taken to be that of an ideal, completely degenerate, gas. Modifications associated with the presence of other particle species and the

strong interactions are discussed in §3.5 and §5.2. We neglect thermal contributions to the Brunt-Väisälä frequency on the grounds that the thermal conductivity of neutron star interiors is so high that they are unimportant for the slow motions of interest here.

We specify the local state of each species by its internal chemical potential, μ_i, which is equal to the Fermi energy including rest mass. The protons and electrons are described as two separate fluids coupled by electromagnetic forces. Drag forces due to elastic binary collisions impede the relative motions of the different particle species. Weak interactions tend to erase perturbations away from chemical equilibrium among the neutrons, protons and electrons.

The neutrons are assumed to form a fixed background in diffusive equilibrium. This assumption, while not entirely realistic, simplifies the algebra and does not lead us astray. Its justification is that the combined fluid of neutrons, protons and electrons is stably stratified (Reisenegger and Goldreich 1992). The stratification is associated with the chemical composition gradient; the equilibrium ratio of the number densities of charged particles to neutrons increases with depth. The ratio of the magnetic field stress to the pressure of the charged particles is small. Thus, the magnetic field cannot force significant displacements of the combined fluid, at least not ones in which the composition is frozen. We show in §V that the interactions which smooth perturbations of chemical equilibrium are so slow that these are the only displacements of practical interest. The density profile of the neutrons, as determined by

$$\mu_n + m_n \psi = \text{constant}, \tag{1}$$

gives rise to a Newtonian gravitational potential, ψ; contributions to ψ by protons and electrons are neglected, as are corrections due to general relativity.

The charged particles satisfy the equations of motion:

$$m_p \frac{\partial \mathbf{v}_p}{\partial t} + m_p (\mathbf{v}_p \cdot \boldsymbol{\nabla}) \mathbf{v}_p = -\boldsymbol{\nabla}\mu_p - m_p \boldsymbol{\nabla}\psi + e(\mathbf{E} + \frac{\mathbf{v}_p}{c} \times \mathbf{B}) - \frac{m_p \mathbf{v}_p}{\tau_{pn}} - \frac{m_p (\mathbf{v}_p - \mathbf{v}_e)}{\tau_{pe}} \quad (2)$$

and

$$m_e^* \frac{\partial \mathbf{v}_e}{\partial t} + m_e^* (\mathbf{v}_e \cdot \boldsymbol{\nabla}) \mathbf{v}_e = -\boldsymbol{\nabla}\mu_e - e(\mathbf{E} + \frac{\mathbf{v}_e}{c} \times \mathbf{B}) - \frac{m_e^* \mathbf{v}_e}{\tau_{en}} - \frac{m_e^* (\mathbf{v}_e - \mathbf{v}_p)}{\tau_{ep}}. \quad (3)$$

Here, $m_e^* = \mu_e / c^2$ is the effective inertia of the electrons, $\mathbf{E}$ and $\mathbf{B}$ are the electric and magnetic fields, $\mathbf{v}_i$ is the mean velocity of the particles of species i, and τ_{ij} is the relaxation time for collisions of particles of species i against particles of species j. The average velocity of the neutrons is assumed to vanish, $\mathbf{v}_n = 0$. Conservation of momentum implies that $m_p / \tau_{pe} = m_e^* / \tau_{ep}$. We ignore relativistic corrections to both the inertia of the neutrons and protons and to the gravitational forces acting upon them. To be consistent, we also drop the gravitational force acting on the electrons and take the neutron and proton masses to be equal. Without the essential additions of the forces due to pressure and gravity, our equations of motion would yield an electrical conductivity tensor similar to that applied by Haensel, Urpin, and Yakovlev (1990).

The processes under consideration involve small velocities that change over timescales much longer than any of the relaxation times. Thus, we neglect the acceleration terms on the left-hand sides of equations (2) and (3). Then, combining equations (1), (2), and (3), we arrive at

$$\frac{\mathbf{f}_B}{n_c} - \boldsymbol{\nabla}(\Delta\mu) = \frac{m_p \mathbf{v}_p}{\tau_{pn}} + \frac{m_e^* \mathbf{v}_e}{\tau_{en}} \equiv \left(\frac{m_p}{\tau_{pn}} + \frac{m_e^*}{\tau_{en}} \right) \mathbf{v}, \quad (4)$$

where $\Delta\mu \equiv \mu_p + \mu_e - \mu_n$ is the departure from chemical equilibrium, $n_c \approx n_p \approx n_e$ is the number density of charged particles, $\mathbf{f}_B$ is the magnetic force density,

$$\mathbf{f}_B = \frac{\mathbf{j} \times \mathbf{B}}{c}, \quad (5)$$

with the electric current, $\mathbf{j}$, given by

$$\mathbf{j} \equiv en_c(\mathbf{v}_p - \mathbf{v}_e). \tag{6}$$

Each of the terms in equation (4) admits a simple interpretation. Clearly, $\mathbf{f}_B/n_c$ is the magnetic force per proton-electron pair. From the thermodynamic identity $(\partial\mu/\partial p)_s = 1/n$, it follows that $-\boldsymbol{\nabla}(\Delta\mu)$ is the net of the forces due to particle pressure plus gravity acting on a proton-electron pair. Equation (4) shows that magnetostatic equilibrium requires $\mathbf{f}_B/n_c$ to be the gradient of a potential. Only in this special circumstance can the gradient of the perturbed chemical potential balance the magnetic force density. If magnetostatic equilibrium does not apply, the forces drive the charged particles through the fixed background of neutrons at the *ambipolar diffusion velocity*, $\mathbf{v}$, defined by the second equality in equation (4).

Weak interactions tend to erase chemical potential differences between the charged particles and neutrons. The difference between the rates, per unit volume, at which the reactions $p + e^- \rightarrow n + \nu_e$ and $n \rightarrow p + e^- + \bar{\nu}_e$ occur is

$$\Delta\Gamma \equiv \Gamma(p + e^- \rightarrow n + \nu_e) - \Gamma(n \rightarrow p + e^- + \bar{\nu}_e) = \lambda\Delta\mu, \tag{7}$$

where the coefficient λ is a temperature-dependent proportionality constant in the limit $\Delta\mu \ll k_B T$.

The protons and electrons each satisfy a continuity equation

$$\frac{\partial n_i}{\partial t} + \boldsymbol{\nabla}\cdot(n_i\mathbf{v}_i) = -\lambda\Delta\mu. \tag{8}$$

Approximate charge neutrality implies $n_p \approx n_e \equiv n_c$ from which it follows that

$$\frac{\partial n_c}{\partial t} + \boldsymbol{\nabla}\cdot(n_c\mathbf{w}) = -\lambda\Delta\mu, \tag{9}$$

where

$$\mathbf{w} \equiv \frac{\mathbf{v}_p + \mathbf{v}_e}{2} = \mathbf{v} - \left(\frac{m_p/\tau_{pn} - m_e^*/\tau_{en}}{m_p/\tau_{pn} + m_e^*/\tau_{en}} \right) \frac{\mathbf{j}}{2n_c e}. \tag{10}$$

Since the Eulerian variations of n_c are of order $n_c B^2/p_e \ll 1$, where p_e is the electron pressure, equation (9) simplifies to

$$\nabla \cdot (n_c \mathbf{w}) \approx -\lambda \Delta \mu. \tag{11}$$

3. OHMIC DISSIPATION AND AMBIPOLAR DIFFUSION

In this section we study the dissipation of magnetic energy in a fluid mixture of neutrons, protons, and electrons that is close to both magnetostatic and chemical equilibrium. To avoid the proliferation of inessential terms, we neglect gravity and treat m_e^*, τ_{pn}, τ_{en}, and λ as constants throughout most of the section. Moreover, we assume that the magnetic field is spatially bounded and that the fluid medium is of infinite extent. In the final subsection, §3.5, we consider extensions and refinements of our results to inhomogeneous, gravitating media.

3.1. Magnetic Field Evolution

The evolution of the magnetic field is related to the electric field, $\mathbf{E}$, by Faraday's induction law,

$$\frac{\partial \mathbf{B}}{\partial t} = -c\nabla \times \mathbf{E}. \tag{12}$$

The electric field, obtained from a suitable combination of equations (2) and (3) without the inertial terms, reads:

$$\mathbf{E} = \frac{\mathbf{j}}{\sigma_0} - \frac{\mathbf{v}}{c} \times \mathbf{B} + \left(\frac{m_p/\tau_{pn} - m_e^*/\tau_{en}}{m_p/\tau_{pn} + m_e^*/\tau_{en}} \right) \frac{\mathbf{j} \times \mathbf{B}}{n_c ec} + \frac{(\tau_{pn}/m_p)\nabla\mu_p - (\tau_{en}/m_e^*)\nabla\mu_e}{e(\tau_{pn}/m_p + \tau_{en}/m_e^*)}, \tag{13}$$

where

$$\sigma_0 = n_c e^2 \left(\frac{1}{\tau_{ep}/m_e^*} + \frac{1}{\tau_{pn}/m_p + \tau_{en}/m_e^*} \right)^{-1} \qquad (14)$$

is the electrical conductivity in the absence of a magnetic field.

Substituting equation (13) into equation (12), we obtain the governing equation for the magnetic field,

$$\frac{\partial \mathbf{B}}{\partial t} = -c \boldsymbol{\nabla} \times \left(\frac{\mathbf{j}}{\sigma_0} \right) + \boldsymbol{\nabla} \times (\mathbf{v} \times \mathbf{B}) - \left(\frac{m_p/\tau_{pn} - m_e^*/\tau_{en}}{m_p/\tau_{pn} + m_e^*/\tau_{en}} \right) \boldsymbol{\nabla} \times \left(\frac{\mathbf{j} \times \mathbf{B}}{n_c e} \right). \qquad (15)$$

where $\mathbf{j}$ is related to $\mathbf{B}$ by Ampère's law,

$$\mathbf{j} = \frac{c \boldsymbol{\nabla} \times \mathbf{B}}{4\pi}. \qquad (16)$$

The terms on the right hand side of equation (15) describe, in order, the effects of ohmic decay, ambipolar diffusion, and Hall drift. Since $\mathbf{j}$ and $\mathbf{v}$ are linear and quadratic functionals of $\mathbf{B}$, these terms scale as B, B^3, and B^2, respectively.

3.2. Dissipation of Magnetic Energy

The total magnetic energy is given by

$$E_B = \frac{1}{8\pi} \int d^3x \, |\mathbf{B}|^2. \qquad (17)$$

We write its time derivative, with the aid of equation (12) and after an integration by parts, in the form

$$\frac{dE_B}{dt} = -\frac{1}{4\pi} \int d^3x \, \mathbf{j} \cdot \mathbf{E}. \qquad (18)$$

Neither the Hall term nor the potential term in the electric field contribute to dE_B/dt. The former is orthogonal to $\mathbf{j}$ and the latter is eliminated by the use of Ampère's law in the derivation of equation (18). Thus,

$$\frac{dE_B}{dt} = \left(\frac{dE_B}{dt}\right)_{\text{ohmic}} + \left(\frac{dE_B}{dt}\right)_{\text{ambip}}. \tag{19}$$

The contribution from ohmic dissipation reads

$$\left(\frac{dE_B}{dt}\right)_{\text{ohmic}} = -\frac{1}{4\pi} \int d^3x \, \frac{|\mathbf{j}|^2}{\sigma_0}. \tag{20}$$

The ambipolar term is given by

$$\begin{aligned}
\left(\frac{dE_B}{dt}\right)_{\text{ambip}} &= -\frac{1}{4\pi} \int d^3x \, \mathbf{v} \cdot \mathbf{f}_B \\
&= -\int d^3x \, n_c \left(\frac{m_p}{\tau_{pn}} + \frac{m_e^*}{\tau_{en}}\right) |\mathbf{v}|^2 - \int d^3x \, n_c \mathbf{v} \cdot \boldsymbol{\nabla}(\Delta\mu), \quad (21)
\end{aligned}$$

where we arrive at the second expression by using equation (4) to eliminate $\mathbf{f}_B$ in favor of $\mathbf{v}$ and $\Delta\mu$. Another integration by parts, together with equation (11), yields

$$\left(\frac{dE_B}{dt}\right)_{\text{ambip}} = -\int d^3x \left[n_c \left(\frac{m_p}{\tau_{pn}} + \frac{m_e^*}{\tau_{en}}\right) |\mathbf{v}|^2 + \lambda(\Delta\mu)^2\right]. \tag{22}$$

The first piece in the integrand arises from energy lost to frictional drag. The second piece accounts for the energy carried away by the neutrinos and anti-neutrinos that are emitted during the inverse and direct beta decays that smooth departures from chemical equilibrium.

As is evident from equations (20) and (22), ohmic dissipation and ambipolar diffusion always act to decrease the magnetic energy.

3.3. Ambipolar Drift Velocity

To relate the chemical potential imbalance, $\Delta\mu$, and the drift velocity, $\mathbf{v}$, to the magnetic force, $\mathbf{f}_B$, we start from equations (4) and (11). It is convenient to resolve $\mathbf{v}$ and $\mathbf{f}_B$ into solenoidal (divergence-free) and irrotational (curl-free) components,

$\mathbf{v}^s$ and $\mathbf{f}_B^s$, and $\mathbf{v}^{ir}$ and $\mathbf{f}_B^{ir}$.[1] Because $\nabla(\Delta\mu)$ is irrotational, the solenoidal and irrotational components of equation (4) can be written as

$$\mathbf{v}^s = \frac{\mathbf{f}_B^s}{n_c(m_p/\tau_{pn} + m_e^*/\tau_{en})}, \tag{23}$$

and

$$\mathbf{v}^{ir} = \frac{\mathbf{f}_B^{ir} - n_c\nabla(\Delta\mu)}{n_c(m_p/\tau_{pn} + m_e^*/\tau_{en})}. \tag{24}$$

Note that $\mathbf{v}^s$ is directly proportional to the local value of $\mathbf{f}_B^s$ with a coefficient that is inversely proportional to the frictional coupling between the charged particles and neutrons. Because $\mathbf{v}^{ir}$ perturbs the chemical equilibrium between the neutrons and charged particles, its response to $\mathbf{f}_B^{ir}$ is more complicated. The details are worked out below.

Since the fractional variations of n_c are of order $B^2/p_e \ll 1$, equation (11) simplifies further to

$$\nabla\cdot\mathbf{v}^{ir} \approx -\frac{\lambda\Delta\mu}{n_c}. \tag{25}$$

Taking the divergence of equation (24) and using equation (25) to eliminate $\nabla\cdot\mathbf{v}^{ir}$, we obtain

$$\nabla^2(\Delta\mu) - \frac{\Delta\mu}{a^2} = \frac{\nabla\cdot\mathbf{f}_B^{ir}}{n_c}, \tag{26}$$

where the length scale a satisfies

$$a \equiv \left[\frac{\lambda}{n_c}\left(\frac{m_p}{\tau_{pn}} + \frac{m_e^*}{\tau_{en}}\right)\right]^{-1/2}. \tag{27}$$

The solution of equation (26) is conveniently expressed in terms of the Green's function

---

[1]This decomposition is unique since the fields are spatially bounded.

$$G(\mathbf{x} - \mathbf{x}') = -\frac{\exp(-|\mathbf{x} - \mathbf{x}'|/a)}{4\pi|\mathbf{x} - \mathbf{x}'|} \tag{28}$$

as

$$\Delta\mu(\mathbf{x}) = \frac{1}{n_c} \int d^3x' \, G(\mathbf{x} - \mathbf{x}') \, \nabla' \cdot \mathbf{f}_B^{ir}(\mathbf{x}'). \tag{29}$$

Next, we relate $\mathbf{v}^{ir}$ to $\mathbf{f}_B^{ir}$ by substituting equation (29) into equation (24) and performing an integration by parts:

$$\mathbf{v}^{ir}(\mathbf{x}) = \frac{\lambda a^2}{n_c^2} \left(\mathbf{f}_B^{ir}(\mathbf{x}) - \int d^3x' \, G(\mathbf{x} - \mathbf{x}')\nabla' \left[\nabla' \cdot \mathbf{f}_B^{ir}(\mathbf{x}') \right] \right). \tag{30}$$

Let us denote by L the characteristic length scale over which $\mathbf{f}_B^{ir}$ varies. The response of $\mathbf{v}^{ir}$ to $\mathbf{f}_B^{ir}$ depends upon the relative sizes of L and a.

For $L/a \gg 1$ the second term in equation (30) is smaller than the first by a factor of order $(a/L)^2 \ll 1$, and

$$\mathbf{v}^{ir} \approx \frac{\lambda a^2}{n_c^2} \mathbf{f}_B^{ir} = \frac{\mathbf{f}_B^{ir}}{n_c(m_p/\tau_{pn} + m_e^*/\tau_{en})}. \tag{31}$$

In this limit chemical equilibrium is achieved so rapidly that only the frictional drag exerted by the neutrons on the charged particles is available to balance the magnetic force.

In the opposite limit, $L/a \ll 1$, the relation between $\mathbf{v}^{ir}$ and $\mathbf{f}_B^{ir}$ is non-local, and therefore more complicated. It is best revealed in Fourier space, since the Fourier components of the irrotational parts of vector fields are parallel to $\mathbf{k}$. Taking the Fourier transforms of equations (25) and (26) yields

$$\mathbf{k} \cdot \mathbf{v}^{ir}(\mathbf{k}) = \frac{\lambda a^2}{n_c^2 (1 + k^2 a^2)} \mathbf{k} \cdot \mathbf{f}_B^{ir}(\mathbf{k}) \approx \frac{\lambda L^2}{n_c^2} \mathbf{k} \cdot \mathbf{f}_B^{ir}(\mathbf{k}), \tag{32}$$

for $L = k^{-1} \ll a$. For $L/a \ll 1$, $\mathbf{f}_B^{ir}$ is balanced by the pressure gradient, leaving only $\mathbf{f}_B^s$ to be balanced by frictional drag.

3.4. Decay Timescales

Here, we collect formulae giving the characteristic timescales over which ohmic decay and ambipolar diffusion dissipate magnetic energy. We reserve until §5 the numerical evaluation of these timescales under different hypotheses concerning the state of matter in neutron star interiors.

The timescale for ohmic decay, which follows immediately from equations (15) and (16), has the familiar form

$$t_{\mathrm{ohmic}} \sim \frac{4\pi\sigma_0 L^2}{c^2}. \tag{33}$$

Ohmic decay involves a diffusion of the magnetic field lines with respect to the charged particles. Note that t_{ohmic} is proportional to L^2 and independent of the field strength.

There are two timescales for ambipolar diffusion, one for the solenoidal component of the charged particle flux and the other for the irrotational component. Following equations (23) and (32), we find

$$t_{\mathrm{ambip}}^s \sim \frac{L}{v^s} \sim \frac{4\pi n_c L^2}{B^2}\left(\frac{m_p}{\tau_{pn}} + \frac{m_e^*}{\tau_{en}}\right), \tag{34}$$

and

$$t_{\mathrm{ambip}}^{ir} \sim \frac{L}{v^{ir}} \sim \frac{4\pi n_c\left(L^2 + a^2\right)}{B^2}\left(\frac{m_p}{\tau_{pn}} + \frac{m_e^*}{\tau_{en}}\right). \tag{35}$$

Ambipolar diffusion involves the motion of the magnetic field lines together with the charged particles relative to the neutrons. Note that both expressions for t_{ambip} are inversely proportional to B^2. Also, for $L/a \ll 1$, $t_{\mathrm{ambip}}^s \approx (L/a)^2 t_{\mathrm{ambip}}^{ir}$.

We show in §5.2 that t_{ambip}^{ir} is larger than the Hubble time. However, if it were not, we would be compelled to consider displacements of the combined fluid of neutrons and charged particles. This is because magnetic forces would drive

a solenoidal flux of baryons (neutrons plus protons) if particle interactions could maintain chemical equilibrium. This solenoidal motion of the combined fluid would not suffer the frictional retardation that the solenoidal component of the charged particle fluid does. It would only have the milder effects of viscosity to contend with.

3.5. Extensions and Refinements

It is easy to extend most of the results obtained in this section so that they apply to inhomogeneous media in gravitational fields.

The expressions for the dissipation of magnetic energy by ohmic decay and ambipolar diffusion given by equations (20) and (22) are unchanged in an inhomogeneous medium. However, the derivation of dE_{ambip}/dt is complicated by the spatial variations of m_e^*, τ_{pn}, τ_{en}, and λ. We leave the proofs to the reader.

The flow of charged particles in a homogeneous medium tends to upset chemical equilibrium if $\nabla{\cdot}(n_c\mathbf{v}) \neq 0$. This generalizes in an inhomogeneous medium to $\nabla{\cdot}(n_c\mathbf{w}) \neq 0$ (cf. eqn. [9]). It is useful to resolve the charged particle flux $n_c\mathbf{w}$ into its solenoidal and irrotational components. If beta reactions do not erase perturbations from chemical equilibrium, the irrotational component is choked by pressure gradients. We note that $\mathbf{w}$ differs from the ambipolar diffusion velocity $\mathbf{v}$ by a term proportional to the current density $\mathbf{j}$. Since $\nabla{\cdot}\mathbf{j} = 0$ as a consequence of charge neutrality,

$$\nabla{\cdot}(n_c\mathbf{w}) = \nabla{\cdot}(n_c\mathbf{v}) - \frac{\mathbf{j}}{2e} \cdot \nabla\left(\frac{m_p/\tau_{pn} - m_e^*/\tau_{en}}{m_p/\tau_{pn} + m_e^*/\tau_{en}}\right). \tag{36}$$

The difference between $\nabla{\cdot}(n_c\mathbf{w})$ and $\nabla{\cdot}(n_c\mathbf{v})$ vanishes in either the limit $m_p\tau_{en} \gg m_e^*\tau_{pn}$ or the limit $m_e^*\tau_{pn} \gg m_p\tau_{en}$. The first limit would be relevant if the protons were normal since that would imply $\tau_{en}/\tau_{pn} \gg 1$ because neutron-proton scatterings are mediated by the strong force, whereas neutron-electron scatterings are due to electromagnetic interactions involving the neutron's magnetic moment. The

consequences of proton superconductivity are less clear. However, we shall assume that $\nabla\cdot(n_c\mathbf{w}) \approx \nabla\cdot(n_c\mathbf{v})$ wherever ambipolar diffusion might be important inside neutron stars. Thus, we write

$$\nabla\cdot(n_c\mathbf{v}) \approx -\lambda\Delta\mu, \tag{37}$$

from here on.

Ambipolar diffusion in a homogeneous medium is driven by unbalanced magnetic stresses. In an inhomogeneous medium subject to a gravitational field buoyancy forces also play a role (Parker 1979). To estimate the buoyancy forces, consider a thin, circular, magnetic flux tube of outer radius r that surrounds the center of a spherical star. The pressure of the charged particles, p_c, mostly due to electrons, is lower inside the tube than outside by $\delta p_c \approx -B^2/(8\pi)$. The density deficit inside the tube is $\delta\rho/\rho \approx -3B^2/(32\pi p_c)$. Thus, the buoyancy force density is given by

$$\mathbf{f}_{\text{buoyancy}} \approx -\frac{3B^2\rho}{32\pi\,p_c}\mathbf{g} \approx \frac{3B^2}{32\pi\,H}\hat{\mathbf{r}}, \tag{38}$$

where $\hat{\mathbf{r}}$ is the radial unit vector, and H is the pressure scale height of the charged particle fluid. It is easy to show that the magnitude of $\mathbf{f}_{\text{buoyancy}}$ exceeds that of the inward directed force density due to magnetic tension provided $H < 3r/4$. The buoyancy force density is to be compared to $B^2/(8\pi L)$, the characteristic magnitude of the force density associated with a magnetic field of scale L. Since $L \lesssim H$ in the fluid core of a neutron star, the addition of buoyancy forces does not alter the timescales for ambipolar diffusion given by equations (34) and (35).

Our treatment of ambipolar diffusion is predicated on the assumption that the charged particle fluid is homogeneous; more specifically, that it is composed of equal number densities of protons and electrons. This crucial assumption insures that the charged particle fluid is neutrally stratified. The solenoidal component of the charged particle flux does not perturb the density and pressure of a homogeneous

fluid. However, it is likely that additional species of charged particles appear in the equilibrium composition at pressures below the central pressure of a neutron star. We refer to this region, where there is a gradient in the charged particle composition, as the inner core. Unfortunately, the size and composition of the inner core are uncertain. However, it is clear that the charged particle fluid in the inner core is stably stratified. This has serious implications for ambipolar diffusion. Displacements of the charged particle fluid at frozen composition would raise the potential energy. Unless particle interactions could rapidly erase perturbations from chemical equilibrium, ambipolar diffusion could not occur in the inner core.

4. HALL DRIFT AND MAGNETIC TURBULENCE

In this section we examine the third term in equation (15), the one that describes advection of the field by Hall drift. This term does not change the total magnetic energy. However, it cannot be ignored in neutron star interiors because, in places, its magnitude exceeds that of the terms which account for ambipolar diffusion and ohmic decay. We begin by describing Hall drift waves. Then, we go on to consider the possibility that the magnetic field in the crust evolves through a turbulent cascade.

We simplify the induction equation (15) by taking the limit $\tau_{pn} \rightarrow 0$ and $\tau_{en} \rightarrow \infty$. With the protons immobilized, the electrons carry all the current and ambipolar diffusion is eliminated. The medium resembles a metallic solid. Then, the reduced version of equation (15) reads

$$\frac{\partial \mathbf{B}}{\partial t} = -\frac{c}{4\pi n_c e} \boldsymbol{\nabla} \times [(\boldsymbol{\nabla} \times \mathbf{B}) \times \mathbf{B}] + \frac{c^2}{4\pi \sigma_0} \nabla^2 \mathbf{B}. \tag{39}$$

Application of dimensional analysis to equation (39) yields a relation between the linear size, L, and characteristic evolution timescale, t_{Hall}, of field structures:

$$t_{\text{Hall}} = \frac{4\pi n_c e L^2}{cB}. \tag{40}$$

Jones (1988) proposed that Hall drift could transport magnetic field from the inner crust where ohmic decay is slow to the outer crust where it proceeds rapidly. Here we show that there is a class of Hall drift waves that carry magnetic energy and whose dispersion relation is closely related to equation (40). To obtain the dispersion relation for linear waves in a uniform magnetic field $\mathbf{B}_0$, we substitute the elementary disturbance $\mathbf{B}_1 = \tilde{\mathbf{B}}_1 \exp i(\mathbf{k} \cdot \mathbf{x} - \omega t)$ into equation (39). After a little algebra, we obtain

$$\omega = \frac{ck|\mathbf{k} \cdot \mathbf{B}_0|}{4\pi n_c e}, \tag{41}$$

where $k \equiv |\mathbf{k}|$. The corresponding group velocity is

$$\mathbf{v}_{gp} = \pm \frac{ck\left[\mathbf{B}_0 + \left(\hat{\mathbf{k}} \cdot \mathbf{B}_0\right)\hat{\mathbf{k}}\right]}{4\pi n_c e}, \tag{42}$$

where $\hat{\mathbf{k}} \equiv \mathbf{k}/k$.

There is reason to doubt whether these waves could transport magnetic energy from the inner to the outer crust. In particular, they might be reflected as they propagate upward toward lower density. To expose the problem, we interpret equation (41) as a WKBJ dispersion relation. Consider a plane parallel model for the crust with n_c decreasing monotonically in the z direction. The validity of the WKBJ approximation requires $k_z H \gg 1$, where H is the local scale height. Let us assume that a wavepacket which satisfies this inequality is launched upward from the lower crust. For the moment, we focus on the special case with $\mathbf{B}_0$ constant and aligned along the x axis. As the wave packet propagates toward lower density, k must decrease in direct proportion to n_c, since ω remains constant. Because of the symmetry of the problem, the decrease of k comes entirely at the expense of k_z. Since H also decreases with height, the inequality $k_z H \gg 1$ must eventually be violated. It is plausible that the wave packet would be reflected downward at about the level where $k_z H \sim 1$. Although the details differ when $\mathbf{B}_0$ is aligned along the z axis, the reflection of upward propagating wave packets still seems

likely.

The above considerations suggest that only disturbances whose wavelengths in the inner crust are very much shorter than the local scale height could propagate to the outer crust. Below, we argue that Hall drift tends to produce short wavelength magnetic structures. This enhances the local rate of ohmic dissipation as well as the ability of Hall waves to transport magnetic energy upward.

We proceed by rewriting equation (39) in dimensionless form as

$$\frac{\partial \mathbf{b}}{\partial \tau} = -\boldsymbol{\nabla}_\xi \times [(\boldsymbol{\nabla}_\xi \times \mathbf{b}) \times \mathbf{b}] + \frac{1}{\mathcal{R}_B} \nabla_\xi^2 \mathbf{b}. \tag{43}$$

Here, $\boldsymbol{\xi} \equiv \mathbf{x}/L$, $\mathbf{b} \equiv \mathbf{B}/B_0$, and $\tau \equiv t/t_{\text{Hall}}$, with L and B_0 scale factors appropriate to the largest magnetic structures. The parameter

$$\mathcal{R}_B = \frac{\sigma_0 B_0}{n_c e c} = \frac{e B_0 \tau_{ep}}{m_e^* c} \tag{44}$$

is the tangent of the Hall angle; $\mathcal{R}_B$ may be large inside neutron stars. Note that $\mathcal{R}_B$ has a couple of interpretations. It is equal to 2π times the ratio of the electron relaxation time to the electron cyclotron period, and it is also equal to $t_{\text{ohmic}}/t_{\text{Hall}}$.

The dimensionless induction equation (43) resembles the vorticity equation for an incompressible fluid. In dimensionless form, the latter equation reads

$$\frac{\partial \omega}{\partial \tau} = \boldsymbol{\nabla}_\xi \times (\mathbf{v} \times \omega) + \frac{1}{\mathcal{R}} \nabla_\xi^2 \omega, \tag{45}$$

where $\mathbf{v}$ and $\omega = \boldsymbol{\nabla}_\xi \times \mathbf{v}$ are the dimensionless velocity and vorticity, and $\mathcal{R}$ is the Reynolds number. The analogy between equations (43) and (45) would be complete if $\mathbf{v}$ were the curl, rather than the inverse curl, of ω.[2]

Turbulence is a generic property of homogeneous, incompressible flows under circumstances where the Reynolds number is large. It is easy to rationalize this

---

[2]The minus sign in front of the nonlinear term in equation (43) is not crucial. It arises because the current carriers have negative charge.

fact from equation (45) by noting that the nonlinear advection term is much larger than the linear diffusion term for $\mathcal{R} \gg 1$. We speculate that, where $\mathcal{R}_B \gg 1$ in the solid crust, the generic magnetic field evolves through a turbulent cascade. In other words, nonlinear couplings transfer magnetic energy from larger to smaller scales where it is ultimately dissipated by ohmic decay. The similarity between equations (43) and (45) leads us to speculate that the generic magnetic field is turbulent for $\mathcal{R}_B \gg 1$. The material in the remainder of this section is based on that speculation. It is so intriguing that we present it in advance of serious investigation.

Having guessed that magnetic fields are turbulent for $\mathcal{R}_B \gg 1$, it is natural to inquire about their spectra. We take a first cut at this problem by adapting a method devised by Kolmogoroff (1941) for fluid turbulence. We assume that the nonlinear interactions transfer magnetic energy from large to small scales where it is ultimately dissipated by ohmic diffusion. The outer, or energy bearing, scale has linear size L, magnetic field strength B_0, and lifetime t_{Hall}. Smaller structures of size λ have magnetic field strengths B_λ and lifetimes t_λ. The inner scale, at which ohmic decay becomes important, is denoted by λ_*. We assume that magnetic turbulence is space filling and that the nonlinear transfer of magnetic energy is local in wave number space. Then, the steady flow of energy toward smaller scales implies

$$\frac{B_\lambda^2}{t_\lambda} \sim \frac{B_0^2}{t_{\text{Hall}}}. \tag{46}$$

We determine t_λ from the form of the nonlinear term in equation (43). A simple scaling argument suggests that

$$\frac{t_\lambda}{t_{\text{Hall}}} \sim \left(\frac{\lambda}{L}\right)^2 \frac{B_0}{B_\lambda}. \tag{47}$$

This is the choice made by Vainshtein (1973) and amounts to assuming that the turbulence is strong. However, the period of Hall waves of wavelength λ is shorter

than t_λ by a factor $\sim B_\lambda / B_0$. Thus, Hall turbulence consists of weakly interacting waves (Kingsep, Chukbar, and Yan'kov 1990). The lowest order nonlinear interactions are those that couple three resonant waves which satisfy, $\omega = \omega_1 + \omega_2$ and $\mathbf{k} = \mathbf{k}_1 + \mathbf{k}_2$. It is easily to verify that the dispersion relation (eqn. [41]) permits these conservation laws to be satisfied simultaneously. The characteristic timescale for the transfer of energy among resonant triplets is

$$\frac{t_\lambda}{t_{\text{Hall}}} \sim \left(\frac{\lambda}{L}\right)^2 \left(\frac{B_0}{B_\lambda}\right)^2, \tag{48}$$

which is longer by the factor B_0 / B_λ than t_λ given in equation (47). The larger value for t_λ arises because the transfer of energy and momentum among wave packets of unit fractional bandwidths in ω and $\mathbf{k}$ takes place in steps of dimensionless size B_λ / B_0, each of duration $\sim 1/\omega_k$ with $\lambda k \sim 1$. Our derivation of t_λ is a heuristic one. However, the same result may also be derived by the rigorous methods described by Zakharov (1971, 1983).

Together, equations (46) and (48) yield

$$\frac{B_\lambda}{B_0} \sim \left(\frac{\lambda}{L}\right)^{1/2}, \tag{49}$$

and

$$\frac{t_\lambda}{t_{\text{Hall}}} \sim \frac{\lambda}{L}. \tag{50}$$

The inner scale is set by $t_{\text{ohmic}} \sim t_\lambda$. From equations (33) and (50), we arrive at

$$\frac{\lambda_*}{L} \sim \frac{1}{\mathcal{R}_B}. \tag{51}$$

The one-dimensional power spectrum of the magnetic field is determined by $k B^2(k) \sim B_\lambda^2$. Thus,

$$B^2(k) \sim \frac{B_0^2}{Lk^2}. \qquad (52)$$

By way of comparison, the Kolmogoroff power spectrum of a turbulent velocity field $v^2(k) \propto k^{-5/3}$. Just as most of the energy in a turbulent flow is contained in the largest eddies, most of the energy in a (Hall) turbulent magnetic field is contained in the largest magnetic structures. However, the small scales dominate the vorticity density in fluid turbulence and the current density in (Hall) magnetic turbulence.

The turbulent cascade of magnetic energy leads to an enhanced ohmic decay of the magnetic field. The large scale components of the field weaken as magnetic energy is conservatively transported to smaller scales.

Hall drift occurs in electrically conducting fluids as well as solids. However, its implications in fluid media are less clear. The reason is that Hall drift changes the magnetic force density, $\mathbf{j} \times \mathbf{B}/c$. In a fluid, the magnetic force density drives motions at the Alfvén speed, $v_A = B/(4\pi\rho)^{1/2}$, which in cases of interest here is much greater than the speed of the Hall drift. The situation in a solid is simpler, because the magnetic force density is ultimately balanced by the divergence of the lattice stress tensor.

5. APPLICATION TO NEUTRON STARS

Our goal is to determine how magnetic fields in neutron stars decay. We discuss the possible roles played by ohmic dissipation, ambipolar diffusion, and Hall drift. Lack of knowledge concerning the states of matter inside neutron stars is a great hindrance. We adopt the following approach for dealing with this problem.

We assess each decay mechanism as it would apply if the modified URCA reactions were the principal means for smoothing departures from chemical equilibrium, if the neutrons and protons were normal, and if neutrons, protons, and

electrons were the only particles present in the fluid core. Then, we relax various combinations of these assumptions and consider how our assessments must be modified.

Many of the uncertainties regarding the properties of matter in neutron star interiors stem from our inadequate knowledge of particle interactions at above nuclear density. This impedes prediction of the equilibrium number densities of different species of particles. It also limits our ability to determine whether and where the neutrons form a superfluid and the protons form a superconductor. These unresolved issues impact the discussion of the decay of the magnetic field in many ways, a few of which are mentioned below.

The relative number densities of protons and electrons to neutrons determines whether the regular URCA process can occur in neutron stars. Until recently, it was thought that only the much slower modified URCA reactions could operate (Chiu and Salpeter 1964). However, this issue seems less settled now (Lattimer, Pethick, Prakash, and Haensel 1991). If the regular URCA reactions function, both neutron star cooling and the smoothing of perturbations away from chemical equilibrium would proceed much faster than previously estimated.

Neutron superfluidity would greatly reduce the collision rates between neutrons and charged particles. The energy gap would impede the reactions that restore chemical equilibrium. The effects of proton superconductivity would depend upon whether the superconductor was type I or II. The prevailing view is that the protons form a type II superconductor (Baym, Pethick, and Pines 1969a). If so, the arrangement of the magnetic field in quantized flux tubes would modify the magnetic stress (Easson and Pethick 1977). In particular, the components of the stress tensor would be proportional to the first power of the mean magnetic field strength. Thus, the timescales for ambipolar diffusion would be inversely proportional to B instead of B^2.

The presence of exotic species of particles would affect the static stability of

neutron star interiors as measured by the Brunt-Väisälä frequency. The dynamics of ambipolar diffusion would be complicated by the presence of additional species of charged particles.

5.1. Ohmic Decay

Shortly after the discovery of pulsars, Baym, Pethick, and Pines (1969b) calculated the electrical conductivity, σ_0, of neutron star interiors under the assumption that the neutrons, protons, and electrons are degenerate but normal (not-superfluid), and that the magnetic field is weak. They found that σ_0 is so high that the timescale for ohmic dissipation of neutron star magnetic fields exceeds the age of the universe. We take the electrical conductivity of the core fluid, as given by equation (14), to be $\sigma_0 = 4.2 \times 10^{28} T_8^{-2} (\rho/\rho_{\rm nuc})^3 {\rm s}^{-1}$, where T_8 denotes the temperature in units of $10^8 {\rm K}$, and $\rho_{\rm nuc} \equiv 2.8 \times 10^{14} {\rm g/cm^3}$ (Haensel, Urpin, and Yakovlev 1990).[3] This corresponds to an ohmic decay timescale (cf. eqn. [33])

$$t_{\rm ohmic} \sim 2 \times 10^{11} \frac{L_5^2}{T_8^2} \left(\frac{\rho}{\rho_{\rm nuc}} \right)^3 {\rm years}, \tag{53}$$

where $L_5 \equiv L/(10^5 \ {\rm cm})$.

We can draw a rigorous, although qualified, conclusion from equation (53). It is that magnetic fields of stellar scale supported by currents in the fluid core of a neutron star would not suffer significant ohmic decay if the core matter were normal. This conclusion can be extended in several directions. Superconductivity of either type would certainly decrease the rate of ohmic decay, but might lead to the expulsion of magnetic fields by other means. If crustal currents support neutron star magnetic fields, ohmic decay would be faster. However, unless the currents are confined to the outer crust, ohmic decay would fall short of accounting for the magnitude of the decline in field strength estimated from observations of neutron stars (Ewart, Guyer, and Greenstein 1975, Sang and Chanmugam 1987).

---

[3]Electrons are the main current carriers and their important collisions are with protons.

Haensel, Urpin, and Yakovlev (1990) reopened the issue of the ohmic decay with the claim that the resistivity is enhanced in directions perpendicular to strong magnetic fields.[4] They proposed that ohmic decay could reduce arbitrary initial fields to strengths below $B \sim 10^{12}$ G in about 10^7 years. However, as we show below, and as has also been recognized by Pethick (1991), the decay mode identified by Haensel, Urpin, and Yakovlev is *ambipolar diffusion* rather than *ohmic dissipation*.

We conclude that large scale magnetic structures in neutron stars do not suffer significant ohmic decay.

5.2. Ambipolar Diffusion

Ambipolar diffusion involves a coupled motion of the magnetic field lines and the charged particles (protons and electrons) relative to the neutrons. The flux of charged particles associated with ambipolar diffusion, $n_c \mathbf{v}$, resolves into a solenoidal and an irrotational component. The solenoidal component does not disturb the chemical equilibrium between neutrons, protons and electrons. Therefore, it is only opposed by friction between the charged particles and the neutrons. However, the irrotational part of $n_c \mathbf{v}$ is also retarded by pressure gradients that build up in response to the departures from chemical equilibrium that it causes. Since the weak interactions that restore chemical equilibrium are very sluggish at low temperatures,[5] the pressure gradients effectively choke $n_c \mathbf{v}^{ir}$.

The square of the length scale ratio L/a provides a quantitative measure of the relative importance of frictional drag and pressure gradients in limiting the irrotational component of the charged particle flux. We find

$$\frac{L}{a} \approx \left(\frac{\lambda m_p}{n_c \tau_{pn}} \right)^{1/2} L \sim 7 \times 10^{-4} T_8^4 L_5 \left(\frac{\rho_{\text{nuc}}}{\rho} \right)^{1/3}, \tag{54}$$

where we use

---

[4]Their work is based on the assumption that the neutrons and protons are normal.

[5]We are assuming that only the modified URCA reactions can operate inside neutron stars.

$$n_c \sim 5 \times 10^{-2} \frac{\rho}{m_n} \approx 8 \times 10^{36} \frac{\rho}{\rho_{\text{nuc}}} \text{cm}^{-3}, \tag{55}$$

and

$$\frac{1}{\tau_{pn}} = 4.7 \times 10^{16} T_8^2 \left(\frac{\rho_{\text{nuc}}}{\rho}\right)^{1/3} \text{s}^{-1} \gg \frac{m_e^*}{m_p} \frac{1}{\tau_{en}}, \tag{56}$$

from Yakovlev and Shalybkov (1990), and

$$\lambda = 5 \times 10^{27} T_8^6 \left(\frac{\rho}{\rho_{\text{nuc}}}\right)^{2/3} \text{erg}^{-1}\text{cm}^{-3}\text{s}^{-1}, \tag{57}$$

due to the modified URCA reactions from Sawyer (1989).

Next, we evaluate the timescales for ambipolar diffusion at $\rho = \rho_{\text{nuc}}$ from equations (34), (35), (54), (55), and (57), and arrive at

$$t_{\text{ambip}}^s \sim 3 \times 10^9 \frac{T_8^2 L_5^2}{B_{12}^2} \text{years}, \tag{58}$$

and

$$t_{\text{ambip}}^{ir} \sim \frac{5 \times 10^{15}}{T_8^6 B_{12}^2} \left(1 + 5 \times 10^{-7} T_8^8 L_5^2\right) \text{years}, \tag{59}$$

where $B_{12} \equiv B/(10^{12}\text{G})$. The expression for t_{ambip}^s is equal to the second term in t_{ambip}^{ir}. They account for the retardation of the charged particle flux by frictional drag and approximately reproduce the timescale that Haensel, Urpin, and Yakovlev (1990) attribute to enhanced ohmic decay. The first term in t_{ambip}^{ir} expresses the choking of the irrotational part of the charged particle flux by pressure gradients. It dominates under conditions expected to hold inside neutron stars. The minimum value of t_{ambip}^{ir} as a function of T is of order $10^{11} L_5^{3/2} B_{12}^{-2}$ years and occurs for $T_8 \approx 7 L_5^{-1/4}$.

If the regular URCA reactions operate, λ would be larger by a factor of order $5 \times 10^7 T_8^{-2}$ than the value given in equation (57) (Lattimer et al., 1991). This

would not affect the value of t^s_{ambip}, but the appropriate expression for t^{ir}_{ambip} would become

$$t^{ir}_{\text{ambip}} \sim \frac{10^8}{T_8^4 B_{12}^2} \left(1 + 3 \times 10^1 T_8^6 L_5^2\right) \text{ years.} \qquad (60)$$

The minimum value of t^{ir}_{ambip} would be reduced to about $10^9 L_5^{4/3} B_{12}^{-2}$ years and occur at $T_8 \approx 0.6 L_5^{-1/3}$. This great reduction of t^{ir}_{ambip} at fixed T would be less significant than one might think because it would be accompanied by very rapid cooling. Thus, it is almost certain that the irrotational part of the charged particle flux would still be choked by pressure gradients.

If the neutrons form a superfluid, the drag associated with ambipolar diffusion would be greatly reduced. This would increase the magnitude of the solenoidal part of the charged particle flux. However, the superfluid energy gap would block the URCA reactions that are required to maintain the irrotational part of the flux. These considerations emphasize that the distinction between ohmic decay and ambipolar diffusion is more than semantic. For example, in their study of the electrical conductivity of magnetized neutron stars, Yakovlev and Shalybkov (1990) conclude that magnetically enhanced ohmic decay of cross field currents does not occur if the neutrons form a superfluid. However, realizing that ambipolar diffusion and not ohmic dissipation is under investigation makes it clear that neutron superfluidity speeds up the dissipation of magnetic energy.

There has been considerable discussion of the loss of magnetic flux from neutron star cores under the assumption that the neutrons are superfluid and the protons form a type II superconductor. The most popular ideas are that the quantized flux tubes rise due to magnetic buoyancy (Muslimov and Tsygan 1985, Jones 1987), or are pinned to and dragged by neutron vortices that migrate away from the rotation axis as the star is despun (Srinivasan, Bhattacharya, Muslimov, and Tsygan 1990). Although it was not recognized by the authors, these proposals are variants of ambipolar diffusion. Because the radii of curvature of the proton and electron orbits

are much larger than the spacing between flux tubes, the charged particle fluids satisfy macroscopic equations of motion. Any drift of magnetic flux tubes faster than that permitted by ohmic decay must be accompanied by a flux of charged particles (Harrison 1991). Of course, the relation between the average magnetic flux density and the magnetic stress is modified by proton superconductivity (Easson and Pethick 1977). Harrison (1991) appreciated the relation between the buoyant rise of flux tubes and ambipolar diffusion. However, he incorrectly surmised that pressure gradients would block the ambipolar drift. In so doing he, like Pethick (1991), overlooked the distinction between the solenoidal and irrotational parts of the charged particle flux. It would be worth reexamining the motion of the flux tubes with the added restriction that the charged particle flux is purely solenoidal. This could spell trouble for the hypothesis that flux tubes are pulled along by neutron vortices.

We have been proceeding as though protons and electrons are the only species of charged particles in the fluid cores of neutron stars. Nevertheless, as discussed in §3.5, it is plausible that other charged particle species make an appearance not far above nuclear density. A composition gradient in the charged particle fraction of the core fluid would impede the solenoidal component of the charged particle flux. The severity of this effect would depend upon the rate at which interactions could act to smooth departures from chemical equilibrium. These rates could be very slow if weak interactions among highly degenerate particles were involved, or if superfluid energy gaps were present. A residual field would be trapped in the inner core if ambipolar diffusion were blocked there. The residual strength of the surface field would be related to that in the inner core by $(R_i/R)^3$, where R_i is the radius of the inner core.

We summarize our discussion of ambipolar diffusion as follows. Ambipolar diffusion is a viable mechanism for the dissipation of magnetic energy in regions where the charged particle fluid is chemically homogeneous. The charged particle flux associated with ambipolar diffusion is purely solenoidal, the irrotational part

being choked by pressure gradients. These qualitative conclusions are independent of whether or not the direct URCA reactions occur, the neutrons form a superfluid, or the protons are superconducting. Charged particle composition gradients would inhibit the solenoidal component of the particle flux.

5.3. Hall Drift

The timescale for Hall drift is obtained from equation (40) using n_c from equation (55) :

$$t_{\text{Hall}} \approx 5 \times 10^8 \frac{L_5^2}{B_{12}} \left(\frac{\rho}{\rho_{\text{nuc}}} \right) \text{ years.} \tag{61}$$

Unlike ohmic decay or ambipolar diffusion, Hall drift is insensitive to the state of matter in the neutron stars. It occurs in both the fluid core and solid crust, although its implications are less obvious in the former than in the latter. Since Hall drift conserves magnetic energy, it cannot be a direct cause of magnetic field decay. However, if the speculative picture of magnetic turbulence advanced in §4 is valid, it could tangle the field, thus enhancing ohmic dissipation. We evaluate the tangent of the Hall angle, $\mathcal{R}_B$, by forming the ratio of t_{ohmic} given in equation (53) to t_{Hall} from equation (61) above:

$$\mathcal{R}_B \sim 4 \times 10^2 \frac{B_{12}}{T_8^2} \left(\frac{\rho}{\rho_{\text{nuc}}} \right)^2. \tag{62}$$

What we are interested in is the Hall drift in the crust. For $\rho = \rho_{\text{nuc}}$, the numerical expressions for t_{Hall} and $\mathcal{R}_B$ apply to the boundary between the core and crust. Higher in the crust, the low temperature electrical conductivity depends on the abundance of lattice impurities. It is likely that these are so rare that $\mathcal{R}_B \gg 1$, at least in the inner crust. Should $\mathcal{R}_B \lesssim 1$, then ohmic dissipation would limit the lifetimes of crustal currents.

Our estimate for t_{Hall} is robust and suggests that Hall drift might be an important process in the decay of a neutron star's magnetic field if the currents that

support the field are confined to the crust (Jones 1988). Should Hall drift be the limiting factor in the decay of a neutron star's magnetic field, the field strengths would decline approximately as t^{-1}, at least while $\mathcal{R}_B \gg 1$. Note that, if the magnetic field as well as the currents that support it is confined to the crust, the surface field strength would be about an order of magnitude smaller than the crustal field strength.

ACKNOWLEDGEMENTS

REFERENCES

Baym, G., Pethick, C., & Pines, D. 1969a, Nature, **224**, 673

Baym, G., Pethick, C., & Pines, D. 1969b, Nature, **224**, 674

Bhattacharya, D., Wijers, R. A. M. J., Hartman, J. W., & Verbunt, F. 1991, A&A, in press

Bisnovatyi-Kogan, G. S., & Komberg, B. V. 1975, Sov. Astr., **18**, 217

Blandford, R. D., Applegate, J. H., & Hernquist, L. 1983, MNRAS, **204**, 1025

Chiu, H., & Salpeter, E. E. 1964, Phys. Rev. Lett., **12**, 413

Easson, I., & Pethick, C. 1977, Phys. Rev. D, **16**, 275

Ewart, G. M., Guyer, R. A., & Greenstein, G. 1975, ApJ, **202**, 238

Haensel, P., Urpin, V. A., & Yakovlev, D. G. 1990, A&A, **229**, 133

Harrison, E. 1991, MNRAS, **248**, 419

Jones, P. B. 1987, MNRAS, **228**, 513

Jones, P. B. 1988, MNRAS, **233**, 875

Kingsep, A. S., Chukbar, K. V., & Yan'kov, V. V. 1990, Rev. Plasma Phys., **16**, 243

Kolmogoroff, A. N. 1941, Dokl. AN SSSR, **30**, 299

Lattimer, J. M., Pethick, C. J., Prakash, M., & Haensel, P. 1991, Phys. Rev. Lett., **66**, 2701

Lyne, A. G., Manchester, R. N., Taylor, J. H. 1985, MNRAS, **213**, 613

Murakami, T., et al. 1988, Nature, **335**, 234

Muslimov, A. G., & Tsygan, A. I. 1985, Sov. Astr. Lett., **11**, 80

Narayan, R., & Ostriker, J. P. 1990, ApJ, **352**, 222

Parker, E. N. 1979, Cosmical Magnetic Fields, Oxford University Press

Pethick, C. J. 1991, Nordita preprint

Reisenegger, A., & Goldreich, P. 1992, ApJ, submitted

Sang, V., & Chanmugam, G. 1987, ApJ, **323**, L61

Sawyer, R. F. 1989, Phys. Rev. D, **39**, 3804

Shibazaki, N., Murakami, T., Shaham, J., & Nomoto, K. 1989, Nature, **342**, 656

Srinivasan, G., Bhattacharya, D., Muslimov, A. G., & Tsygan, A. I. 1990, Curr. Sci., **59**, 31

Vainshtein, S. I. 1973, JETP, **37**, 73

Yakovlev, D. G. & Shalybkov, D. A. 1990, Sov. Astr. Lett., **16**, 86

Zakharov, V. E. 1971, JETP, **33**, 927

Zakharov, V. E. 1983, Basic Plasma Physics, vol 2, ed. A. A. Galeev & R. N. Sudan (North Holland), p. 1

Chapter 4

THE SPIN-UP PROBLEM IN HELIUM II

ABSTRACT

The laminar spin-up of helium II is studied by solving the linearized equations of motion for the normal and superfluid components and the quantized vortex lines in a simple case. The fluid is taken to be confined between two parallel planes whose angular velocity increases at a small, steady rate. The vortex lines are treated as a continuum. No direct interactions between the vortex lines and the walls are included. Two mechanisms are identified for the transfer of angular momentum from the container to the interior fluid. In the first place, classical Ekman pumping occurs in the normal fluid component. Secondly, mutual friction between the normal Ekman layer and the vortex lines produces an (Ekman-like) secondary flow in the superfluid component. In both mechanisms, mutual friction in the interior couples the normal and superfluid components together, so that both components spin up. Normal-fluid Ekman pumping is found to dominate at temperatures close to the λ-point ($T_\lambda = 2.17\,\mathrm{K}$), while the second mechanism becomes progressively more important at lower temperatures. In the small-Ekman-number limit, when the vertical container dimension $2a$ is much larger than the Ekman layer thickness, the spin-up time (i. e., the time lag between the container and the interior fluid) for both components is $t_{spin-up} \approx f(T)a\Omega_0^{-1/2}$, where Ω_0 is the angular velocity and $f(T)$ is a decreasing function of temperature. Although some experimental spin-up times in He II have been reported in the literature, their analysis involves many uncertainties. Thus, new experiments to test this model should be highly desirable.

1. INTRODUCTION

Two distinct motivations exist for the theoretical study of the hydrodynamics of superfluid spin-up and spin-down. Firstly, a complete description of spin-up in superfluid ^{4}He (and ^{3}He) could be checked in the laboratory, providing an important test of our present understanding of quantum fluids (Campbell & Krasnov 1982) and, especially, a basis for the study of related phenomena, like vortex pinning and depinning, vortex nucleation, and the transition to superfluid turbulence (Donnelly 1991). On the other hand, superfluid spin-up processes are likely to be relevant to the interpretation of variations of the rotation rate of pulsars on several different time scales (Sauls 1989, Lamb 1991, Baym, Epstein, & Link 1992; see Lyne, Graham Smith, & Pritchard 1992 for intriguing new observations).

Greenspan and Howard (1963) solved the spin-up problem for a homogeneous, classical fluid in an axially symmetric container whose angular velocity Ω is impulsively changed by a small fraction, the Rossby number (Greenspan 1968) $\varepsilon = \Delta\Omega/\Omega$. They showed that in the generic case it occurs in three stages: 1) Formation of a viscous boundary layer in a time scale of the order of the rotation period, 2) spin-up of the interior fluid by a secondary flow that "returns" through the boundary layer, in an Ekman time (geometric mean of rotation period and viscous diffusion time), and 3) decay of the residual oscillations (inertial modes), in the usually much longer viscous time (see also Greenspan 1968, Chapter 2, for a complete discussion). The more general (non-linear) problem in which the angular velocity is changed by a fraction of order unity or greater (e. g., spin-up from rest) has also been studied by several authors (Benton & Clark 1974). Although it presents some new features, the main time scales are usually the same as in the linear limit, unless the fluid becomes turbulent (Wedemeyer 1964, Greenspan 1968, Benton & Clark 1974).

Systematic measurements of the spin-up time in a superfluid were performed by Tsakadze and Tsakadze (1973, 1975, 1980), who attempted to model a pulsar in

the laboratory as a glass sphere containing He II (liquid ^{4}He at temperatures below the lambda point, $T_\lambda = 2.17\,\text{K}$). In particular, they measured the spin-up time as a function of temperature, T, initial rotation rate, Ω_0, and change in rotation rate, $\Delta\Omega$, for moderate to large Rossby numbers, and fitted their results by an analytical function partially justified by dimensional analysis.

Alpar (1978) tried to explain their data[1] by postulating that the spin-up process in a superfluid might be similar in character to that occurring in a classical fluid, but with the quantum of circulation, $\kappa = h/m$, playing the role of an effective viscosity. (Here, $h = 2\pi\hbar$ is Planck's constant, and m is the mass of the elementary boson, i. e. of one atom in superfluid ^{4}He, and of a Cooper pair in fermionic superfluids.)

Theoretical models for superfluid spin-up were constructed by Campbell and Krasnov (1982) and by Adams, Cieplak, and Glaberson (1985), mainly for the purpose of studying the interaction between the superfluid vortex lines and the walls of the container. In both cases, the authors took the friction coefficient between the vortices and the walls as a free parameter, and in the second case a pinning force was included in the same way. Campbell and Krasnov compared their results with experimental data for spin-up from rest (Reppy, Depatie, & Lane 1960, Reppy & Lane 1961, 1965) and found a reasonable agreement for appropriate choices of their free parameter. Adams et al. performed low-Rossby-number spin-up experiments in containers with smooth and rough walls. Their results at 1.3 K agreed well with their model (setting the pinning force equal to zero in the smooth-wall experiments, and otherwise adjusting the parameters to fit the data), but not those at 2.1 K. Neither model, however, allowed for a poloidal secondary flow, which plays such a crucial role in classical spin-up. It was to this fact that Adams et al. (1985) attributed the failure of their model at 2.1 K, where most of the

---

[1]Alpar (1978), Adams et al. (1985), and Donnelly (1991) state that the spin-up in He II is *quicker* than in He I, in contradiction with the graphs of Tsakadze and Tsakadze (1973, 1980), which show the opposite effect, consistent with the monotonically increasing kinematic viscosity (as a function of T) in the region around T_λ.

fluid is normal. Furthermore, there is no explanation so far for the frictional force used in both models, although Adams et al. pointed out that its magnitude, as derived from the experimental data, is about what would be expected from the friction between the vortex lines and the normal fluid that is viscously coupled to the container in a classical Ekman layer.

A study of superfluid spin-up from rest was also done by Poppe and Schmidt (1987), who solved the full equations of motion for the coupled superfluid and normal fluid numerically. The main features of their results were reproduced by approximate analytical calculations of Peradzynski, Filipkowski, and Fiszdon (1990), who included a poloidal secondary flow, but took the radial velocities of the superfluid and the normal fluid to be equal to each other, and guessed their value by analogy with the classical spin-up problem.

The purpose of this paper is a careful examination of the linear, laminar spin-up problem in incompressible superfluids. In §2, the linearized equations of motion (Chandler & Baym 1986) for a superfluid/normal fluid mixture (such as He II), and the boundary conditions at the containing walls are presented and written in a form convenient for this problem, with suitable approximations made. In §3, the quasi-steady-state motion of such a fluid confined between two infinite, parallel, smooth planes spinning up (or down) at a constant, slow, rate is found by solving these equations analytically. (The similar, but simplified, problem of a pure superfluid with vortex lines interacting via a frictional force with the boundaries is studied in the Appendix, with the purpose of clarifying the mechanism of superfluid spin-up.) In §4, the spin-up times and secondary flows are found as functions of the container dimension along the rotation axis, the rotation rate, and the temperature, and the physical content of the solution is discussed. The range of validity of the analysis of §3 is examined in §5. In §6, a very tentative comparison to the empirical expression of Tsakadze and Tsakadze (1975, 1980) for the spin-up time shows similar numbers and similar qualitative behavior, but no detailed quantitative agreement. However, several uncertainties involved in analyzing their results make this comparison not

very meaningful. Thus, new experiments of a similar kind, specially designed to test the model given here, should be crucial to probe our present understanding of the superfluid spin-up process.

2. ASSUMPTIONS AND EQUATIONS

The equations of motion used in this paper are those derived by Chandler and Baym (1986; see also Baym & Chandler 1983). These equations treat the distribution of quantized vortices as a continuum, much in the same way as the classical theory of elasticity treats the ions in a crystal. The underlying assumption is, of course, that there are many vortices present in the system, and that all important (macroscopic) length scales are much larger than the separation between vortex lines. In ^{4}He rotating at an angular velocity $\Omega_0 = 1\,\mathrm{s}^{-1}$, the separation between vortex lines is $b_0 \approx 0.02\,\mathrm{cm}$, so this assumption is correct for most experiments.

Except for including terms that take into account the finite compressibility and shear modulus of the vortex lattice in the plane perpendicular to the axis of rotation, these equations are equivalent to the simpler and more popular HVBK (Hall-Vinen-Bekarevich-Khalatnikov) equations (Hall 1963; see Donnelly 1991, §6.2.4, for the HVBK equations in a rotating reference frame). As is shown below, the additional terms do not play any role in the spin-up dynamics.

It will also be assumed that the maximal differences in angular velocity between different fluid elements or between these and the container are small compared to the container's angular velocity, and that in some finite time interval all relevant variables change only by a small fraction. Thus, the problem to be solved reduces, for the same time interval, to one of small perturbations with respect to a state of solid-body rotation at a constant angular velocity Ω_0. It is therefore convenient to use a frame of reference rotating with angular velocity $\boldsymbol{\Omega}_0 = \Omega_0\hat{\mathbf{z}}$ and linearize the equations of motion, as Greenspan and Howard (1963) did in their analysis of the classical spin-up problem, and Chandler and Baym (1986) in their study of

the oscillations of the superfluid vortex lattice. In this rotating reference frame, cylindrical coordinates, r, ϕ, and z, and the corresponding unit basis vectors, $\hat{\mathbf{r}}$, $\hat{\phi}$, and $\hat{\mathbf{z}}$, are used.

The superfluid and normal components can be described by densities ρ_s, ρ_n and velocities $\mathbf{v}_s$, $\mathbf{v}_n$. The equation of mass conservation reads

$$\frac{\partial \rho}{\partial t} + \boldsymbol{\nabla} \cdot \mathbf{j} = 0, \tag{1}$$

where $\rho \equiv \rho_s + \rho_n$ is the total mass density, and $\mathbf{j} \equiv \rho_s \mathbf{v}_s + \rho_n \mathbf{v}_n$ is the mass current or momentum density. In the linear approximation, entropy is also conserved, and the equation of entropy conservation becomes

$$\frac{\partial(\rho s)}{\partial t} + \boldsymbol{\nabla} \cdot \left(\rho s \mathbf{v}_n - \kappa_{th} \frac{\boldsymbol{\nabla} T}{T} \right) = 0, \tag{2}$$

where s is the entropy per unit mass, κ_{th} is the thermal conductivity, and T is the temperature. The two terms acted upon by the divergence operator represent the entropy transport by normal-fluid convection and by thermal diffusion. In typical experiments with He II, the convection overwhelms the diffusion by several orders of magnitude, so the thermal conductivity may be set equal to zero (Wilks 1967). Furthermore, it is well known that spatial variations in the total density produce waves of first (usual) sound, and variations in the entropy density produce emission of second sound (Wilks 1967, Tilley & Tilley 1990). Since the velocities of interest in spin-up experiments are much smaller than the velocities of both first and second sound, and no external sources of heat or mass are present, the fluid can be assumed to be incompressible[2] and isentropic, so that in the linear approximation the equations (1) and (2) simplify to

---

[2] The density will not only be taken as constant in time, but also the equilibrium density will be assumed to be independent of position, although the pressure in the rotating fluid of course increases with radius.

$$\nabla \cdot \mathbf{v}_s = \nabla \cdot \mathbf{v}_n = 0. \tag{3}$$

These equations are complemented by the conservation laws for superfluid vorticity (or number of quantized vortex lines) and momentum, and by the force balance on the (virtually massless) vortex lines, given as eqs. (22) in Chandler and Baym (1986). By using eq. (3), these can be written as

$$\frac{\partial \mathbf{v}_s}{\partial t} + 2\Omega_0 \times \dot{\epsilon} = -\nabla \mu', \tag{4}$$

$$\frac{\partial \mathbf{j}}{\partial t} + 2\Omega_0 \times \mathbf{j} - \eta_n \nabla^2 \mathbf{v}_n = -\nabla P' - \sigma, \tag{5}$$

and

$$\rho_s 2\Omega_0 \times (\mathbf{v}_s - \dot{\epsilon}) = -\sigma - \mathbf{D}. \tag{6}$$

Here, ϵ is the displacement of the vortex lines from the positions they would occupy if the superfluid were in solid-body rotation at angular velocity Ω_0 (ϵ is taken to be perpendicular to Ω_0), P' and μ' are the reduced pressure and chemical potential per unit mass, defined in terms of the true pressure and chemical potential per unit mass as $P' = P - \frac{1}{2}\rho(\Omega_0 \times \mathbf{r})^2$ and $\mu' = \mu - \frac{1}{2}(\Omega_0 \times \mathbf{r})^2$, and η_n is the dynamic viscosity of the normal fluid component. The force due to elastic deformations of the vortex lattice is

$$\sigma = 2\Omega_0 \rho_s \left(-\nu_s \frac{\partial^2 \epsilon}{\partial z^2} + \frac{\kappa}{16\pi} \left[2\nabla_\perp (\nabla \cdot \epsilon) - \nabla_\perp^2 \epsilon \right] \right), \tag{7}$$

where $\nabla_\perp \equiv \nabla - \hat{\mathbf{z}} \partial / \partial z$. The "vortex line tension parameter" ν_s is given in terms of the vortex line separation $b_0 = (\kappa/2\Omega_0)^{1/2}$ and the vortex core radius a_0 as

$$\nu_s \equiv (\kappa/4\pi) \ln(b_0/a_0). \tag{8}$$

It has dimensions of kinematic viscosity (or circulation) and behaves, in a restricted way that will become clearer below, like an effective kinematic viscosity of the superfluid component (cf. Alpar 1978). Finally, the mutual friction force is written as

$$\mathbf{D} = -\beta_0 \rho_s \hat{\mathbf{z}} \times [2\mathbf{\Omega}_0 \times (\dot{\epsilon} - \mathbf{v}_n)] - \beta_0' \rho_s 2\mathbf{\Omega}_0 \times (\dot{\epsilon} - \mathbf{v}_n), \tag{9}$$

where β_0 and β_0' are dimensionless friction coefficients.

From eqs. (4), (5), and (6), it is possible to derive an equation of motion for the normal component that closely resembles the classical Navier-Stokes equation in a rotating reference frame:

$$\frac{\partial \mathbf{v}_n}{\partial t} + 2\mathbf{\Omega}_0 \times \mathbf{v}_n = -\mathbf{\nabla} \left(\frac{P' - \rho_s \mu'}{\rho_n} \right) + \nu_n \nabla^2 \mathbf{v}_n + \frac{\mathbf{D}}{\rho_n}, \tag{10}$$

where $\nu_n \equiv \eta_n / \rho_n$ is the kinematic viscosity of the normal fluid. Finally, eq. (4) can be replaced by its time-integral:

$$\mathbf{v}_s + 2\mathbf{\Omega}_0 \times \epsilon = -\mathbf{\nabla}\lambda, \tag{11}$$

with $\partial \lambda / \partial t = \mu'$.

If the container has axial symmetry, and its walls are thermally insulating,[3]

$$\hat{\mathbf{n}} \cdot \mathbf{v}_s |_{walls} = \hat{\mathbf{n}} \cdot \mathbf{v}_n |_{walls} = 0, \tag{12}$$

where $\hat{\mathbf{n}}$ is a unit vector normal to the wall. The boundary condition for the tangential component of the normal fluid velocity is simply the usual no-slip condition; if the container rotates with a time-dependent angular velocity $\Omega_1(t)\hat{\mathbf{z}}$ (with respect to the rotating reference frame), this can be written as

---

[3]If there is heat flow through the walls, only the normal component of the total mass current $\mathbf{j}$ is zero, and the normal component of the normal-fluid velocity is given in terms of the heat flux $\mathbf{q}$ by $\hat{\mathbf{n}} \cdot (\mathbf{q} - \rho s \mathbf{v}_n) = 0$.

$$\hat{n} \times v_n|_{walls} = r\Omega_1(t)\hat{n} \times \hat{\phi}. \tag{13}$$

Thermal counterflow experiments (Yarmchuk and Glaberson 1979, Hedge and Glaberson 1980) show that the studied container walls fall into two distinct groups, "rough" and "smooth," of which only those of the first group seem to show any signs of vortex-surface interaction (pinning or friction). For simplicity, only walls of the second group will be considered here, so that the remaining boundary condition becomes

$$\hat{n} \times \left(\hat{z} + \frac{\partial \epsilon}{\partial z}\right)|_{walls} = 0. \tag{14}$$

Of course, this condition applies only to those walls at which some vortex lines end, not to those which are parallel to the lines everywhere (like the sidewalls of a cylindrical container rotating around its axis of symmetry), for which the condition is $\hat{n} \cdot (\hat{z} + \partial\epsilon/\partial z)|_{walls} = 0$. Furthermore, it has to be noted that the use of the linearized expression for σ (eq. [7]) requires that $|\partial\epsilon/\partial z| \ll 1$ everywhere. Applied to the walls satisfying eq. (14), this condition translates into $\hat{n} \approx \pm\hat{z}$, i. e., all walls at which vortex lines end must be nearly perpendicular to the axis of rotation.

The equations of motion, eqs. (6), (10), and (11), together with the explicit expressions for σ and D (eqs. [7] and [9]) and the boundary conditions, (12), (13), and (14), give a complete description of the dynamics of the system.

3. A MODEL PROBLEM

The problem to be studied here consists of a normal fluid/superfluid mixture (such as He II) confined between two parallel, infinite, smooth, thermally insulating planes (at $z = \pm a$) whose angular velocity varies synchronously as $\Omega(t) = \Omega_0 + \alpha t$, where Ω_0 and α are constants, and the ratio α/Ω_0 is small enough for the linear theory presented in the previous section to apply. (Precisely how small it has to

be is examined in §5.) It is assumed that the planes have been spinning up (if $\alpha/\Omega_0 > 0$) or down (if $\alpha/\Omega_0 < 0$) for a time long enough for all transients and residual oscillations (Greenspan & Howard 1963) to have died away, so that only a quasi-steady-state spin-up process is observed. The analogous problem for a classical fluid was solved by Bondi and Lyttleton (1948), who were interested in the secular retardation of the Earth's core.

Clearly, the three vector fields, $\mathbf{v}_n$, $\mathbf{v}_s$, and ϵ, will have both azimuthal symmetry (their components in cylindrical coordinates are independent of the azimuthal angle ϕ) and reflection symmetry with respect to the plane $z = 0$. The solution to the classical spin-up problem (Greenspan & Howard 1963) suggests that the velocity fields have the "von Kármán similarity" form (von Kármán 1921)

$$\mathbf{v}_c = r[U_c(z,t)\hat{\mathbf{r}} + V_c(z,t)\hat{\boldsymbol{\phi}}] - 2\int_0^z U_c(z',t)dz'\hat{\mathbf{z}}, \qquad (15)$$

where the subscript $c = s, n$ labels the superfluid and normal components. This choice is consistent with the symmetry requirements (U_c and V_c have to be even functions of z) and with the boundary conditions, and automatically satisfies the incompressibility conditions, eqs. (3). Furthermore, in the quasi-steady-state situation described above, both the normal fluid and the superfluid spin up with angular acceleration α, i. e.

$$V_c(z,t) = \alpha[t - T_c(z)], \qquad (16)$$

and the secondary flows are independent of time:

$$U_c(z,t) = U_c(z). \qquad (17)$$

From the z-component of eq. (11), it is clear that $\lambda = R(r,t) + Z(z)$, with $dZ/dz = 2\int_0^z U_s dz$, and R (so far) an arbitrary function. The other two components yield

$$\epsilon = \frac{r}{2\Omega_0}\left(-\alpha[t - T_s(z)]\hat{\mathbf{r}} + \left[U_s(z) + \frac{1}{r}\frac{\partial R(r,t)}{\partial r}\right]\hat{\phi}\right). \tag{18}$$

Therefore, from the radial component of eq. (6), one obtains

$$(1 + \beta_0')\left(\frac{1}{2\Omega_0 r}\frac{\partial^2 R}{\partial r\partial t} - \alpha t\right) = -\alpha\left(T_s - \delta_s^2\frac{d^2 T_s}{dz^2}\right) - \alpha\beta_0' T_n + \beta_0\left(\frac{\alpha}{2\Omega_0} + U_n\right), \tag{19}$$

where

$$\delta_s = \left(\frac{\nu_s}{2\Omega_0}\right)^{1/2} \tag{20}$$

is a constant with units of length. Since the left-hand side of eq. (19) depends only on r and t, and the right-hand side, only on z, their equality implies that both are constants, independent of r, z, and t. Imposing, furthermore, that the components of ϵ scale with r (like the radial and azimuthal components of the velocities), it is possible to write[4]

$$R(r,t) = \frac{1}{2}\Omega_0\alpha r^2(t - T_0)^2, \tag{21}$$

where T_0 is a constant to be determined from the boundary conditions. Thus, the vortex displacement vector becomes

$$\epsilon = r\left(-\frac{\alpha}{2\Omega_0}[t - T_s(z)]\hat{\mathbf{r}} + \left[\frac{U_s(z)}{2\Omega_0} + \frac{\alpha}{2}(t - T_0)^2\right]\hat{\phi}\right). \tag{22}$$

From the azimuthal component of eq. (10), one obtains the differential equation

$$\left(1 - \beta_0'\frac{\rho_s}{\rho_n}\right)\left(U_n + \frac{\alpha}{2\Omega_0}\right) - \alpha\beta_0\frac{\rho_s}{\rho_n}(T_n - T_0) + \frac{\alpha}{2}\delta_n^2\frac{d^2 T_n}{dz^2} = 0, \tag{23}$$

---

[4]In principle, an arbitrary function of t could be added to this expression, without any effect on the dynamics.

and eliminating the gradient term from its other two components yields

$$\alpha \left(1 - \beta_0' \frac{\rho_s}{\rho_n}\right) \frac{dT_n}{dz} + \beta_0 \frac{\rho_s}{\rho_n} \frac{dU_n}{dz} - \frac{1}{2}\delta_n^2 \frac{d^3 U_n}{dz^3} = 0, \tag{24}$$

where

$$\delta_n = \left(\frac{\nu_n}{\Omega_0}\right)^{1/2} \tag{25}$$

is the classical Ekman layer thickness for the normal fluid. Similarly, eq. (6) yields

$$T_s - \delta_s^2 \frac{d^2 T_s}{dz^2} = T_0 + \frac{\beta_0}{\alpha}\left(U_n + \frac{\alpha}{2\Omega_0}\right) - \beta_0'(T_n - T_0), \tag{26}$$

and

$$U_s - \delta_s^2 \frac{d^2 U_s}{dz^2} = -\frac{\alpha}{2\Omega_0} - \alpha\beta_0(T_n - T_0) - \beta_0'\left(U_n + \frac{\alpha}{2\Omega_0}\right). \tag{27}$$

The boundary conditions, eqs. (12), (13), and (14), can be written in terms of T_s, T_n, U_s, and U_n as

$$\int_0^{\pm a} U_s(z)dz = \int_0^{\pm a} U_n(z)dz = T_n(\pm a) = U_n(\pm a) = \frac{dT_s}{dz}(\pm a) = \frac{dU_s}{dz}(\pm a) = 0. \tag{28}$$

Elimination of U_n from the normal-fluid equations ([23] and [24]) gives the single equation

$$\left[\left(1 - \beta_0' \frac{\rho_s}{\rho_n}\right)^2 + \left(\beta_0 \frac{\rho_s}{\rho_n}\right)^2\right] \frac{dT_n}{dz} - \delta_n^2 \beta_0 \frac{\rho_s}{\rho_n} \frac{d^3 T_n}{dz^3} + \frac{1}{4}\delta_n^4 \frac{d^5 T_n}{dz^5} = 0, \tag{29}$$

which has solutions of the forms $T_n = $ constant and $T_n \propto \exp(\pm k_R z \pm i k_I z)$, with

$$(k_R^2 - k_I^2)\delta_n^2 = 2\beta_0 \frac{\rho_s}{\rho_n}, \tag{30}$$

and

$$k_R k_I \delta_n^2 = 1 - \beta_0' \frac{\rho_s}{\rho_n}, \tag{31}$$

or, solving for k_R and k_I,

$$k_R \delta_n = \left\{ \left[\left(1 - \beta_0' \frac{\rho_s}{\rho_n} \right)^2 + \left(\beta_0 \frac{\rho_s}{\rho_n} \right)^2 \right]^{\frac{1}{2}} + \beta_0 \frac{\rho_s}{\rho_n} \right\}^{\frac{1}{2}}, \tag{32}$$

and

$$k_I \delta_n = \pm \left\{ \left[\left(1 - \beta_0' \frac{\rho_s}{\rho_n} \right)^2 + \left(\beta_0 \frac{\rho_s}{\rho_n} \right)^2 \right]^{\frac{1}{2}} - \beta_0 \frac{\rho_s}{\rho_n} \right\}^{\frac{1}{2}}. \tag{33}$$

By convention, k_R is taken to be positive, and k_I to have the same sign as $(1 - \beta_0' \rho_s / \rho_n)$. Clearly, it is always the case that $k_R \geq |k_I|$.

The most general solution for $T_n(z)$ that respects the reflection symmetry with respect to the central plane is

$$T_n(z) = T_{n0} + A_0 \cosh(k_R z) \cos(k_I z) + B_0 \sinh(k_R z) \sin(k_I z), \tag{34}$$

where T_{n0}, A_0, and B_0 are constants to be determined from the boundary conditions. An analogous result can be obtained for $U_n(z)$. Both T_n and U_n decay exponentially to a constant value over a distance k_R^{-1} away from the boundary. Typically,

$$k_R a \gtrsim \frac{a}{\delta_n} = \left(\frac{\Omega_0 a^2}{\nu_n} \right)^{\frac{1}{2}} \gtrsim 20 \tag{35}$$

for He II at $T > 1.3\,\mathrm{K}$, with $a = 1\,\mathrm{cm}$ and $\Omega_0 = 1\,\mathrm{s}^{-1}$. In most experimental situations, the boundary layer thickness will be significantly smaller than the dimensions of the container. In the interior of the container, the z-dependent terms

will be exponentially small. Thus, it is possible to treat one boundary layer at a time when applying the boundary conditions, and drop terms of order $\exp(-k_R a)$. Although this is not really necessary, it substantially simplifies the algebra, allowing more insight into the physics involved.

It is useful to define, for each boundary layer, a coordinate ζ that measures the distance from the wall into the fluid, i. e.,

$$\zeta \equiv a - z \tag{36}$$

in the upper boundary layer (at $z = a$), and

$$\zeta \equiv z + a \tag{37}$$

in the lower boundary layer (at $z = -a$). The solution for T_n is of the "Ekman spiral" form (Greenspan 1968),

$$T_n(\zeta) = T_{n0} + [A \cos(k_I \zeta) + B \sin(k_I \zeta)]e^{-k_R \zeta}, \tag{38}$$

in both boundary layers. (Terms of $O[\exp(-k_R a)]$ have already been dropped.)

Imposing the boundary conditions (at $\zeta = 0$) on this and the corresponding expression for U_n, one obtains

$$T_n(\zeta) = T_{n0} \left\{ 1 - [\cos(k_I \zeta) - c \sin(k_I \zeta)]e^{-k_R \zeta} \right\}, \tag{39}$$

and

$$U_n(\zeta) = U_{n0} \left\{ 1 - [c^{-1} \sin(k_I \zeta) + \cos(k_I \zeta)]e^{-k_R \zeta} \right\}, \tag{40}$$

where

$$T_{n0} = \frac{(1/2\Omega_0) + bT_0}{b + c} = -\frac{U_{n0}}{\alpha c}, \tag{41}$$

$$b \equiv \frac{\beta_0 \rho_s / \rho_n}{1 - \beta_0' \rho_s / \rho_n}, \tag{42}$$

and

$$c \equiv \frac{k_I}{(k_R^2 + k_I^2)a - k_R}. \tag{43}$$

In the limit of thin Ekman layers, $k_R a \gg 1$ (cf. eq. [35]),

$$c \approx \frac{k_I}{(k_R^2 + k_I^2)a} = \frac{k_I \delta_n}{(k_R \delta_n)^2 + (k_I \delta_n)^2} E^{\frac{1}{2}} \leq (k_R a)^{-1} \ll 1, \tag{44}$$

where

$$E \equiv \nu_n / (\Omega_0 a^2) = (\delta_n / a)^2 \tag{45}$$

is the normal-fluid Ekman number (Greenspan 1968).

Solving the equations (26) and (27) and imposing the remaining boundary conditions, one obtains[5]

$$T_s(\zeta) = T_{s0} + T_{n0} \left\{ [\tilde{A} \cos(k_I \zeta) + \tilde{B} \sin(k_I \zeta)] e^{-k_R \zeta} + [k_I \tilde{B} - k_R \tilde{A}] \delta_s e^{-\zeta/\delta_s} \right\}, \tag{46}$$

and

$$U_s(\zeta) = U_{s0} + \alpha T_{n0} \left\{ [\tilde{B} \cos(k_I \zeta) - \tilde{A} \sin(k_I \zeta)] e^{-k_R \zeta} - [k_R \tilde{B} + k_I \tilde{A}] \delta_s e^{-\zeta/\delta_s} \right\}, \tag{47}$$

with the dimensionless constants

$$\tilde{A} = \frac{(\beta_0' + \beta_0 c)(1 - \beta_0 \rho_s \nu_s / \rho_n \nu_n) - (\beta_0 - \beta_0' c)(1 - \beta_0' \rho_s / \rho_n) \nu_s / \nu_n}{(1 - \beta_0 \rho_s \nu_s / \rho_n \nu_n)^2 + [(1 - \beta_0' \rho_s / \rho_n) \nu_s / \nu_n]^2} \tag{48}$$

---

[5]Terms of order $\exp(-a/\delta_s)$ and higher are also being neglected here, since $a/\delta_s \approx 40$ for He II with $a = 1 \, \text{cm}$ and $\Omega_0 = 1 \, \text{s}^{-1}$.

and

$$\tilde{B} = \frac{(\beta_0 - \beta_0'c)(1 - \beta_0\rho_s\nu_s/\rho_n\nu_n) + (\beta_0' + \beta_0 c)(1 - \beta_0'\rho_s/\rho_n)\nu_s/\nu_n}{(1 - \beta_0\rho_s\nu_s/\rho_n\nu_n)^2 + [(1 - \beta_0'\rho_s/\rho_n)\nu_s/\nu_n]^2}. \tag{49}$$

The remaining constants (which determine the behavior of the interior fluid) come out to be

$$T_{n0} = \frac{1/c}{[(\rho_n/\rho) + (\rho_s/\rho)g](2\Omega_0)}, \tag{50}$$

$$T_{s0} = T_{n0} + \frac{(1 - g)[(\rho_n/\rho)(1 + \beta_0') - (\rho_s/\rho)(\beta_0' + \beta_0^2 + (\beta_0')^2)]}{\beta_0[(\rho_n/\rho) + (\rho_s/\rho)g](2\Omega_0)}, \tag{51}$$

$$T_0 = T_{n0} + \frac{(1 - g)[(\rho_n/\rho) - (\rho_s/\rho)\beta_0']}{\beta_0[(\rho_n/\rho) + (\rho_s/\rho)g](2\Omega_0)}, \tag{52}$$

$$U_{n0} = -\frac{1}{[(\rho_n/\rho) + (\rho_s/\rho)g]}\frac{\alpha}{2\Omega_0}, \tag{53}$$

and

$$U_{s0} = -\frac{g}{[(\rho_n/\rho) + (\rho_s/\rho)g]}\frac{\alpha}{2\Omega_0}, \tag{54}$$

where

$$g \equiv \left(\frac{k_R}{k_I} - \frac{1}{k_I a}\right)\beta_0 - \beta_0'. \tag{55}$$

4. RESULTS AND DISCUSSION

In He II, the mutual friction force is strong (typically, β_0 is not much smaller than unity). In the usual small-Ekman-number limit ($c \ll 1$), it couples the normal

and superfluid components on time scales much shorter than the spin-up time: For temperatures in the range $1.3\,\mathrm{K} \lesssim T \leq T_\lambda$,

$$\left|\frac{T_{s0} - T_{n0}}{T_{n0}}\right| = \left|\frac{c}{\beta_0}(1-g)\left[\frac{\rho_n}{\rho}(1+\beta_0') - \frac{\rho_s}{\rho}(\beta_0' + \beta_0^2 + (\beta_0')^2)\right]\right|$$

$$\lesssim 10^{-2}\left(\frac{a}{\mathrm{cm}}\right)^{-1}\left(\frac{\Omega_0}{\mathrm{s}^{-1}}\right)^{-1/2}. \tag{56}$$

Thus, a single spin-up time $t_{spin-up} = T_{n0} \approx T_{s0}$ can be used for both components. In the same limit, this time scale can be written as

$$t_{spin-up} \approx f(T)\frac{a}{\Omega_0^{\frac{1}{2}}}, \tag{57}$$

where the function

$$f(T) = \frac{\rho}{\rho_n}\left\{\left[\left(1 - \beta_0'\frac{\rho_s}{\rho_n}\right)^2 + \left(\beta_0\frac{\rho_s}{\rho_n}\right)^2\right]^{\frac{1}{2}} + \beta_0\frac{\rho_s}{\rho_n}\right\}^{-\frac{1}{2}} \nu_n^{-\frac{1}{2}}, \tag{58}$$

plotted in Fig. 1, depends only on temperature (through the viscosity, the density ratios, and the friction coefficients), and not on the container dimension a and the rotation rate Ω_0. The values of $f(T)$ as a function of T are found by using the data in Table I of Barenghi, Donnelly, and Vinen (1983), and converting from the mutual friction parameters B, B' shown there[6] to the parameters β_0, β_0' by the relations given in Chandler and Baym (1986).

The presence of the two terms ρ_n/ρ and $g\rho_s/\rho$ in the denominator of the expressions for T_{n0}, T_{s0}, T_0, U_{n0}, and U_{s0} (eqs. [50] to [54]) suggests the combined

---

[6]The friction coefficients, usually measured by second-sound and thermal counterflow experiments, depend on frequency in the first case, and on the relative velocity, $u_{rel} = |\mathbf{v}_n - \dot{\epsilon}|$, in the second. (References and conversion formulae are given in Swanson, Wagner, Donnelly, & Barenghi 1987.) However, when the values of B (from second-sound experiments) given in Barenghi et al. (1983) are replaced by the values for zero frequency and $u_{rel} = 0.1\,\mathrm{cm}$ from Table II in Swanson et al. (1987), which are probably the most appropriate ones for the present problem, $f(T)$ does not change by more than $\sim 5\%$ anywhere in the range $1.3\,\mathrm{K} \leq T \leq 2.17\,\mathrm{K}$. The effect of the variations of B' should be even less significant. A detailed comparison with a particular experiment can, of course, be made with the values of B and B' appropriate for that experiment, calculated by the algorithm of Swanson et al. (1987).

action of two spin-up mechanisms. The nature of these two mechanisms can be seen most clearly by considering two limiting cases:

1) If $\beta_0 \rho_s / \rho_n$ and $\beta_0' \rho_s / \rho_n$ are small ($\ll 1$), then the spin-up time becomes

$$t_{spin-up} \approx \frac{\rho}{\rho_n} \frac{a}{(\nu_n \Omega_0)^{1/2}}. \tag{59}$$

Except for the correction factor ρ/ρ_n, this is the classical Ekman time. The dominant spin-up process is Ekman pumping in the normal fluid component. The superfluid is also being spun up because it is coupled to the normal fluid by the mutual friction force. (This is true even in the limit of vanishing mutual friction coefficients, since in the steady state the angular velocity difference will adjust to be exactly as large as needed to have both components spinning up with angular acceleration α.) The extra factor arises because both components are being spun up, while only the normal fluid is involved in the Ekman pumping process.

2) If, on the other hand, $\beta_0 \rho_s / \rho_n \gg |1 - \beta_0' \rho_s / \rho_n|$, the spin-up time can be written as

$$t_{spin-up} \approx \frac{\rho}{\rho_s} \frac{k_R a}{2\Omega_0 \beta_0}. \tag{60}$$

If one sets $\gamma = \beta_0 k_R^{-1}$, this expression becomes the same (again, except for the density ratio) as that for the spin-up time in a pure superfluid with a frictional force between the walls and the ends of the vortex lines, which is studied in the Appendix. In the present case, the frictional force is the mutual friction between the superfluid vortex lines and the normal fluid that is viscously coupled to the container in the Ekman layer, as suggested by Adams et al. (1985), and thus it is proportional to the Ekman layer thickness, k_R^{-1}. This friction produces a secondary flow in the superfluid that transports the vortex lines inward. The factor ρ/ρ_s accounts for the fact that, again, both components are being spun up, although only one (in this case the superfluid) is involved in the pumping process.

Which of the two spin-up mechanisms dominates is determined by the values of the variables $\beta_0 \rho_s / \rho_n$ and $\beta_0' \rho_s / \rho_n$, plotted in Fig. 2. At temperatures close to the λ-point, both are small, and normal-fluid Ekman pumping dominates. As the temperature decreases, the friction between the vortex lines and the normal-fluid Ekman layer becomes increasingly important, thus qualitatively confirming the argument given by Adams et al. (1985) to explain the disagreement between their theory and experimental data at 2.1 K, as opposed to the agreement at 1.3 K. Unfortunately, their paper does not provide enough experimental data to make a quantitative comparison with the present model.

Fig. 3 shows that, in disagreement with the assumption of Peradzynski et al. (1990), the radial inflow velocities of the normal and superfluid components are different from each other and from the radial velocity of the vortex lines, given by $\dot{\epsilon}_r = -r\alpha/(2\Omega_0)$. However, it is interesting to see that the average radial mass-flow velocity is the same as the radial velocity of the vortex lines,

$$\frac{j_{r0}}{\rho} = \frac{r}{\rho}(\rho_n U_{n0} + \rho_s U_{s0}) = -\frac{\alpha r}{2\Omega_0} = \dot{\epsilon}_r. \tag{61}$$

That this has to be the case can be seen by subtracting eq. (4), multiplied by ρ, from eq. (5), neglecting the viscous and vortex lattice stress terms, which are irrelevant in the interior, and using the fact that the accelerations (in the rotating frame) of the normal fluid and the superfluid are equal. One obtains

$$2\Omega_0 \times (\mathbf{j} - \rho \dot{\epsilon}) = -\nabla P' + \rho \nabla \mu' = -\rho s \nabla T. \tag{62}$$

The azimuthal symmetry of this problem guarantees that no azimuthal temperature gradients will exist, and thus $j_r/\rho = \dot{\epsilon}_r$ in the interior fluid. This average radial mass-flow velocity is the same as that obtained in the classical spin-up problem (Greenspan & Howard 1963, Wedemeyer 1964), which was used by Peradzynski et al. (1990) as a guess for the radial velocities of both components.[7]

---

[7]This may be a better approximation in the highly nonlinear problem studied by these authors

It is also worth noticing that the interior flows are independent of the parameters characterizing the elasticity of the vortex lattice. This is to be expected in the limit where the normal-fluid Ekman process dominates, since in this case the vortex lines play only a passive role. That it is also true in the opposite limit, when the vortex tension is crucial for the spin-up process, is examined more carefully in the Appendix.

5. RANGE OF VALIDITY

The assumption underlying the linearization of the equations of motion is that all internal velocities of the fluid are much smaller than the velocities due to the overall rotation of the system, i. e.,

$$\left|\frac{\alpha T_c(z)}{\Omega_0}\right| \ll 1, \quad \text{and} \quad \left|\frac{U_c(z)}{\Omega_0}\right| \ll 1, \tag{63}$$

for all z and for both components, $c = n, s$. In the usually appropriate small-Ekman-number limit, this can be reduced to the single (low-Rossby-number) condition

$$\varepsilon \equiv \left|\frac{\alpha T_{n0}}{\Omega_0}\right| \approx \frac{\rho}{\rho_n} \frac{a}{k_R \delta_n^2} \frac{|\alpha|}{\Omega_0^2} \ll 1. \tag{64}$$

This condition also makes sure that the vortex instability found by Glaberson, Johnson, and Ostermeier (1974; see also Ostermeier & Glaberson 1975) does not occur.

It does *not* guarantee, however, that the vortex lines are nearly parallel to the rotation axis, $|\partial\epsilon/\partial z| \ll 1$, as is required for the linearized form of the force due to vortex lattice deformations to be valid. In the interior fluid, this derivative is very nearly zero, but in the boundary layers

---

than in the linear problem studied here.

$$\left|\frac{\partial \epsilon}{\partial z}\right| = \left|\frac{r}{2\Omega_0}\left(\alpha\frac{dT_s}{dz}\hat{\mathbf{r}} + \frac{dU_s}{dz}\hat{\phi}\right)\right|$$
$$\lesssim \left|\frac{\alpha T_{n0}}{2\Omega_0}\right|k_R r(\tilde{A}^2 + \tilde{B}^2)^{\frac{1}{2}}. \tag{65}$$

The normal-fluid Ekman layer can be characterized by a Reynolds number

$$\mathcal{R} \equiv \frac{\alpha T_{n0}r\delta_n}{\nu_n} = \frac{\varepsilon}{E^{\frac{1}{2}}}\frac{r}{a}, \tag{66}$$

in terms of which the condition $|\partial\epsilon/\partial z| \ll 1$ can be written as

$$\mathcal{R} \ll 2(\tilde{A}^2 + \tilde{B}^2)^{-\frac{1}{2}}(k_R\delta_n)^{-1}. \tag{67}$$

The expression on the right-hand side depends only on temperature (not on the container dimensions, or Ω_0, or α), and is ≥ 20 for He II, except very close to T_λ. It is likely that the spin-up times derived do not change significantly if this condition is violated. In the limit in which the normal-fluid Ekman pumping dominates, the vortex lines play only a passive role, so this is certainly the case. In the opposite limit, the situation is not as clear-cut, but considering that the spin-up time in the simplified problem studied in the Appendix does not depend on whether this condition is true, and that the thickness of the Ekman layer does not depend on the bending of the vortex lines, one might not expect a large change either.

Of course, a simple solution of the form given by eq. (15) will only represent the generic behavior of the fluid as long as the boundary layers remain laminar. In a classical fluid, the Ekman layer becomes unstable once its characteristic Reynolds number (defined as in eq. [66]) reaches a critical value of (Greenspan 1968)

$$\mathcal{R}_{crit} \approx 56.3 + 58.4\varepsilon. \tag{68}$$

Thus, it may be expected that the boundary layer in the problem studied here also becomes unstable at some critical Reynolds number. In other types of flow,

particularly flows through thin capillaries, He II is found to become turbulent when either component (the superfluid or the normal fluid) reaches a critical Reynolds number which is usually of the same order as (or even lower than) the critical Reynolds numbers for classical fluids (Staas, Taconis, & van Alphen 1961, Courts & Tough 1988, Oestereich & Xie 1991). However, the onset of turbulence in a superfluid is still a problem far from being well understood (Tough 1982, Schwarz 1992).

In summary, the solution derived in §3 should be applicable as long as eq. (64) is satisfied, and the Ekman-layer Reynolds number defined in eq. (66) is much smaller than a critical value $\mathcal{R}_0 \approx 20$.

6. COMPARISON TO EXPERIMENTAL DATA

Of course, the spin-up time given in eq. (57) has been derived for a very idealized geometry, impossible to reproduce in an experiment. However, in the classical spin-up problem, the same time scale (the Ekman time $t_E = a/(\nu\Omega_0)^{1/2}$ calculated by taking a to be some characteristic dimension of the container in the direction parallel to the rotation axis) is relevant for almost any simple, azimuthally symmetric, container geometry (as long as the dimension perpendicular to the axis is not so small as to make viscous diffusion effective in a shorter time), and for any time-dependence of the container's angular velocity (Greenspan & Howard 1963, Greenspan 1968), as long as it respects the low-Rossby-number constraint and the flow remains laminar. For the best-studied case of a sudden change $\Delta\Omega$ in the angular velocity of the container, the azimuthal velocity of the fluid (in a reference frame rotating with the initial angular velocity Ω_0) varies as

$$v_\phi(\tilde{r}, \tilde{t}) = \Delta\Omega a\tilde{r} \left\{ 1 - \exp\left[-\frac{(1 + f'^2)^{1/4} + (1 + g'^2)^{1/4}}{f + g}\tilde{t} \right] \right\}, \qquad (69)$$

where the container walls are located at $z = af(\tilde{r})$ and $z = -ag(\tilde{r})$, with the

dimensionless distance from the rotation axis defined as $\tilde{r} \equiv r/a$, and the dimensionless time as $\tilde{t} \equiv t/t_E$. (f' and g' denote derivatives with respect to $\tilde{r}$.)

Since the spin-up process studied in the present paper is very similar (particularly in its mathematical expression) to the classical spin-up process, one may expect a similar formula to hold in this case, if it were not for one generic feature of the superfluid spin-up problem in finite containers that does not show up in the model of §3: the necessity of creating new vortex lines at the walls (Campbell & Krasnov 1982, Peradzynski et al. 1990). The problem of vortex nucleation is not fully understood at present (Donnelly 1991), but it is to be expected that a finite velocity difference between the wall and the superfluid next to it is necessary for new vortex lines to form. This could, in principle, slow down the spin-up process, but the magnitude of this effect is hard to estimate and may be small if a large number of vortex lines is present in the fluid. This uncertainty may be avoided in particular experiments by letting the container spin *down* ($\alpha/\Omega_0 < 0$, or $\Delta\Omega/\Omega_0 < 0$) rather than up, and will be ignored in what follows.

Thus, the present theory of superfluid spin-up can be tested experimentally by measuring the spin-up time for different values of the (vertical) container dimensions, angular velocity, and temperature. Experiments of this kind have been done by Tsakadze and Tsakadze (1973, 1975, 1980), who studied the relaxation of He II (and He I) to sudden spin-up of a spherical container. After a spin-up, they measured the evolution of the angular velocity of the container. From this, they extracted a spin-up time t_0, for which they assumed the functional form

$$t_0 = \frac{A}{\Omega_0} \left(\frac{\Omega_0 R^2}{\hbar/m} \right)^{\beta} \left(\frac{\rho_n}{\rho} \right)^{-\alpha} \ln(1 + c'\Delta\Omega), \qquad (70)$$

and found the best-fit parameters $A = 1.0 \pm 0.1$, $\beta = 0.40 \pm 0.05$, $\alpha = 0.25 \pm 0.01$, and $c' = (5.1 \pm 0.2)\,$s, by making measurements at various temperatures, rotation rates, and changes in the rotation rate (Tsakadze & Tsakadze 1975, 1980).

Since only the motion of the container was observed, the dynamical variable

of interest for the fluid is its total angular momentum, which can conveniently be written as

$$L(\tilde{t}) = L(\tilde{t} = 0) \left(1 + \frac{\Delta\Omega}{\Omega_0} l(\tilde{t}) \right). \tag{71}$$

The dimensionless function $l(\tilde{t})$ is equal to zero at $\tilde{t} = 0$ (the instant at which the container spins up) and tends to unity as $\tilde{t} \to \infty$. It can only be found numerically by integrating the appropriate form of eq. (69) (multiplied by $\tilde{r}$) over the interior volume of the spherical container. The result can be fit reasonably well as

$$l(\tilde{t}) \approx 1 - e^{-\tilde{t}/\tilde{t}_s}, \tag{72}$$

where $\tilde{t}_s \approx 1/2$ if the characteristic length scale used is the radius R of the spherical container. Both the exact and the approximate form of $l(\tilde{t})$ are plotted in Fig. 4.

Unfortunately, several problems are encountered when trying to use the results of Tsakadze and Tsakadze (1975, 1980) to test the model presented here:

1) The fact that the experimental results correspond to Rossby numbers $\varepsilon = \Delta\Omega/\Omega_0$ ranging from about 0.3 to 1 (rather than being $\ll 1$) makes the applicability of the linear theory at least questionable. Even if it could be extended to such high Rossby numbers, it is not clear which angular velocity in the range $(\Omega_0, \Omega_0 + \Delta\Omega)$ has to be used, for example, in the expression for the spin-up time, leading to uncertainties of order ε. Furthermore, even in the experiments with the smallest Rossby numbers (~ 0.3), the Reynolds numbers characterizing the Ekman layers (see eq. [66]), are of order 30 to 90 if the radius of the container is 1.7 cm, and twice these numbers if it is 3.4 cm (see point 3 in this list). Thus, the assumption of small bending of the vortex lines is at best marginally satisfied, and it is possible that at least in some of these experiments the Ekman layers become unstable, making the model inapplicable.

2) The precise definition of the spin-up time t_0 is not given in their papers.

It is clearly not identical with the time constant for exponential relaxation since exponential fits (Alpar 1978) of their data yield time constants significantly shorter than the spin-up times shown in their graphs. For spin-up from rest to $\Omega = 4\,\text{s}^{-1}$, and from $3\,\text{s}^{-1}$ to $4\,\text{s}^{-1}$ (in both cases at $T = 1.57\,\text{K}$), the time constants (Alpar 1978) are 52 s and 47 s, whereas, from Fig. 9 of Tsakadze and Tsakadze (1980), one can read off the (approximate) values 280 s and 120 s. These particular numbers also suggest that the spin-up time variable measured by Tsakadze and Tsakadze may be much more dependent on $\Delta\Omega$ than the time constant for exponential relaxation. The logarithmic dependence of t_0 on $\Delta\Omega$ suggests that t_0 may be the time it takes for the angular velocity difference between the container and the interior fluid to decrease below some specified, small value $\Delta\Omega_c$.[8] Of course, in this case one would expect a dependence of the form

$$t_0 = t_e \ln(\Delta\Omega/\Delta\Omega_c), \tag{73}$$

where t_e is the exponential relaxation time. This is slightly different from the form chosen by Tsakadze and Tsakadze, but by choosing appropriate values for $\Delta\Omega_c$ ($\approx 0.136\,\text{s}^{-1}$) and for the constant of proportionality, these two functions can be made to agree very well in the range of $\Delta\Omega$ spanned by their experiments, $1\,\text{s}^{-1} \leq \Delta\Omega \leq 4\,\text{s}^{-1}$ (see Fig. 5).

3) The spherical container used for the experiments is first reported as having a *radius* (Tsakadze & Tsakadze 1973, 1975) of 3.4 cm, then as having a *diameter* (Tsakadze & Tsakadze 1980) of 3.4 cm, but the same plots are given for the relaxation time as a function of temperature (Fig. 3 of Tsakadze & Tsakadze 1973, Fig. 9 of Tsakadze & Tsakadze 1980). Of course, if Ω_0, $\Delta\Omega$, and T are the same, the relaxation times can only be identical if the radius of the sphere is also the

---

[8]This particular definition of t_0 appears not to have been deliberately chosen by these authors, who define t_0 as "the time interval from the start of the rotation to the assumption of uniform attenuation of the vessel" (Tsakadze & Tsakadze 1973), but it seems to be the only viable operational definition, since a perfectly uniform attenuation of the vessel (with the fluid rotating exactly as a solid body with the same angular velocity as the vessel) will not occur within a finite time interval.

same. Whether this is $R = 3.4\,\text{cm}$ or $R = 1.7\,\text{cm}$ can be decided, e. g., by considering the data points above T_λ, which correspond to a classical fluid. For these, the spin-up time (defined in the manner discussed in the previous paragraph) is expected to be $t_0 \approx 0.5 R (\nu\Omega)^{-1/2} \ln(\Delta\Omega/0.136\,\text{s}^{-1})$. At $T = 2.2\,\text{K}$, the kinematic viscosity is $\nu = 1.84 \times 10^{-4}\,\text{cm}^2\,\text{s}^{-1}$ (Wang, Howald, & Meyer 1990). Thus, for spin-up from $\Omega = 3\,\text{s}^{-1}$ to $4.2\,\text{s}^{-1}$, one obtains $105\,\text{s} \le t_0 \le 124\,\text{s}$ if $R = 3.4\,\text{cm}$, and $53\,\text{s} \le t_0 \le 62\,\text{s}$ if $R = 1.7\,\text{cm}$ (the ranges reflect the uncertainty in the value of Ω to be used in the formula), while for spin-up from $\Omega = 0$ to $4.2\,\text{s}^{-1}$, one can only obtain the lower limits $t_0 \ge 166\,\text{s}^{-1}$ for $R = 3.4\,\text{cm}$ and $t_0 \ge 83\,\text{s}^{-1}$ for $R = 1.7\,\text{cm}$ (which should be reasonably good order-of-magnitude estimates for the correct values). The plotted values ($t_0 \approx 70\,\text{s}$ in the first case, $t_0 \approx 130\,\text{s}$ in the second) are approximately consistent with $R = 1.7\,\text{cm}$, but not with $R = 3.4\,\text{cm}$. However, eq. (70) does not reproduce the plots mentioned above, unless the value $R = 3.4\,\text{cm}$ is used. Thus, if $R = 1.7\,\text{cm}$ is adopted, the constant of proportionality in that equation should be changed to $A = 1.0 \times 2^{2\beta} = 1.74$.

4) Finally, the range of validity of eq. (70) with the given parameters is by no means clear. The formula itself was arrived at by a mixture of dimensional analysis, physical intuition, and guesswork, and the parameters were fitted by varying one of the three variables Ω_0, $\Delta\Omega$, and T while holding the other two fixed at particular values. This procedure does not check whether the spin-up time can really be written as a product of three functions, each of which depends only on one variable. This could have been checked by changing the values of the variables being held constant and repeat the determination of the unknown parameters.

Ignoring the problems mentioned in point 1, and using the definition arrived at in point 2, one can write down a theoretical prediction for the spin-up time,

$$t_0 \approx 0.5 \frac{R}{\Omega_0^{1/2}} f(T) \ln\left(\frac{\Delta\Omega}{\Delta\Omega_c}\right), \tag{74}$$

where $f(T)$ is the function shown in eq. (58) and in Fig. 1. Like in eq. (70), it

is also the case here that t_0 is a product of functions of R, Ω_0, $\Delta\Omega$, and T. The dependence on R and Ω_0 corresponds to setting $\beta = 0.5$ in eq. (70), rather than the measured value $\beta = 0.40 \pm 0.05$. The theoretical dependence on temperature, given by the function $f(T)$, cannot be written simply as a power of ρ_n/ρ.

Fig. 6 shows t_0 as a function of temperature for $R = 1.7$ cm as predicted by eqs. (70) (with A=1.74) and (74), in the two cases $\Omega_0 = 2\,\text{s}^{-1}$, $\Delta\Omega = 4\,\text{s}^{-1}$, and $\Omega_0 = 3.5\,\text{s}^{-1}$, $\Delta\Omega = 1\,\text{s}^{-1}$. One sees that the empirical and theoretical curves do not agree in detail, although the qualitative dependence on temperature is similar, and the values at particular temperatures agree within a factor of 1.8.[9] If the correct values are $R = 3.4$ cm and $A = 1.0$, the empirical curves stay where they are, but the theoretical curves move up by a factor of 2, making the disagreement worse. (However, as pointed out already, this would also make the experimental spin-up times of He I different from the values expected from the well-tested Ekman circulation model.)

In principle, the theoretical spin-up time should also include a correction for the relaxation of the container's angular velocity. If the fluid's relaxation occurred with a single, well-defined time constant, the effect of the container's relaxation would be to reduce this time constant by a factor $(1 + I_f/I_c)^{-1} \approx 0.8 - 0.85$, where I_f and I_c are the moments of inertia of the fluid and the container, and the numerical values are those given by Tsakadze and Tsakadze (1973, 1975). However, this is clearly not the case for a spherical container, where the effect is much more complicated and will not be considered here.

That the experimental curve is less temperature-dependent would be consistent with the Ekman layers in these experiments being turbulent. In this case, the angular momentum would be transported from the container to the Ekman layer by the turbulent Reynolds stress, which does not depend on temperature, rather

---

[9]Alpar (1978) claims that "the relaxation times observed [by Tsakadze and Tsakadze] turn out to be higher by a factor of $35 - 120$ than the Ekman time," but this seems to be due to his omitting a factor 10^{-4} in the kinematic viscosity.

than by viscosity, which is temperature dependent (though not very strongly in this case). A clear signature of the formation of a turbulent Ekman layer would be a progressive reduction of the measured spin-up time relative to the theoretical prediction when the Reynolds number is increased beyond some critical value.

7. CONCLUSIONS

A consistent model for linear, laminar spin-up of He II (or a superfluid of similar properties) without any free parameters has been presented. This model is found by solving generally accepted, coupled equations of motion for the quantized vortex lines and the normal and superfluid components. Two basic spin-up mechanisms are identified: 1) Classical, viscosity-induced, Ekman pumping of the normal component, and 2) Ekman-like circulation in the superfluid component, caused by friction exerted by the normal Ekman layer on the vortex lines. In both cases, the normal fluid and the superfluid are coupled by the Magnus and mutual friction forces acting between them and the vortex lines.

The spin-up time scales with $a/\Omega_0^{1/2}$ (where $2a$ is the height of the container parallel to the rotation axis, and Ω_0 is the rotation rate), and increases with decreasing temperature. Unfortunately, the interpretation of the available experimental results involves many uncertainties and the model is likely not to be applicable in the parameter region covered. Thus new experiments are highly desirable. These should preferably be performed in cylindrical containers with smooth walls being spun up or down at a constant, slow rate (in which case one should measure the difference between the rotation rates of the container and the interior fluid at a given instant), or suddenly by a small amount, as in the experiments discussed in this section. Such experiments could determine whether this relatively simple model gives a complete description of superfluid spin-up, or whether additional elements (vortex nucleation, vortex-boundary friction, or vortex pinning) should be included.

Of course, the model presented here cannot be directly applied to spin-up and spin-down of neutron stars. The response of the interior of a neutron star is complicated by several factors, only a few of which will be mentioned here: 1) the plausible existence of superconducting protons threaded by a dense array of magnetic flux tubes that may interact strongly with the (also magnetized) neutron superfluid vortices (Sauls 1989); 2) pinning of the neutron vortices to the nuclei inside the solid stellar crust (Baym et al. 1992), and 3) strong stratification of the fluid in the stellar interior (Reisenegger & Goldreich 1992). However, some features of this model may also be relevant to neutron star spin-up, in particular that vortex lines will generally move with the fluid, unless frictional forces are present locally, and that superfluid spin-up, like classical spin-up, usually occurs due to secondary flows that transport the vorticity.

ACKNOWLEDGEMENTS

APPENDIX. A SIMPLIFIED MODEL PROBLEM

In this Appendix, a simplified model problem is examined, in order to clarify the physical mechanism for the spin-up of the superfluid component in the absence of viscosity. The physical situation studied here is, as in §3, a fluid confined between two parallel, infinite planes, whose rotation rate is $\Omega(t) = \Omega_0 + \alpha t$. However, no normal (viscous) component is present in this case, only the superfluid component

threaded by its array of vortex lines. The container and the vortex lines are coupled by a frictional force like that used in Campbell and Krasnov (1982) and Adams et al. (1985).

Using the same variables as in §3, one obtains a very simplified form of eqs. (26) and (27):

$$T_s - \delta_s^2 \frac{d^2 T_s}{dz^2} = T_0, \tag{75}$$

and

$$U_s - \delta_s^2 \frac{d^2 U_s}{dz^2} = -\frac{\alpha}{2\Omega_0}. \tag{76}$$

The boundary condition $\int_0^{\pm a} U_s(z)dz = 0$, imposing that there is no flow into the wall, is kept, but the free-end conditions for the vortex lines are modified to include friction:

$$\left[\gamma(\dot{\epsilon} - r\alpha t\hat{\phi}) \pm \nu_s \frac{\partial \epsilon}{\partial z} \right]_{z=\pm a} = 0. \tag{77}$$

The frictional force, parametrized by a friction coefficient γ (with dimensions of length), is balanced by the horizontal component of the tension of the deformed vortex lines. Equivalently,

$$\frac{dT_s}{dz}(z = \pm a) = \pm \frac{\gamma}{2\Omega_0 \delta_s^2}, \tag{78}$$

and

$$\frac{dU_s}{dz}(z = \pm a) = \pm \frac{\alpha \gamma T_0}{\delta_s^2}. \tag{79}$$

The (exact) solutions are

$$T_s(z) = \frac{1}{2\Omega_0} \left[\frac{a}{\gamma} + \frac{\gamma}{\delta_s} \frac{\cosh(z/\delta_s)}{\sinh(a/\delta_s)} \right], \tag{80}$$

and

$$U_s(z) = -\frac{\alpha}{2\Omega_0} \left[1 - \frac{a}{\delta_s} \frac{\cosh(z/\delta_s)}{\sinh(a/\delta_s)} \right]. \tag{81}$$

If $\delta_s \ll a$, the terms containing the factor $\cosh(z/\delta_s)/\sinh(a/\delta_s)$ are negligible except in boundary layers of thickness $\sim \delta_s$ at the walls of the container. In the interior $(a - |z| \gg \delta_s)$, both T_s and U_s are independent of z. The vortex line velocity,

$$\dot{\epsilon} = \alpha r \left[-\frac{1}{2\Omega_0} \hat{\mathbf{r}} + \left(t - \frac{a/\gamma}{2\Omega_0} \right) \hat{\phi} \right], \tag{82}$$

is independent of z everywhere,[10] and is the same as the fluid velocity far from the boundaries.

In the interior, the fluid carries the vortex lines inward (assuming $\alpha/\Omega_0 > 0$), giving rise to spin-up. The fluid moves back outward in the boundary layers. The angular velocity of the interior fluid (together with the vortex lines) increases at the same rate as that of the container, but with a time lag $(a/\gamma)(2\Omega_0)^{-1}$. The boundary layer fluid lags behind the interior fluid by an additional time $\sim (\gamma/\delta_s)(2\Omega_0)^{-1}$. The relative motion of the fluid and the vortex lines in the boundary layer produces a Magnus force that allows the vortex lines to bend, so that the fluid velocity is different near the boundaries and in the interior.

This process has interesting similarities, but also important differences, with the spin-up mechanism for classical fluids. In both cases, there is a secondary flow that carries the vorticity inward in the interior of the container, and returns through the boundary layers, whose thickness is determined by the kinematic viscosity in the

---

[10]If this were not the case, the vortex lines would be stretching indefinitely.

classical fluid and by the "effective viscosity" ν_s in the superfluid, in this respect confirming Alpar's (1978) speculation mentioned in §1.

However, the superfluid spin-up time scale is independent of ν_s; there is no superfluid analog for the classical Ekman time. In both cases (classical fluid and superfluid), the torque exerted by the container has to be simply αI_f, where I_f is the moment of inertia of the fluid. In a classical fluid, this is set equal to the viscous stress across the boundary layer, determining the required angular velocity difference, and from it the Ekman time. In a superfluid, it can be set equal to the frictional torque due to the interior fluid (and thus the vortex lines) spinning slower than the container by $\Delta\Omega = -\alpha T_0$, and this immediately determines $T_0 = (a/\gamma)(2\Omega_0)^{-1}$, without involving ν_s. (This argument also shows that this result does not require the assumption that $|\partial\epsilon/\partial z| \ll 1$, although the more explicit derivation given previously depends on it.) Physically, this means that the vortex lines in the boundary layer region will be stretched as much as needed to transmit the frictional torque from the walls to the interior fluid. Of course, the amount by which they have to be stretched depends on ν_s, but the effect on the interior fluid does not. For related reasons, the characteristic "Ekman spiral" of spinning-up classical fluids (Greenspan 1968) is also absent in a pure superfluid.

Finally, the fluid close to the wall, whose velocity is equal to that of the container (and therefore faster than that of the interior fluid) in a classical fluid, can have a velocity very different from that of the container (and always slower than that of the interior fluid, if $\alpha/\Omega_0 > 0$) in the superfluid case. The reason for this last difference is that in the classical fluid the walls interact directly with the fluid, preventing it from "slipping," whereas in the superfluid the walls interact with the ends of the vortex lines, preventing them from moving quickly, and therefore maintaining the fluid velocity at the boundaries closer to its original value.

REFERENCES

Adams, P. W., Cieplak, M., & Glaberson, W. I. 1985, *Phys. Rev. B* **32**, 171.

Alpar, M. A. 1978, *J. Low Temp. Phys.* **31**, 803.

Barenghi, C. F., Donnelly, R. J., & Vinen, W. F. 1983, *J. Low Temp. Phys.* **52**, 189.

Baym, G. & Chandler, E. 1983, *J. Low Temp. Phys.* **50**, 57.

Baym, G., Epstein, R. I., & Link, B. 1992, *Physica B* **178**, 1.

Benton, E. R. & Clark, A. 1974, *Ann. Rev. Fluid Mech.* **6**, 257.

Bondi, H. & Lyttleton, R. A. 1948, *Proc. Camb. Phil. Soc.* **44**, 345.

Campbell, L. J. & Krasnov, Yu. K. 1982, *J. Low Temp. Phys.* **49**, 377.

Chandler, E. & Baym, G. 1986, *J. Low Temp. Phys.* **62**, 119.

Courts, S. C. & Tough, J. T. 1988, *Phys. Rev. B* **38**, 74.

Donnelly, R. J. 1991, *Quantized Vortices in Helium II* (Cambridge Univ. Press, Cambridge).

Glaberson, W. I., Johnson, W. W., & Ostermeier, R. M. 1974, *Phys. Rev. Lett.* **33**, 1197.

Greenspan, H. P. 1968, *The Theory of Rotating Fluids* (Cambridge Univ. Press, Cambridge).

Greenspan, H. P. & Howard, L. N. 1963, *J. Fluid Mech.* **17**, 385.

Hall, H. E. 1963, in *Liquid Helium*, International School of Physics "Enrico Fermi," Course XXI, G. Careri, ed. (Academic Press, New York).

Hedge, S. G., & Glaberson, W. I. 1980, *Phys. Rev. Lett.* **45**, 190.

Lamb, F. K. 1991, in *Frontiers of Stellar Evolution*, D. L. Lambert, ed. (Astron. Society of the Pacific), p. 299.

Lyne, A. G., Graham Smith, F., & Pritchard, R. S. 1992, *Nature* **359**, 706.

Oestereich, T. & Xie, J. K. 1991, *J. Low Temp. Phys.* **83**, 57.

Ostermeier, R. M. & Glaberson, W. I. 1975, *J. Low Temp. Phys.* **21**, 191.

Peradzynski, Z., Filipkowski, S., & Fiszdon, W. 1990, *Eur. J. Mech. B/Fluids* **9**, 259.

Poppe, W. & Schmidt, D. W. 1987, *Theoretical Investigation of the Development of the Normal Fluid and Superfluid Velocity Distributions During Spin-up for He II-Filled Cylinder*, MPI Strömungsforsch., Göttingen, Bericht 6; graphs of their results are also given by Peradzynski et al. 1990.

Reisenegger, A. & Goldreich, P. 1992, *Astrophys. J.* **395**, 240.

Reppy, J. D., Depatie, D., & Lane, C. T. 1960, *Phys. Rev. Lett.* **5**, 541.

Reppy, J. D. & Lane, C. T. 1961, in *Proceedings of the VII International Conference on Low Temperature Physics*, G. M. Graham and A. C. H. Hallett, eds. (Univ. of Toronto Press, Toronto), p.443.

Reppy, J. D. & Lane, C. T. 1965, *Phys. Rev.* **140**, A106.

Sauls, J. A. 1989, in *Timing Neutron Stars*, H. Ögelman & E. P. J. van den Heuvel, eds. (Kluwer Academic Publishers), p. 457.

Schwarz, K. W. 1992, *Phys. Rev. Lett.* **69**, 3342.

Staas, F., Taconis, K. W., & van Alphen, W. M. 1961, *Physica* **27**, 893.

Swanson, C. E., Wagner, W. T., Donnelly, R. J., & Barenghi, C. F. 1987, *J. Low Temp. Phys.* **66**, 263.

Tilley, D. R. & Tilley, J. 1990, *Superfluidity and Superconductivity*, third edition (Adam Hilger, Bristol & New York), §3.9.

Tough, J. T. 1982, in *Progress in Low Temperature Physics*, vol. VIII, D. F. Brewer, ed., p. 133 (North-Holland, Amsterdam).

Tsakadze, J. S. & Tsakadze, S. J. 1973, *Sov. Phys.-JETP* **37**, 918.

Tsakadze, J. S. & Tsakadze, S. J. 1975, *Sov. Phys.-Uspekhi* **18**, 242.

Tsakadze, J. S. & Tsakadze, S. J. 1980, *J. Low Temp. Phys.* **39**, 649.

von Kármán, T. 1921, *Zeitschrift für Angewandte Mathematik und Mechanik* **1**, 233, also in *Collected Works of Theodore von Kármán*, vol. II, p. 70 (Butterworths Scientific Publications, London, 1956).

Wang, S., Howald, C., & Meyer, H. 1990, *J. Low Temp. Phys.* **79**, 151.

Wedemeyer, E. H. 1964, *J. Fluid Mech.* **20**, 383.

Wilks, J. 1967, *The Properties of Liquid and Solid Helium* (Clarendon Press, Oxford), Chapters 3 and 7.

Yarmchuk, E. J., & Glaberson, W. I. 1979, *J. Low Temp. Phys.* **36**, 381.

Fig. 1: The function $f(T)$ that contains the temperature- dependence of the spin-up time (see eqs. [57] and [58]) as predicted by the theoretical model discussed in this paper, using the data in Table I of Barenghi et al. (1983). It gives the spin-up time (in seconds) for the container dimension $a = 1$ cm and the angular frequency $\Omega_0 = 1$ s.
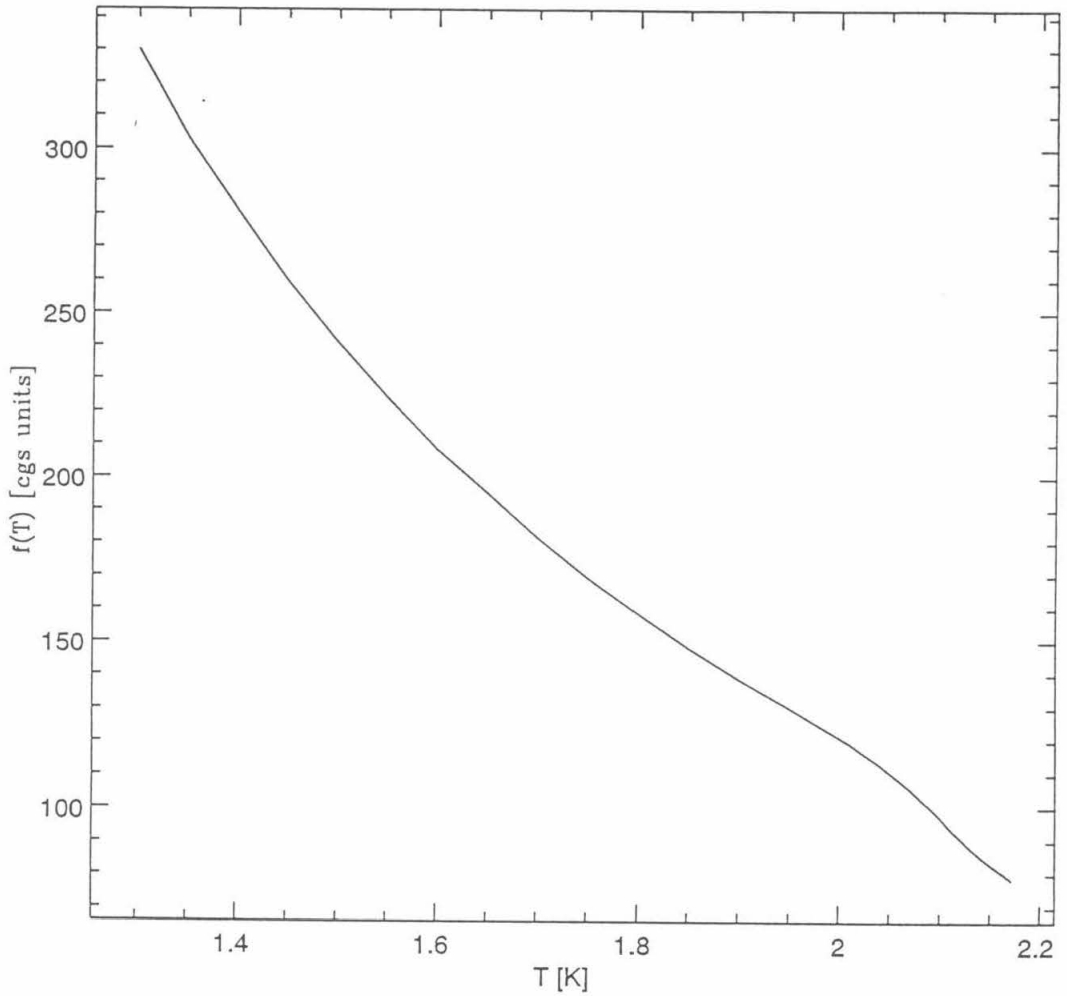
Fig. 2: The mutual-friction variables, $\beta_0\rho_s/\rho_n$ (solid curve) and $\beta_0'\rho_s/\rho_n$ (dashed curve), as functions of temperature.
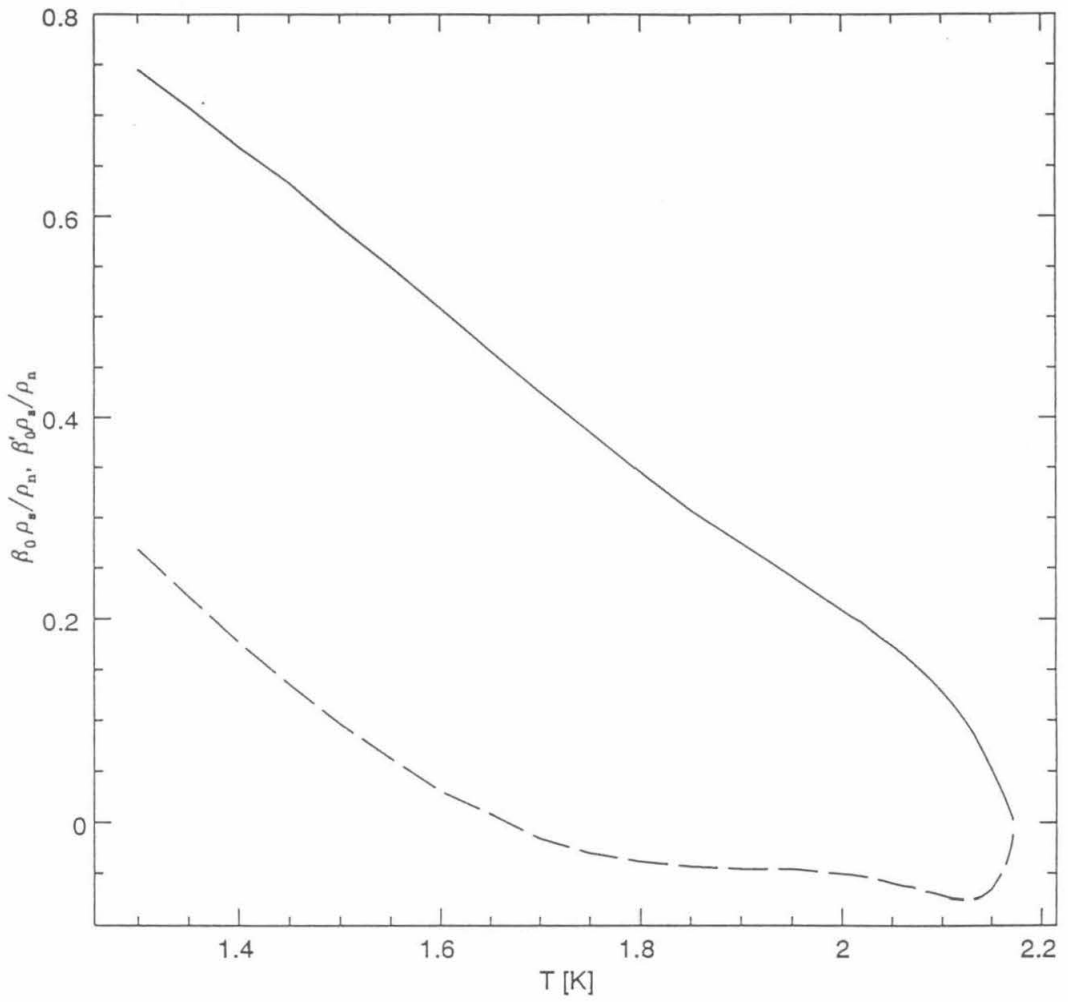
Fig. 3: The variables $-(2\Omega_0/\alpha)U_{n0}$ (solid line) and $-(2\Omega_0/\alpha)U_{s0}$ (dashed line), giving a dimensionless measure of the secondary flow velocities of the normal fluid and the superfluid. The corresponding variable for the vortex lines is equal to 1 everywhere (dotted line).
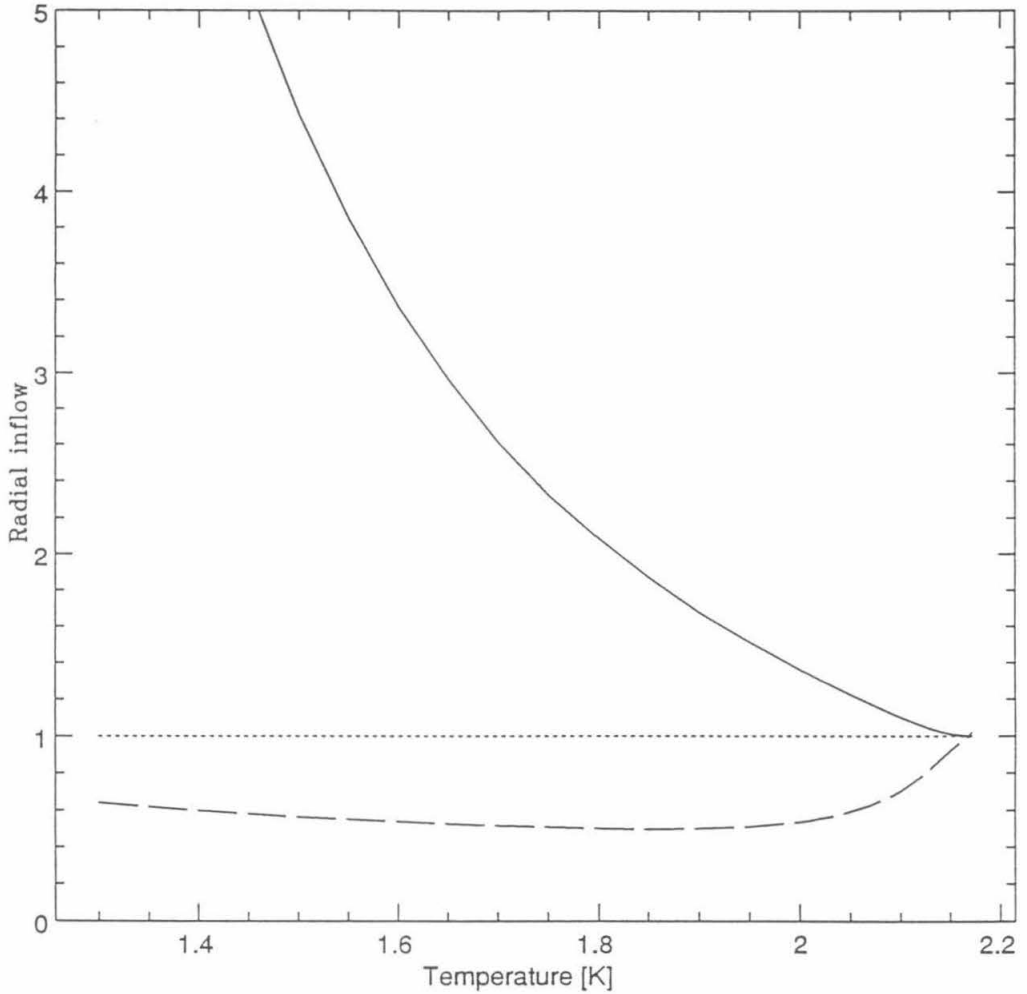
Fig. 4: The function $l(\tilde{t})$ (solid line), giving the time-evolution of the total angular momentum of the fluid enclosed in a sphere that is spun up impulsively at $\tilde{t} = 0$ (see eq. [71]), and its analytical approximation (dashed line), given by eq. [72].
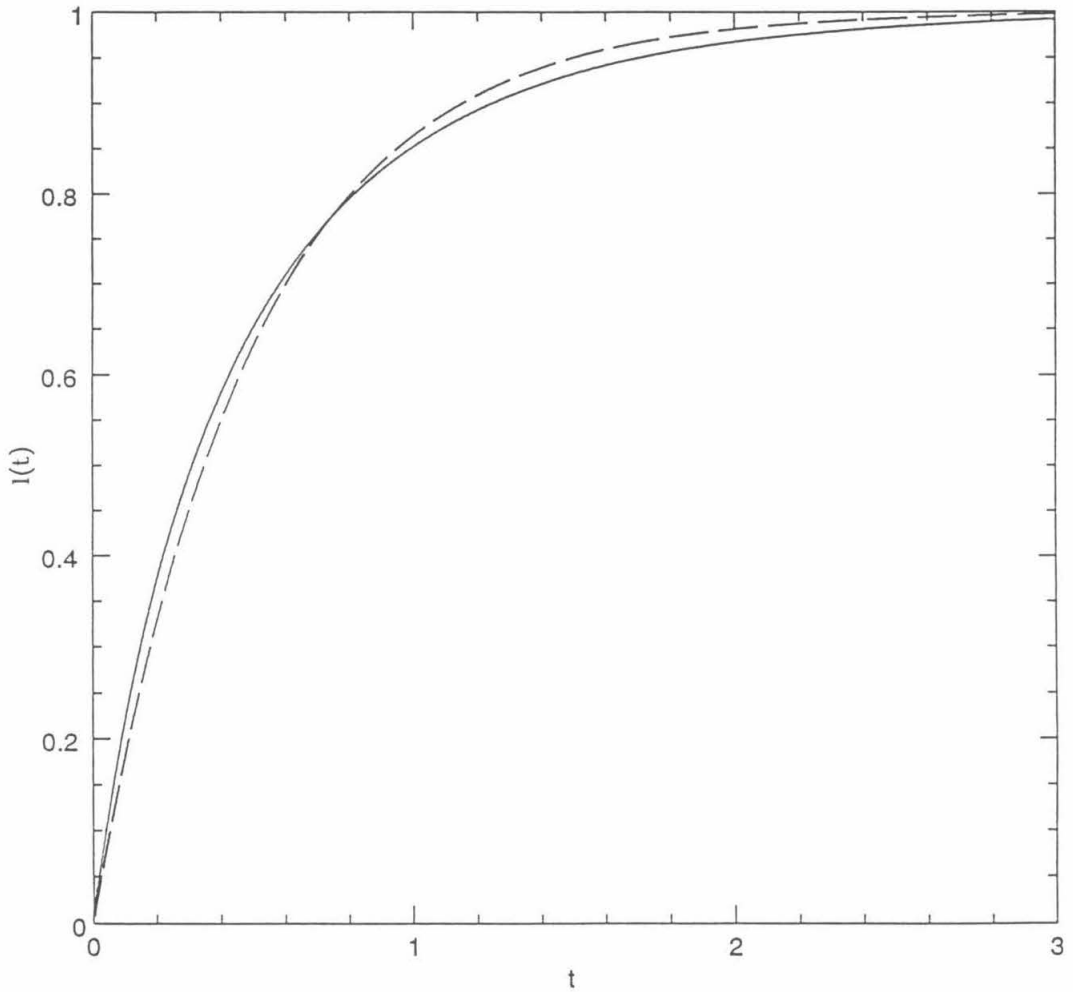
Fig. 5: The functions giving the dependence of the spin-up time on the magnitude of the sudden change in the angular velocity of the container. The solid curve gives $\ln(1 + 5.1\Delta\Omega)$, the form used by Tsakadze and Tsakadze (1975, 1980); the dotted curve, $(1.38 + 2.1\Delta\Omega)^{1/2}$, is the alternative suggested by Alpar (1978), and the dashed curve, $0.905\ln(\Delta\Omega/\Delta\Omega_c)$, with $\Delta\Omega_c = 0.136$, is the form favored in the present paper. (In all formulae, cgs units have been used.)
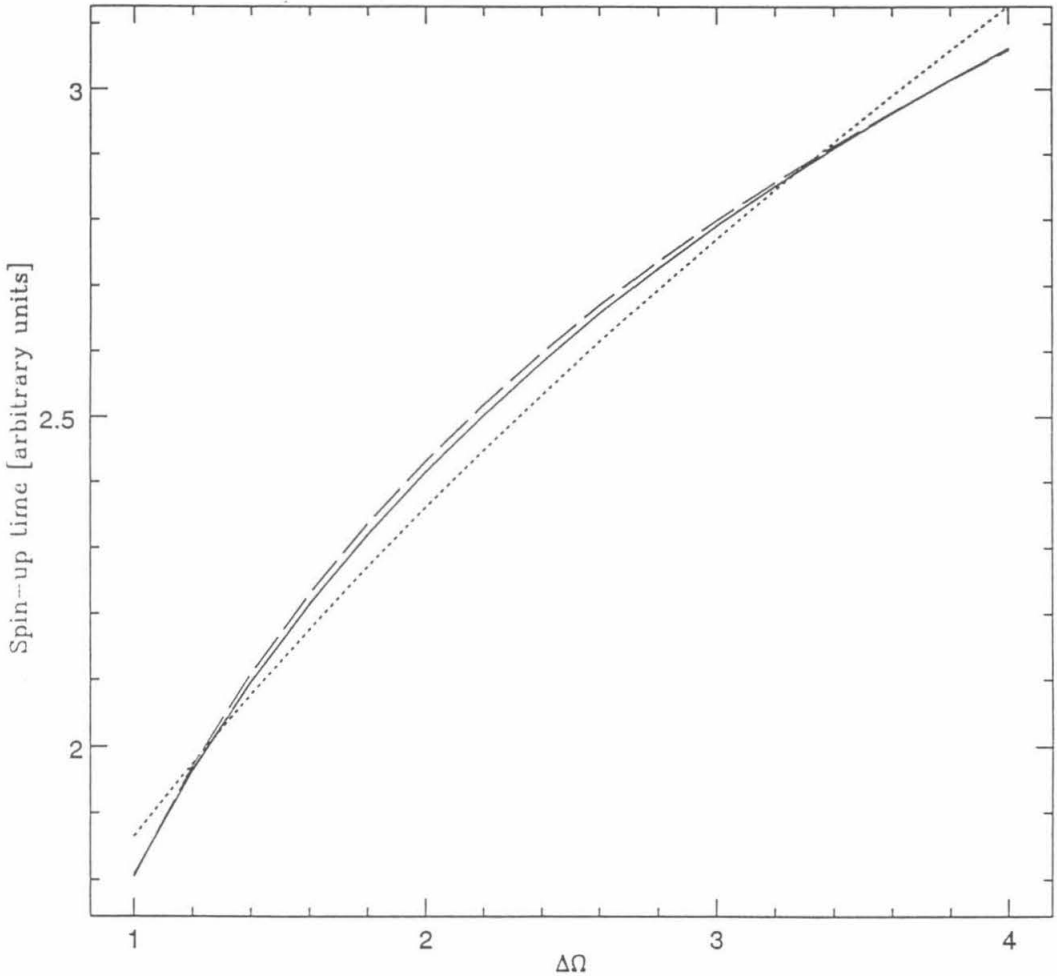
Fig. 6: Comparison of the spin-up times $t_0(T)$ given by the semi-empirical formula of Tsakadze and Tsakadze (1975, 1980) (eq. [70] with $A = 1.74$, $\alpha = 0.25$, $\beta = 0.4$, and $c' = 5.1$ s; solid curves) and the formula derived from the theoretical model (eq. [74] with $\Delta\Omega_c = 0.136$ s^{-1}; dashed curves). The upper two curves correspond to the parameter values $\Omega_0 = 2$ s^{-1} and $\Delta\Omega = 4$ s^{-1}, and the lower two curves to the values $\Omega_0 = 3.5$ s^{-1} and $\Delta\Omega = 1$ s^{-1}. In all cases, $R = 1.7$ cm.